

**UNIVERSIDADE DE SÃO PAULO
INSTITUTO DE QUÍMICA**

Programa de Pós-Graduação em Ciências Biológicas (Bioquímica)

RAILMARA PEREIRA DA SILVA

**Investigation of Oxidative Metabolism of Uric Acid
and its Role in Redox Processes in Inflammation**

**Versão corrigida da Tese conforme Resolução CoPGr 5890
A original se encontra disponível na Secretaria de Pós-Graduação do IQ-USP**

São Paulo

Data do Depósito na SPG:

07/07/2020

RAILMARA PEREIRA DA SILVA

**Investigação do Metabolismo Oxidativo do Ácido
Úrico e seu Papel sobre Processos Redox na
Inflamação**

*Tese apresentada ao Instituto de Química da
Universidade de São Paulo para obtenção do
Título de Doutora em Ciências (Bioquímica).*

Orientadora: Prof^a. Dr^a. Flavia Carla Meotti

São Paulo
2020

Autorizo a reprodução e divulgação total ou parcial deste trabalho, por qualquer meio convencional ou eletrônico, para fins de estudo e pesquisa, desde que citada a fonte.

Ficha Catalográfica elaborada eletronicamente pelo autor, utilizando o programa desenvolvido pela Seção Técnica de Informática do ICMC/USP e adaptado para a Divisão de Biblioteca e Documentação do Conjunto das Químicas da USP

Bibliotecária responsável pela orientação de catalogação da publicação:
Marlene Aparecida Vieira - CRB - 8/5562

S581i Silva, Railmara Pereira da
Investigação do Metabolismo Oxidativo do Ácido
Úrico e seu Papel sobre Processos Redox na Inflamação
/ Railmara Pereira da Silva. - São Paulo, 2020.
157 p.

Tese (doutorado) - Instituto de Química da
Universidade de São Paulo. Departamento de
Bioquímica.

Orientador: Meotti, Flavia Carla

1. Ácido Úrico. 2. Hidroperóxido de urato. 3.
Mieloperoxidase. 4. Inflamação. 5. Infecção. I. T.
II. Meotti, Flavia Carla , orientador.



Universidade de São Paulo
Instituto de Química

"Investigação do metabolismo oxidativo do ácido úrico e seu papel sobre processos redox na inflamação"

RAILMARA PEREIRA DA SILVA

Tese de Doutorado submetida ao Instituto de Química da Universidade de São Paulo como parte dos requisitos necessários à obtenção do grau de Doutora em Ciências obtido no Programa Ciências Biológicas (Bioquímica) - Área de Concentração: Bioquímica.

Profa. Dra. Flavia Carla Meotti
(Orientadora e Presidente)

APROVADO(A) POR:

Profa. Dra. Ohara Augusto
IQ - USP

Prof. Dr. Niels Olsen Saraiva Câmara
ICB - USP

Prof. Dr. Daniel Martins de Souza
IB - UNICAMP

SÃO PAULO
23 de setembro de 2020

***Dedico esse trabalho:
À minha família e em especial à minha querida avó, Vanda
Pereira da Silva (in memoriam).***

AGRADECIMENTOS

E mais um objetivo é alcançado na minha vida. A jornada vivida em direção desse objetivo me permitiu crescer cientificamente e, muito mais que isso, transformou o meu Eu. Portanto, muitos são os agradecimentos a todos aqueles que de forma direta ou indireta estiveram ao meu lado durante essa jornada.

Começo agradecendo a Deus pelo dom da Vida e por guiar os meus passos diariamente.

À minha querida Orientadora e Amiga Flávia Meotti pelos seus ensinamentos científicos e por ter acreditado na minha capacidade a todo momento. Por me mostrar que é possível desenvolver ciência com rigor científico, leveza, entusiasmo e amor. Pelo exemplo de Ser, que me fez reconhecer que é possível fazermos desse Mundo Bem Melhor. A você todo meu Respeito e Admiração.

Ao meu querido supervisor do *Center Free Radical Research – New Zealand*, Anthony Kettle pelos seus ensinamentos científicos que foram muito além da academia, foram para vida. Por ter acreditado nas minhas capacidades e por ter me mostrado que eu estava no caminho certo. Seu entusiasmo e determinação ficarão para sempre marcados dentro de mim.

Aos meus pais Maria Perpetua e Raimundo Batatinha pelo amor incondicional, pelo incentivo à educação, pelo acolhimento a cada volta para casa e por todos os esforços para que eu pudesse realizar meus sonhos.

Ao meu irmão Rony, suas orações e apoio foram fundamentais para que eu chegasse até aqui.

À minha querida avó Vanda Pereira (*in memoriam*) pelo seu exemplo de Ser e pelo seu espírito educador que nos fez tão parecidas.

À toda minha família pelo amor e por sempre me acolher de braços abertos em cada retorno a Bahia. Em especial, agradeço à minha tia Iara Matos pelo seu amor, por ter acreditado nas minhas capacidades e por sempre me incentivar a alcançar meus objetivos.

Ao Lucas Dantas, seu apoio e incentivo foram fundamentais durante essa jornada. E em seu nome, agradeço toda a família Souza-Dantas pelo carinho de sempre.

Aos meus queridos amigos Adriano Britto e Isabella Pinto, aqueles que tive a oportunidade de compartilhar a mesma casa. A amizade, carinho e companheirismo de vocês fizeram da nossa convivência uma verdadeira família.

À Marcela Mineiro, uma querida amiga que esse processo me apresentou, sua amizade, companheirismo e força diários fizeram dos meus dias no laboratório mais felizes. E por me mostrar o verdadeiro significado do que é vencer e seguir brilhando.

Ao Álberty Peixoto pelo brilho nos olhos em fazer aquilo que ama, pelas risadas soltas e amizade. Essa jornada não teria sido a mesma sem você por perto.

Ao meu Amigo e Teacher Marco Marchi pela Amizade, pelos ensinamentos de inglês e por me mostrar que era possível eu chegar onde queria.

Ao Dr. Celso Charuri pelos ensinamentos que mudaram o meu Ser e me fizeram enxergar esse processo como um verdadeiro presente de Vida.

A todos os meus Amigos de Vida, em especial, Gustavo Belchior e Heloisa Nogueira pelo apoio, carinho e pela Amizade em momentos tão importantes durante meu caminhar. E à minha querida Amiga Giovana Furquim, sua Amizade e carinho tornaram os meus dias mais leves e felizes durante a reta final dessa jornada.

Aos meus bons e velhos amigos, Aline, Clara, Júlia e Yuri pelos fortes abraços em cada retorno a Bahia e por vibrarem comigo em cada passo meu.

Aos colegas e amigos do laboratório, Márcia, Bianca, Litiele, Luiz, Gustavo, Carol, Laura Mortara, Peter, Lorena, Mikaela, Greice, Laura Farkuh, Filipe, Cheila e Isaac pelas discussões científicas, ajudas experimentais, pelos momentos de descontração e por tornarem o ambiente tão leve. E em especial à amiga Amanda, pela amizade, almoços filosóficos e pelo seu jeito de pensar que nos faz tão parecidas.

À minha querida labmate and roommate Beatriz, ela que foi minha aluna de iniciação científica e que já brilha no doutorado. Obrigada por topar cada ideia experimental proposta. Seu carinho e cuidado foram fundamentais na reta final desse processo.

A todos do grupo *Center Free Radical Research* e em especial, Mark Hampton, Christine Winterbourn, Nick, Jefry, Martina, Nina, Louisa, Bee, Lisa, Louise, Lorna, Cidra e Tess pelo acolhimento e ensinamentos científicos durante meu período na Nova Zelândia.

Aos colegas do laboratório de lipídeos, Alex e Larissa por me auxiliarem em qualquer necessidade. Em especial, à Professora Sayuri, Marcos e Adriano pela amizade e ensinamentos de espectrometria de massas, os quais foram fundamentais para o desenvolvimento desse trabalho.

À Professora Iolanda Cuccovia pelo carinho e conhecimentos transmitidos diariamente.

À Professora Graziella Rosein pelos seus ensinamentos de proteômica.

Ao Professor Humberto Reis pela oportunidade que me foi dada de conhecer o Instituto de Química ainda durante minha graduação.

Ao Vanderson Bispo pela amizade e por ter me apresentado a Prof^a Flávia Meotti.

A todos os colegas e pacientes pelas amostras de sangue cedidas em prol do desenvolvimento desse estudo.

Aos técnicos do Instituto de Química Berê, Celinha, Fernanda, Edilaine, Janaína e Fernando por sempre me auxiliarem em qualquer necessidade.

As agências de fomento a pesquisa CAPES, CNPq e especialmente a FAPESP (2015/21563-8) e CEPID-Redoxoma pelo apoio financeiro.

A todos vocês, muito obrigada!

A razão de existência é o exercício da função útil no ponto em que o meio precisa. Aí se plenificará. Ao reconhecer-se útil, você está no encadeamento lógico das coisas...

The reason for existing is the exercise of the function of Usefulness, at the point that the environment needs it. Then, one achieves plenitude. In recognizing yourself as useful, you are in the logical chain of things...

Dr. Celso Charuri

RESUMO

Silva, R.P. **Investigação do Metabolismo Oxidativo do Ácido Úrico e seu Papel sobre Processos Redox na Inflamação**. 2020. 157p – Tese – Programa de Pós-Graduação em Ciências Biológicas (Bioquímica). Instituto de Química – Universidade de São Paulo – São Paulo.

Essa tese estuda a oxidação do ácido úrico durante a inflamação e o seu papel em patologias associadas ao ácido úrico. O ácido úrico é o produto final do metabolismo de purinas em humanos e primatas. Sua concentração no plasma é mais elevada do que em outros mamíferos, devido à repressão do gene da enzima que o decompõe, a uricase. Essa repressão foi considerada uma vantagem evolutiva, devido ao caráter antioxidante do ácido úrico. Por outro lado, níveis aumentados de ácido úrico no plasma têm sido associados à hipertensão, gota, aterosclerose e um pior prognóstico em doenças infecciosas. Embora a patogênese destas doenças seja extremamente complexa e pouco compreendida, estas associações sugerem um papel causal do ácido úrico nestas patologias. Entretanto, o exato mecanismo do papel do ácido úrico nessas patologias ainda não está bem esclarecido. Nosso grupo já havia demonstrado que o ácido úrico é um substrato para a mieloperoxidase, uma heme peroxidase abundante em neutrófilos, e que a combinação do produto desta oxidação, o radical livre de urato, com o radical ânion superóxido gera o oxidante hidroperóxido de urato. Uma vez que o cloreto é o principal substrato à mieloperoxidase, um dos objetivos desta tese foi investigar se a formação do hidroperóxido de urato ocorreria mediante o *burst* oxidativo de neutrófilos, uma condição onde há vários substratos para a enzima e mais próxima ao fisiológico. Nesse sentido, através de um método sensível de cromatografia líquida acoplada à espectrometria de massas, nós demonstramos que mediante a ativação de neutrófilos de sangue periférico, mimetizando um estímulo inflamatório, há formação do hidroperóxido de urato, comprovando de forma inédita a formação deste oxidante na inflamação. A presença do ácido úrico durante o *burst* oxidativo inflamatório aumentou a oxidação da glutatona e a produção do radical

ânion superóxido, ocasionando um ambiente celular mais oxidativo. Além do hidroperóxido de urato, a oxidação do ácido úrico gera outros intermediários capazes de formar adutos covalentes em resíduos de lisina da albumina. Nesta tese quantificou-se, através de espectrometria de massas, os níveis destes adutos em plasma, verificando-se um aumento bastante significativo, juntamente com o produto final da oxidação do ácido úrico, a alantoína, em plasmas de paciente com insuficiência cardíaca e diabetes. A formação destes adutos pode modificar a função da albumina e estar relacionada à patologia vascular nestes pacientes. Além disso, os peptídeos uratilados da albumina tem potencial uso como biomarcadores nestas doenças inflamatórias. A oxidação do ácido úrico pelos neutrófilos diminui a produção de ácido hipocloroso devido à competição entre o ácido úrico e o cloreto pela mieloperoxidase e isso atenua a atividade microbica dessas células contra *Pseudomonas aeruginosa*, como demonstrou um trabalho do nosso grupo. No presente trabalho, nós demonstramos que a oxidação do ácido úrico também está mais acentuada em pacientes com septicemia. Quando comparado aos indivíduos saudáveis houve um aumento significativo nos níveis plasmáticos de alantoína e de um peptídeo uratilado da albumina. A infecção de neutrófilos isolados de sangue periférico com *Pseudomonas aeruginosa* na presença de ácido úrico levou a um aumento nos níveis de alantoína, oxidação da glutatona e glutatilação de proteínas com função microbica como a calprotectina (S100A8). O ácido úrico também induziu um aumento de triacilgliceróis (TAGs) em neutrófilos, incluindo TAGs esterificados ao ácido araquidônico. Desta forma, concluímos que, em processos infecciosos, o ácido úrico afeta de forma diferencial a função de algumas proteínas, através da indução da glutatilação e pode remodelar a constituição lipídica de células inflamatórias. É possível que estas alterações tenham um papel relevante na patogênese da doença infecciosa e poderiam explicar, pelo menos em parte, o pior prognóstico encontrado entre os níveis plasmáticos de ácido úrico na sepse. Neste sentido, a medida dos níveis de alantoína e peptídeos uratilados da albumina

podem ser uma ferramenta útil no monitoramento da progressão de doenças infecciosas e inflamatórias.

Palavras-chaves: Ácido úrico, Hidroperóxido de urato, Mieloperoxidase, Inflamação, Infecção, *Pseudomonas aeruginosa*.

ABSTRACT

Silva, R.P. **Investigation of Oxidative Metabolism of Uric Acid and its Role in Redox Processes in Inflammation. 2020. 157p.** PhD Thesis – Graduate Program in Biochemistry. Instituto de Química – Universidade de São Paulo – São Paulo.

This thesis studied the oxidation of uric acid during inflammation and its role in uric acid associated-pathologies. Uric acid is the end product of purine metabolism in humans and primates. Its concentration in plasma is higher than in other mammals, due to the repression of uricase gene. This repression was considered an evolutionary advantage since accumulation of uric acid in plasma increases the total blood antioxidant capacity. On the other hand, increased plasma uric acid has been associated with hypertension, gout, atherosclerosis and a worse prognosis in infection. Although the pathogenesis of these diseases is extremely complex and poorly understood, these associations suggest a causal role for uric acid. However, the exact mechanism for it is still unclear. Our group showed recently that uric acid is a substrate for myeloperoxidase, a heme-peroxidase abundant in neutrophils. The oxidation of uric acid by the enzyme generates urate free radical that combines with the radical anion superoxide to generate the oxidant urate hydroperoxide. Since chloride is the main substrate for myeloperoxidase, the present study aimed to investigate whether urate hydroperoxide would be formed during the oxidative burst in neutrophils. Through the sensitive liquid chromatography coupled to mass spectrometry method, we demonstrated the formation of urate hydroperoxide by peripheral blood neutrophils activated with phorbol myristate acetate, mimicking an inflammatory stimulus. Thus, we confirmed our hypothesis and demonstrated, for the first time, the formation of this new oxidant in inflammation. The presence of uric acid during the inflammatory oxidative burst increased the oxidation of glutathione and the production of the radical anion superoxide, promoting a more oxidative environment. Besides the urate hydroperoxide, the oxidation of uric acid generates other intermediates that react

with lysine residues to form covalent adducts in albumin, a process named uratylation. These urate covalent adducts, as well as the end product of uric acid oxidation, allantoin, were elevated in plasma albumin from patients with heart failure and diabetes. Therefore, allantoin and uratylated peptides from albumin could be useful biomarkers of inflammatory and cardiovascular diseases. The oxidation of uric acid by neutrophils decreases the production of hypochlorous acid due to the competition between uric acid and chloride by myeloperoxidase and this hinders the microbicide activity of these cells against *Pseudomonas aeruginosa*, as previously demonstrated by our group. In the present study we demonstrated that the oxidation of uric acid is also more pronounced in patients with septicaemia. There was a significant augment of plasma allantoin and an uratylated peptide from albumin in these patients compared to health individuals. By incubating peripheral blood neutrophils with uric acid and *Pseudomonas aeruginosa* we detected an increase in allantoin, in the oxidation of glutathione and glutathionylation of the microbicide protein calprotectin (S100A8). Uric acid also increased total neutrophil triacylglycerols (TAGs), including those esterified with arachidonic acid. These data suggest that, in infectious processes, uric acid may indirectly affect protein function through the induction of glutathionylation and can also remodel lipid constitution in inflammatory cells. These alterations may have a relevant role in the pathogenesis of sepsis and could explain, at least in part, the worse correlation between sepsis and higher levels of plasma uric acid. In this context, we propose the assessment of allantoin and uratylated albumin peptides as useful tools to monitor the progression of infectious and inflammatory diseases.

Keywords: Uric acid, Urate hydroperoxide, Myeloperoxidase, Inflammation, Infection, *Pseudomonas aeruginosa*.

LIST OF ABBREVIATIONS

ACN	Acetonitrile
BIOGEE	Glutathione ethyl ester, biotin amide
CVD	Cardiovascular diseases
DAGs	Diacylglycerols
DTNB	5,5-dithiobis (2-nitrobenzoic acid)
DTPA	Diethylenetriamine penta acetic acid
DTT	Dithiothreitol
FOX	Ferrous Oxidation Xylenol Orange
FBS	Fetal bovine serum
GAPDH	Glyceraldehyde-3-phosphate dehydrogenase
GSH	Reduced glutathione
GSSG	Oxidized glutathione
HOOU	Urate hydroperoxide
HOU	Hydroxyisourate
HX	Hypoxanthine
HSA	Human serum albumin
HL-60	Human promyelocytic leukemia cell line
HOCl	Hypochlorous acid
HPLC	High performance liquid chromatogram
IAM	Iodoacetamide
MS	Mass spectrometry
MPO	Myeloperoxidase
NAC	N-acetylcysteine
NADPH	Nicotinamide adenine dinucleotide phosphate
NEUT	Neutrophils cells

NOX	Nicotinamide adenine dinucleotide phosphate oxidase
PA14	<i>Pseudomonas aeruginosa</i> strain 14
PMA	Phorbol 12-myristate 13-acetate
PRX	Peroxiredoxin
PBS	Phosphate buffer saline
SDS	Sodium dodecyl sulfate
SOD	Superoxide dismutase
TIC	Total ion chromatogram
TAGs	Triacylglycerols
XO	Xanthine Oxidase
UA	Uric acid
UrOOH	Urate hydroperoxide
UrOH	Hydroxyisourate
K	Lysine

Summary

1. Introduction	19
1.1 Uric acid metabolism	19
1.2 Uric acid, inflammation, and associated-pathologies	24
1.3 Oxidative metabolism of uric acid: the anti and pro-oxidant paradox	31
Chapter 1	36
Abstract	37
1. Introduction	37
2. Experimental section	38
2.1 Oxygen consumption, Assessment of superoxide and Hypochlorous acid production	38
2.2 Detection of urate hydroperoxide and hydroxyisourate	24
2.3 Quantification of hydroxyisourate, GSH and GSSG.....	39
2.4. Statistical analysis	39
3.Results	40
4.Discussion.....	42
5.Conclusion	44
Chapter 2	47
Abstract	49
1.Introduction	49
2. Experimental section	52
2.1 Quantification of urate hydroperoxide by FOX	52
2.2 Detection of urate-derived adducts on human serum albumin	53
2.3 Quantification of urate-derived adducts	54
2.4 Formation of uratylated peptides by the products of uric acid photo-oxidation	54
2.5 Quantification of urate-derived adducts on serum albumin from patients	56
2.6 Quantification of myeloperoxidase and allantoin	57
2.7 Statistical Analysis	57
3. Results	59
3.1 Oxidation of urate by enzymatic system and by photo-oxidation	59
3.2 Urate-derived intermediates from myeloperoxidase catalysed reaction modify lysine residues in human serum albumin	61
3.3 Fragmentation pattern and multiple reaction monitoring of the uratylated peptides	63
3.4 Quantification of uratylation using different oxidation systems	63
3.5 Uratylation of albumin is elevated in plasma of patients with heart failure and diabetes	71

3.6 Uratylation is associated with heart failure and death	75
4. Discussion	83
5. Conclusion	86
6. Material Supplementary	90
Chapter 3.....	94
Abstract	96
1. Introduction	97
2. Experimental section	99
2.1 Clinical samples	99
2.2 Bacterial cell culture	100
2.3 Quantification of allantoin in plasma	100
2.4 Quantification of urate-derived adducts on human serum albumin in patients with sepsis	101
2.5 Quantification of allantoin in neutrophils infected with <i>Pseudomonas aeruginosa</i> (PA14)	102
2.6 Quantification of 2-hydroxiethidium (2-OH-E ⁺)	103
2.7 Quantification of glutathione reduced (GSH) and oxidized (GSSG)	104
2.8 Oxidation of Peroxiredoxin 1	105
2.9 Proteomic analysis	106
2.10 Lipidomic of neutrophils	108
2.11 Statistical analysis	110
3. Results	110
3.1 Allantoin is elevated in plasma of septic patients and in neutrophils infected with bacterial ..	110
3.2 Urate-derived adducts are elevated in plasma albumin from septic patients	112
3.3 Effect of uric acid on superoxide production	115
3.4 Effect of uric acid on glutathione oxidation	117
3.5 Effect of uric acid on the oxidation of Peroxiredoxin 1	119
3.6 Effect of uric acid on protein glutathionylation	120
3.7 Effect of uric acid on the lipid profile	123
4. Discussion	126
5. Conclusion	131
6. Material Supplementary	136
3. Final Remarks	145
4. References	146
5. Curriculum vitae	153

1. INTRODUCTION

1.1. Uric acid metabolism

Uric acid (UA; 7,9-Dihydro-1H-purine-2,6,8(3H)-trione) is an heterocyclic organic compound and a final product of purine metabolism in humans and great apes. It is a weak organic acid with a pK_{a1} of 5.4 being present principally (~99%) as monosodium urate at physiological pH. Normal uric acid levels in serum are around 2.6–6 mg/dL (155–339 μ M) in premenopausal women and 3.5–7.0 mg/dL (208–416 μ M) in men and postmenopausal women (Desideri et al. 2014).

In humans, uric acid is formed by the catabolism of purine nucleotides from endogenous nucleic acid, adenosine triphosphate (ATP) and their derivatives or exogenous purines from dietary sources (Ndrepepa 2019). After phosphorolysis and deamination of the nucleosides adenosine and guanosine, the xanthine/hypoxanthine products are oxidized to uric acid by xanthine oxidoreductase catalysis (**Figure 1**). Xanthine oxidoreductase (XOR) acts as a dehydrogenase (XDH) (xanthine dehydrogenase; EC 1.17.1.4) when the final electron acceptor is nicotinamide adenine dinucleotide (NAD^+). Structural changes in this enzyme, as the reversible oxidation of sulfhydryl groups or irreversible proteolysis in specific sites, converts it into an oxidase (XO, xanthine oxidase; EC 1.17.3.2) that uses oxygen as final electron acceptor to generate superoxide (Kuwabara et al. 2003; Doehner and Landmesser 2011; Harris and Massey 1997). The conversion of XHD to XO occurs predominantly in conditions with a low O_2 tension and acidic pH, including hypoxia, ischemia, glutathione depletion and increase of oxidants such as hydrogen peroxide (Battelli, Polito, and Bolognesi 2014; Saksela, Lapatto, and Raivio 1999; Cantu-Medellin and Kelley 2013). XO is one important source of superoxide, and consequently, hydrogen peroxide. Thus, the imbalance towards a pro-oxidant environment

increases the production of the radical anion superoxide and hydrogen peroxide along with the oxidation of xanthine/hypoxanthine to uric acid by XO (Kuwabara et al. 2003).

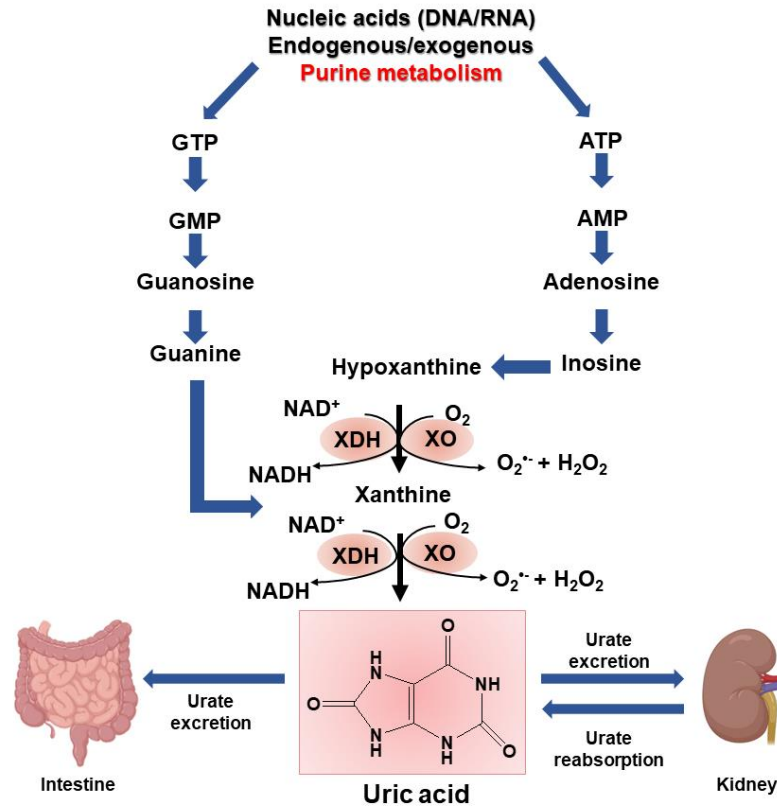


Figure 1. Synthesis, excretion and reabsorption of uric acid. Purines can be absorbed from the diet, synthesized from amino acids or derived from the degradation of endogenous DNA and RNA. They are further oxidized by xanthine oxidase/xanthine dehydrogenase to produce uric acid in humans. The majority of uric acid is excreted by the kidney and the remaining by the intestine, although a substantial amount of uric acid is reabsorbed at the proximal tubule of the kidney. AMP: adenosine monophosphate; ATP: adenosine triphosphate; GMP: guanosine monophosphate; GTP: guanosine triphosphate; NAD⁺: nicotinamide adenine dinucleotide; XO: xanthine oxidase; XDH: xanthine dehydrogenase.

Uric acid does not move freely across the cellular membranes and, therefore, depends on specific transporters for its homeostasis. It involves a complex array of reabsorptive and secretory mechanisms in the kidney and gut (Mandal and Mount 2015). Approximately 90–

95% of the uric acid that is filtered in the kidney is re-absorbed in the proximal tubule. The small portion that is excreted occurs at 70% by the kidneys and 30% through the gastrointestinal system (Richette and Bardin 2010).

Uric acid transporters, such as the organic anion transporters OAT4, OAT10 and the OAT-mimetic, URAT1, are localized in the apical membrane of the epithelial cells in the kidney, being important for reabsorption of urate (Mandal and Mount 2015). This reabsorption occurs through counter-transport with mono or divalent anions, generally organic acids, that are reabsorbed in a co-transport with sodium (**Figure 2A**). The passage of urate through the basolateral membrane occurs by a member of the glucose transporter family (GLUT9) (**Figure 2A**) (Mandal and Mount 2015).

For the excretion, the transport across the basolateral membrane occurs through a counter-transport with alpha-ketoglutarate using OAT1 and OAT3 or with other anions not yet identified by OAT2. The passage through the apical membrane happens through MRP4, ABCG2, NPT1, and NPT4 (**Figure 2B**) (So and Thorens 2010; Hediger et al. 2005). Thus, uric acid homeostasis in humans depends on the balance between ingestion/degradation of purines, renal reabsorption, and renal/intestinal excretion. Genome-wide association studies (GWAS) showed that variants in the loci that contain the genes for the transporters ABCG2, URAT1, OAT4, and GLUT9 are associated with increased levels of uric acid, the most strongly associated is GLUT9 (Mandal and Mount 2015; So and Thorens 2010).

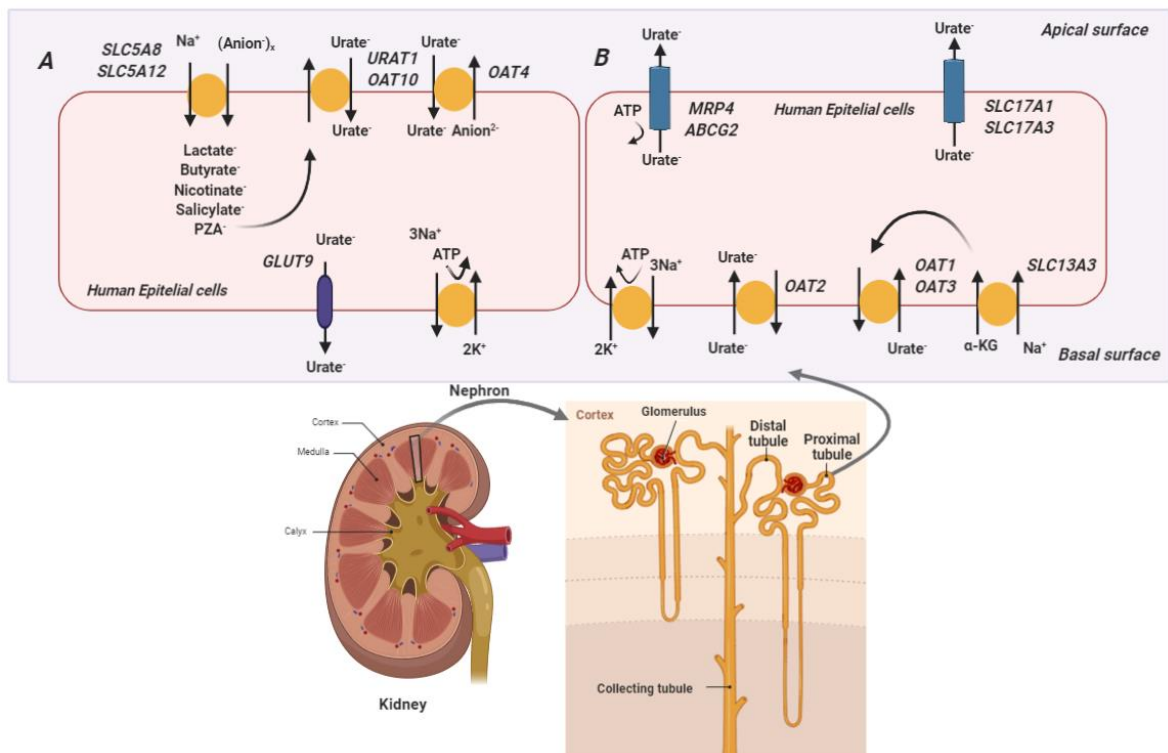


Figure 2. Urate transporters in cells of the proximal tubule. (A) Urate reabsorption. The transport of sodium through the anion dependent transporters SLC5A8 and SLC5A12 leads to the intracellular increase of organic anions that exchange with luminal urate through URAT1/OAT10. Urate also exchanges with divalent anions by OAT4. GLUT9 acts as the epithelial cell efflux of urate, completing the reabsorption. (B) Urate secretion. Urate enters in the cell at the basolateral membrane in exchange with α -ketoglutarate (α -KG), mediated by OAT1 and OAT3, or in exchange with unknown anions via OAT2; urate is secreted via MRP4, ABCG2, NPT1, and/or NPT4 at the apical membrane. PZA: pyrazinoate; GLUT9: glucose transporter 9; GMP: guanosine monophosphate; MRP4=multidrug resistance protein 4; OAT=organic anion transporter; URAT=urate transporter; SLC5A8 solute carrier family 5 member 8; SLC5A12 solute carrier family 5 member 12. Figure adapted from Mandal et al, 2015 (Mandal and Mount 2015).

In most mammals, uric acid is degraded to allantoin by uricase enzyme. Allantoin is more water-soluble than uric acid and hence, more promptly excreted than uric acid (Johnson et al. 2009; Desideri et al. 2014; Chen, Lü, and Yao 2016). However, in human and higher primates, the purine metabolism ends with uric acid due to the absence of uricase. The loss of uricase activity occurred due to mutations in the coding region of uricase gene. Point mutations in the promoter region has also been identified as the cause of a lower affinity of transcription factors

and a consequent loss of gene transcription (Oda et al. 2002; Wu et al. 1989). A series of evolutionary advantages has been related with the silencing of uricase. For example, accumulation of uric acid in plasma was associated with the ability to maintain the blood pressure adequate to postural evolution during lower salt intake due to scarcity of food in the Miocene Period (Cenozoic Era) (Wu et al. 1989; Johnson and Rideout 2004). Higher levels of uric acid have also been related to upper intelligence (Orowan 1955; Sofaer and Emery 1981; Watanabe et al. 2002). Another hypothesis is due to the antioxidant properties of uric acid. The accumulation of uric acid would compensate for the loss of ascorbate (vitamin C) biosynthesis due to the mutation of the L-gulonolactone synthase enzyme. The mutation of L-gulonolactone synthase (~ 55 - 24 million years) preceded uricase mutations (~ 23 - 5 million years) (Proctor 1970; Ames et al. 1981). Therefore, uric acid would provide the antioxidant capacity of plasma that was compromised by the deficiency in ascorbate synthesis (Ames et al. 1981; Johnson et al. 2008). This has been discussed as a key event to the survival of our ancestors during the climate changes in the mid-Miocene.

In spite of the evolutive advantages hypothesized for the accumulation of uric acid in humans, an imbalance in urate homeostasis and hyperuricemia is associated with several diseases and suggests deleterious effects due to high concentrations of urate in the circulation (So and Thorens 2010). A decrease in renal excretion is responsible for hyperuricemia in 90% of individuals (Terkeltaub, Bushinsky, and Becker 2006; Terkeltaub 2003; Ichida et al. 2012). Furthermore, purine rich and alcohol dietary, genetic and disease, such as myeloproliferative disorders and hemolytic anaemia, are associated with enhanced uric acid production and may contribute to hyperuricemia (Terkeltaub, Bushinsky, and Becker 2006; Richette and Bardin 2010; Terkeltaub 2003).

Changes in the activity of enzymes from purine metabolism pathway are also a factor for hyperuricemia. The deficiency of hypoxanthine-guanine phosphoribosyl transferase (HGPRT)

from the purine salvage pathway, an innate error in the metabolism responsible for Lesch-Nyhan syndrome, is associated with increased levels of uric acid. In the *denovo* purine synthesis, the increased activity of 5-phosphoribosyl-1-pyrophosphate (PRPP) synthetase, responsible for the first step of the pathway and the increase in total ATP degradation are associated with hyperuricemia and gout (Mandal and Mount 2015; Ahmed et al. 1999).

Hyperuricemia has been described as a risk factor for gout since the mid-20th century along with an increase in hyperuricemia incidence. Some potential explanations for these findings include lifestyle changes and increased life expectancy (So and Thorens 2010).

1.2. Uric acid, inflammation, and associated-pathologies

Beside the protective effect attributed to the increase of plasma antioxidant capacity by uric acid (Ames et al. 1981), some studies have shown that a low concentration of uric acid is detrimental in neurodegenerative diseases, whereas a high concentration is neuroprotective against Parkinson disease, multiple sclerosis, Alzheimer disease and amyotrophic lateral sclerosis (Álvarez-Lario and Macarrón-Vicente 2010; Drulović et al. 2001; Schwarzschild et al. 2008; Kutzing and Firestein 2008). Despite these evidences, accumulation of uric acid exacerbates inflammation and is associated with gout, hypertension, kidney disease, and atherosclerosis (Feig, Kang, and Johnson 2008; Lotufo et al. 2015; Gur et al. 2013; Gur et al. 2008).

The association between uric acid and cardiovascular diseases or mortality has been extensively investigated (Li et al. 2016). Some studies have demonstrated that uric acid is strongly and independently correlated with cardiovascular events, mortality or stroke (Meisinger et al. 2008; Niskanen et al. 2004; Bos et al. 2006). Other investigations showed that the increase of uric acid is correlated with diastolic and endothelial dysfunction (Krishnan et al.

2012; Cicoira et al. 2002), impaired oxidative metabolism and decreased in oxygen consumption (Leyva et al. 1997). Despite these evidences, other studies failed to demonstrate an independent association between high uric acid levels and cardiovascular events (Culleton et al. 1999; Wheeler et al. 2005). Thus, the question whether the hyperuricemia is an independent risk factor with a causal component, or simply a circumstantial event in cardiovascular disease remains to be answered. To better understand this matter, it is necessary to investigate the role of uric acid in vascular pathologies, evaluating a possible causal effect of this metabolite in the vascular injury.

In this context, studies in cells and animals point to a causal role of uric acid in vascular pathologies because it increases the activation of circulating platelets (Mustard et al. 1963), decreases the availability of nitric oxide (Khosla et al. 2005), increases the activity of the renin-angiotensin system and induces proliferation and migration of arterial smooth muscle cells (Kanellis et al. 2003; Corry et al. 2008). Besides, an elegant study demonstrated that uric acid can induce chemokine (C-C motif) ligand 2, CCL2, formation in vascular smooth muscle cells, and this can explain the elevated CCL2 production found in hyperuricemia with implications in cardiovascular disease (Grainger et al. 2013; Kanellis et al. 2003; Kang et al. 2005). High levels of uric acid and CCL2 increase circulating CD14⁺ monocytes, even in absence of site inflammation and thus, the priming of monocytes induces a faster response to inflammatory stimulus (Rollins 1996; Serbina and Pamer 2006; Matsukawa et al. 1998). This effect can facilitate the production of pro-inflammatory cytokines and amplify inflammation (Crişan et al. 2016; Davis, Wen, and Ting 2011). Despite these evidences, the exact mechanism on how soluble uric acid activates inflammatory cells is still unknown.

The inflammation is an underlying event in several diseases. In physiological situations, inflammatory response halts as soon as the invader microorganism or the initial stimuli are swept from the system and so, homeostasis is re-established. However, inflammation becomes

a pathological event when its resolution is compromised. The basic mechanisms that perpetuate inflammation can vary and they are not fully understood so far.

During infection the specialised white blood cells neutrophils are recruited to phagocyte and kill pathogens (Winterbourn, Kettle, and Hampton 2016). The initial recruitment occurs by the release of chemoattractants produced by resident immune cells, such as macrophages, dendritic and endothelial cells (Nathan 2006; Rigby and DeLeo 2012). These signals act directing neutrophils through a chemotactic movement from circulation to the damaged or infected site (**Figure 3**) (Rigby and DeLeo 2012).

Neutrophils trigger a potent oxidative and non-oxidative response against the invader (Nathan 2006). The oxidative mechanism is initiated by the activation of the NADPH oxidase complex with formation of superoxide anion radical (**Figure 3**) (Bylund et al. 2010). NADPH oxidase can be activated by sterile stimuli independent of phagosome formation. The phorbol myristate acetate (PMA) is a classical activator of NADPH oxidase because it binds and activates protein kinase C, as does diacylglycerol (Lundqvist et al. 1996). The dismutation of superoxide to hydrogen peroxide provides the substrate for myeloperoxidase, an abundant heme-peroxidase in neutrophils. Myeloperoxidase constitutes approximately 5% of total protein in these cells (Winterbourn, Kettle, and Hampton 2016). (Kettle and Winterbourn 1997).

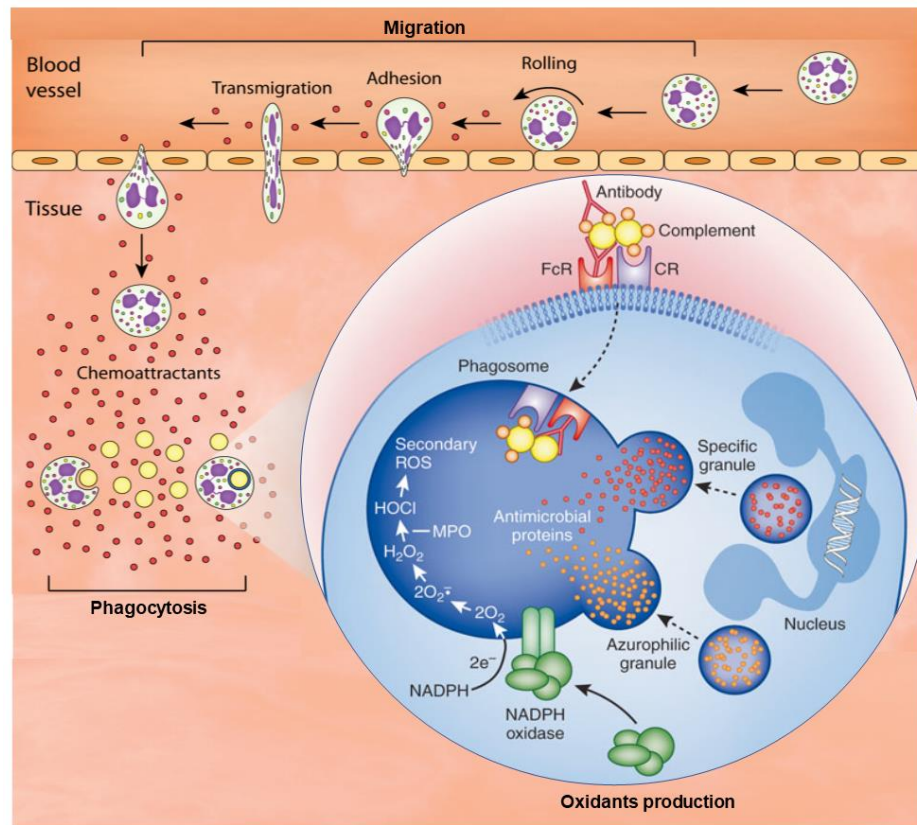


Figure 3. Neutrophil migration to the site of infection leading to phagocytosis and oxidants production. In the presence of invading microorganisms, chemotactic molecules are released recruiting neutrophils to the site of injury or infection. Endothelial cells are activated and facilitate neutrophils rolling along the endothelium to the inflamed tissue. Neutrophils recognize the invading pathogens through a range of surface receptors and thus, the phagocytosis process follows. When the phagosome is formed in the activated neutrophil, the NADPH oxidase is activated to produce superoxide. Superoxide dismutates spontaneously or by catalysis of the superoxide dismutase to hydrogen peroxide. The latter is a substrate for myeloperoxidase along with chloride to form hypochlorous acid, the main microbicide oxidant. Antimicrobial proteins are released upon granule fusion with the phagosome (degranulation) that also contribute to the killing of microbes. CR complement, receptor, FcR Fc receptor, MPO myeloperoxidase. Figure adapted from Rigny et al 2012 (Rigby and DeLeo 2012).

The reaction of hydrogen peroxide with myeloperoxidase triggers the oxidation of a wide range of substrates to reactive products, which include nonradical oxidants and radicals generated from organic (Meotti et al. 2011; Ximenes et al. 2010; Marquez and Dunford 1995; Marquez, Dunford, and Van Wart 1990; Allegra et al. 2001) and inorganic substrates (**Figure 4**) (Abu-Soud and Hazen 2000; Burner et al. 2000; Kettle et al. 2007; Winterbourn 2016; Meotti

et al. 2011). Briefly, the ferric form of myeloperoxidase (Fe^{III}) reacts with hydrogen peroxide to form an oxyferril radical ($\text{Fe}^{\text{IV}}\text{O}\dots\text{Por}^{\bullet}$). This intermediary denominated Compound I can react with chloride to yield hypochlorous acid (HOCl) and regenerate the ferric form (Fe^{III}) of the enzyme. Alternatively, Compound I can react with other substrates, abstracting one electron, to form the intermediate Compound II ($\text{Fe}^{\text{IV}}\text{O}$). Compound II abstracts a second electron from a second substrate to regenerate the ferric form (Fe^{III}) of the enzyme. The first mechanism, with HOCl formation, is called chlorinating activity, while the second mechanism is called peroxidase activity (Davies 2011; Kettle and Winterbourn 1997; Winterbourn 2016). A scheme of these mechanisms is presented in the **Figure 4**. Endogenous substrates for myeloperoxidase include iodide, thiocyanate, bromide, nitrite, superoxide (Kettle et al. 2007; van Dalen et al. 1997; van der Vliet et al. 1997) ascorbate, serotonin, tyrosine, (Ximenes et al. 2010; Marquez and Dunford 1995; Marquez, Dunford, and Van Wart 1990) and uric acid (Meotti et al. 2011). Uric acid is oxidized by Compound I and Compound II producing urate free radical with rate constants of $4.6 \times 10^5 \text{ M}^{-1}\text{s}^{-1}$ and $1.7 \times 10^4 \text{ M}^{-1}\text{s}^{-1}$, respectively (Meotti et al. 2011). These rate constants are similar to those calculated for the oxidation of ascorbate, tyrosine, and serotonin (Marquez and Dunford 1995; Marquez, Dunford, and Van Wart 1990; Ximenes et al. 2010). However, uric acid is the most abundant organic substrate in plasma and biological fluids (Becker 1993). Hence, it can be considered a relevant substrate for the enzyme. In the inflammatory environment, where there is plenty of superoxide both, urate free radical and superoxide can combine to form the oxidant urate hydroperoxide (Meotti et al. 2011; Silva et al. 2018). The formation of urate hydroperoxide would reveal a new reported oxidant in inflammation. However, the detection of this oxidant in cells and biological fluids is challenging regarding the high reactivity of the molecule. To identify whether urate hydroperoxide would be a relevant product in the neutrophil oxidative burst, the **first goal** of the thesis was to detect it using mass spectrometry and to evaluate its effects in these cells.

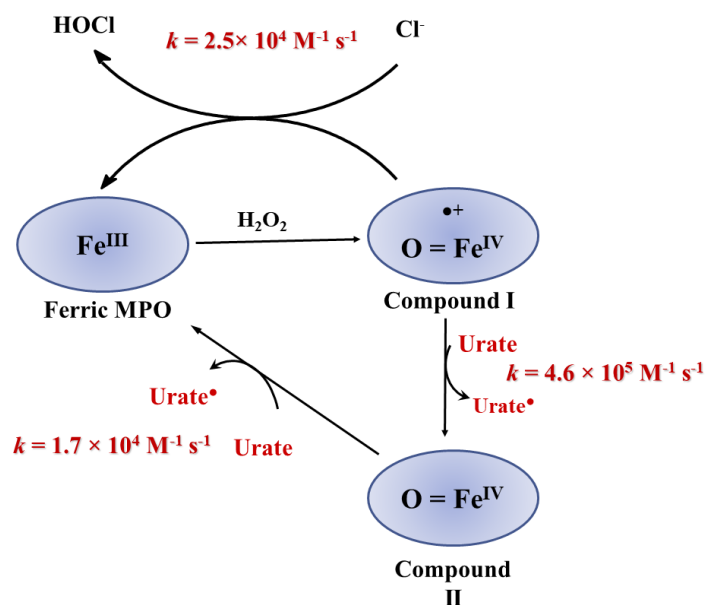


Figure 4. Scheme of myeloperoxidase catalytic cycle. Native ferric MPO reacts with hydrogen peroxide (H₂O₂) to form Compound I. Chloride (Cl⁻) is oxidized to form hypochlorous acid (halogenation cycle) regenerating the native ferric MPO. Alternatively, Compounds I and II oxidize urate by abstraction of a single electron to form urate free radical (Urate•) in the peroxidatic cycle. The redox states of the heme iron are shown as described in several studies (Winterbourn, Kettle, and Hampton 2016; Kettle and Winterbourn 1997; Winterbourn and Kettle 2013).

Considering that uric acid and myeloperoxidase are associated with cardiovascular disease (Anatoliotakis et al. 2013; Cameron et al. 2006; Johnson et al. 2018; Johnson and Rideout 2004) it is plausible that the reaction and generation of highly reactive intermediates, arising from the oxidation of uric acid, could be the responsible by endothelial dysfunction, maintenance of inflammation and vascular tissue damage. This would explain, at least in part, the association between uric acid and cardiovascular disease (Mineiro et al. 2020). Therefore, the **second goal** of this thesis was to evaluate whether the oxidation of uric acid would be more pronounced in patients suffering from heart failure and would predict death events. As described in the second manuscript, the reaction of the intermediates generated from uric acid oxidation with albumin was evaluated. Since albumin is the most abundant protein in plasma, covalent modifications

in this protein can be an useful biomarker in cardiovascular disease. Such permanent modifications are also important to assess how harmful an oxidant can be.

Soluble uric acid has long being recognized as a DAMP (damage-associated molecular pattern), i.e. a danger signal recognized by innate immune cells that induces the production of cytokines, the priming and activation of inflammatory cells (Medzhitov and Janeway 2000; Crisan et al. 2015; Crişan et al. 2017; Patel 2018; Shi, Evans, and Rock 2003). However, no binding of a specific receptor has been demonstrated for uric acid. What we know so far are the effects of uric acid upon inflammation but not the exact mechanisms behind these effects. Soluble uric acid activates the inflammasome pathway (Braga et al. 2017), sensitizes immune cells potentiating the effect of Toll-like receptor ligands (Crisan et al. 2015), induces the expression of chemokine MCP-1 (Kanellis et al. 2003), recruits neutrophils (Shi 2010; Kono et al. 2010), increases superoxide production by NADPH oxidase (Thomas 1992; Sautin et al. 2007) and the formation of NETs (neutrophil extracellular traps) (Arai et al. 2014). During necrosis or any other harmful process cells produce more uric acid than in physiological conditions by an increase in purine degradation. The release of intracellular uric acid contributes to inflammation (Shi, Evans, and Rock 2003; Kono et al. 2010). Under infection, uric acid competes with chloride by myeloperoxidase oxidation disrupting hypochlorous acid production and thus, affecting microbicide activity (Carvalho et al. 2018). These evidences corroborate the data showing that uric acid is associated with the progression of sepsis (Akbar et al. 2015; Chuang et al. 2006), a serious medical condition characterized by a systemic inflammatory response, that can progress to multiple organ failure initiated by an infection (Zarjou and Agarwal 2011).

Together clinical and experimental studies support a role for uric acid in inflammatory and infectious processes. However, the correlation between the oxidation of uric acid and sepsis or other infectious diseases has not been investigated so far. Therefore, the **third goal** of this thesis

was to investigate the mechanisms by which uric acid propagates redox imbalance and sustain inflammation in infectious conditions.

1.3. Oxidative metabolism of uric acid: the anti and pro-oxidant paradox

To pursue any putative causal effect of uric acid in inflammatory diseases, it is important to know the reactions that it participates and which one would be preponderant in the biological system. Uric acid is an excellent electron donor (one-electron reduction potential = 0.59 V, pH 7.0, $\text{HU}^{\bullet-}$, H^+/UH_2^-) (Simic and Jovanovic 1989). Studies that investigate the antioxidant properties of uric acid have shown that it chelates transition metals, reacts with oxidants such as hydroxyl radical, nitrogen dioxide radical, carbonate radical, hypochlorous acid, singlet oxygen, ozone and neutralizes free radicals in proteins (Ames et al. 1981; Kaur and Halliwell 1990; Domazou, Zhu, and Koppenol 2012; Becker 1993; Cross et al. 1992; Squadrito et al. 2000; Ford, Hughes, and Wardman 2002; Iida et al. 2017). Uric acid is considered a powerful plasma antioxidant as it comprises approximately half of the total antioxidant capacity in this fluid (Ames et al. 1981; Davies et al. 1986). Taking these evidences into account, animal models and clinical studies suggest that these antioxidant properties could explain the protective effect of uric acid against neurodegenerative disease (Álvarez-Lario and Macarrón-Vicente 2010; Drulović et al. 2001; Schwarzschild et al. 2008; Paganoni and Schwarzschild 2017), as already mentioned.

Despite this apparent beneficial effect, the products of uric acid oxidation are not inert. For example, the reaction of uric acid with peroxynitrite generates the aminocarbonyl radical, responsible for amplifying lipid peroxidation in LDL particles (Santos, Anjos, and Augusto 1999). Interestingly, free radical adducts from the oxidation of uric acid by peroxynitrite were also detected in plasma (Vásquez-Vivar et al. 1996). Other non-radical intermediates produced in the reaction with peroxynitrite alkylated biomolecules, but the real impact of these

alkylations in the biological system needs to be better understood (Gersch et al. 2009). Besides, under aerobic conditions, urate can directly react with nitric oxide (NO) to produce an unstable nitrosated uric acid that transfers NO to other molecules, as glutathione (Suzuki 2007). Studies with enzymes sensitive to oxidation, such as alpha-1-antiproteinase, alcohol dehydrogenase, and glyceraldehyde phosphate dehydrogenase, reveal that reactive intermediates from uric acid oxidation inactivate these enzymes (Aruoma and Halliwell 1989; Kittridge and Willson 1984; Turner et al. 2018).

The paradoxical anti and pro-oxidant role of uric acid is most evident when analyzing its reaction mechanism (**Figure 5**). For example, the two electrons oxidation of uric acid by oxidants, such as hypochlorous acid and singlet oxygen, produces the dehydrourate which is subsequently hydrated to hydroxyisourate (Kaur and Halliwell 1990; Volk, Yost, and Brajter-Toth 1989; Iida et al. 2017). The decomposition the hydroxyisourate follows four reactions until the final product, allantoin (**Figure 5**). The breakdown products from uric acid oxidation can be different depending on the reagents present in the medium. However, allantoin seems to be the predominant end product in biological environment (Gersch et al. 2009; Volk, Yost, and Brajter-Toth 1989). There is no free radicals intermediates in this two-electron oxidation and the main oxidation product, allantoin, is considered inert.

Uric acid can also undergo one electron abstraction in reactions with free radicals, such as hydroxyl radical, and in the oxidation by heme peroxidases (Maples and Mason 1988; Meotti et al. 2011). This oxidation generates urate free radical which reacts with biomolecules in a diffusion-limiting rate. When a high amount of this radical is formed, two of them can dismutate to generate dehydrourate and uric acid. In the presence of ascorbate, urate free radical can abstract one electron from ascorbate regenerating uric acid and forming the ascorbyl radical. The latter dismutates to ascorbate and dehydroascorbate (Halliwell and Gutteridge 2015; Frei, Stocker, and Ames 1988). The abstraction of one electron from other biomolecules by urate

free radical can trigger a free radical chain reaction (**Figure 5**). The one-electron transference from superoxide to the urate radical has been described to occur at $8 \times 10^8 \text{ M}^{-1}\text{s}^{-1}$. (Santus et al. 2001). However, the combination of these radicals with the formation of hydroperoxide is very reasonable. Based on this, we characterized and identified the production of urate hydroperoxide in cells (Patricio et al. 2015; Silva et al. 2018), as we mentioned earlier.

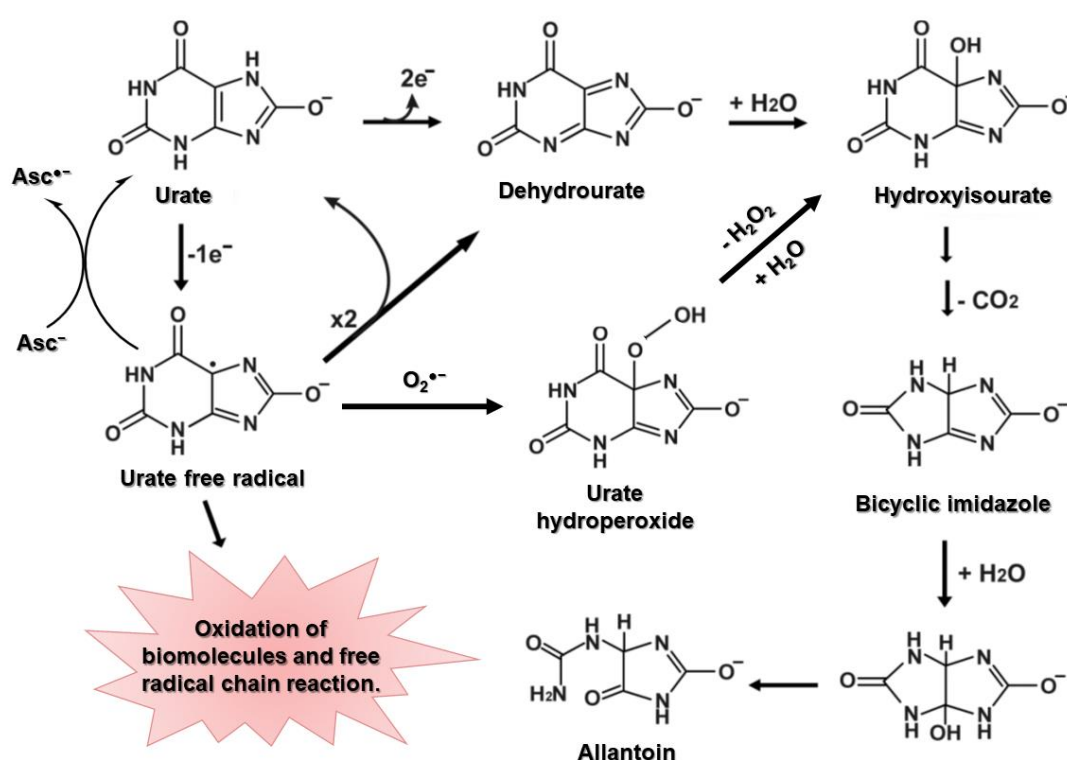


Figure 5. Mechanisms of uric acid oxidation. Oxidation by two electrons generates dehydrourate, which is subsequently hydrated to hydroxyisourate and, after four reactions, it forms allantoin. The one electron oxidation generates urate free radical. Two urate free radicals can dimerize to yield urate and dehydrourate. In the presence of ascorbate, urate free radical can be reduced to urate forming the ascorbyl radical. Alternatively, urate free radical can abstract one electron from other biomolecules triggering a free radical chain reaction or it can combine with superoxide to generate urate hydroperoxide.

Considering that the superoxide anion radical, hydrogen peroxide, myeloperoxidase and uric acid are present in significant amounts in an inflammatory environment, urate hydroperoxide would likely be a relevant product from the inflammatory oxidative burst (Silva et al. 2018). In this context, a study from our group evaluated the reactivity of urate hydroperoxide against biomolecules. In a comparison with different amino acids, urate hydroperoxide reacted specifically with methionine and cysteine but not with histidine, tryptophan, and lysine. It oxidized glutathione (GSH) at a rate constant of $13.7 \text{ M}^{-1}\text{s}^{-1}$, suggesting that it can oxidize GSH in the biological system independently from enzymatic catalysis (Patricio et al. 2015). In spite of that, reactive thiol groups from proteins are likely more prone to oxidation by urate hydroperoxide. In fact, urate hydroperoxide oxidized peroxiredoxin 1 and 2 at rate constants of 4.5×10^5 and $2.6 \times 10^6 \text{ M}^{-1}\text{s}^{-1}$, respectively (Carvalho et al. 2017). Although these values are around two-orders of magnitude lower than the rate constants of the oxidation of these enzymes by hydrogen peroxide (Cox et al. 2009; Manta et al. 2009), they are very high and suggest that these proteins are preferential targets to urate hydroperoxide in the cytosol. Of relevance, peroxiredoxins work as relay proteins in redox signaling because they can transfer their oxidizing equivalents to other thiol proteins and modulate cellular response. In this context, the production of urate hydroperoxide could have an important role in redox signaling in inflammatory process.

Moreover, urate hydroperoxide selectively oxidizes the catalytic cysteine in protein disulfide isomerase (PDI), an oxidoreductase and isomerase involved in platelet activation and aggregation, thrombus formation and vascular remodeling (Cho et al. 2012; Tanaka et al. 2016; Essex 2004). The rate constant for this oxidation is $6 \times 10^3 \text{ M}^{-1}\text{s}^{-1}$, which is much higher than the oxidation of this protein by hydrogen peroxide and glutathione disulfide (Peixoto Á et al. 2018; Mineiro et al. 2020; Ali Khan and Mutus 2014) and slightly lower than by peroxynitrite (Peixoto Á et al. 2018). Therefore, extracellular surface PDI is a putative target to urate

hydroperoxide. The oxidation of this protein by urate hydroperoxide occasioned alterations in endothelial cell adherence, pointing out a possible causal role for this oxidant in vascular disease.

In summary, the inflammatory and oxidative response caused by uric acid indicates that it has complex chemical and biological effects. The oxidation uric acid by hemeperoxidases and the formation of reactive intermediates could be a preponderant event during inflammation and would explain how uric acid causes cell damage and propagates inflammation. Therefore, the **main goal** of this thesis was to investigate the oxidative metabolism of uric acid and its involvement in redox-sensitive mechanisms to better understand the role of uric acid in the progression of inflammation, bringing new insights to a causal role of uric acid in inflammatory-related pathologies.

CHAPTER 1



Contents lists available at ScienceDirect

Free Radical Biology and Medicine

journal homepage: www.elsevier.com/locate/freeradbiomed

Original article

Identification of urate hydroperoxide in neutrophils: A novel pro-oxidant generated in inflammatory conditions

Railmara P. Silva, Larissa A.C. Carvalho, Eliziane S. Patricio, João P.P. Bonifacio, Adriano B. Chaves-Filho, Sayuri Miyamoto, Flavia C. Meotti*

Departamento de Bioquímica, Instituto de Química (IQUSP), Universidade de São Paulo, São Paulo, SP, Brazil

ARTICLE INFO

Keywords

Uric acid
Urate free radical
Urate hydroperoxide
Oxidant
Respiratory burst
Neutrophils

ABSTRACT

Uric acid is the final product of purine metabolism in humans and is considered to be quantitatively the main antioxidant in plasma. *In vitro* studies showed that the oxidation of uric acid by peroxidases, in presence of superoxide, generates urate free radical and urate hydroperoxide. Urate hydroperoxide is a strong oxidant and might be a relevant intermediate in inflammatory conditions. However, the identification of urate hydroperoxide in cells and biological samples has been a challenge due to its high reactivity. By using mass spectrometry, we undoubtedly demonstrated the formation of urate hydroperoxide and its corresponding alcohol, hydroxyisourate during the respiratory burst in peripheral blood neutrophils and in human leukemic cells differentiated in neutrophils (dHL-60). The respiratory burst was induced by phorbol myristate acetate (PMA) and greatly increased oxygen consumption and superoxide production. Both oxygen consumption and superoxide production were further augmented by incubation with uric acid. Conversely, uric acid significantly decreased the levels of HOCl, probably because of the competition with chloride by the catalysis of myeloperoxidase. In spite of the decrease in HOCl, the overall oxidative status, measured by GSH/GSSG ratio, was augmented in the presence of uric acid. In summary, the present results support the formation of urate hydroperoxide, a novel oxidant in neutrophils oxidative burst. Urate hydroperoxide is a strong oxidant and alters the redox balance toward a pro-oxidative environment. The production of urate hydroperoxide in inflammatory conditions could explain, at least in part, the harmful effect associated to uric acid.

1. Introduction

Uric acid is the end product of purine metabolism in humans and higher primates and occurs predominantly as urate mono-anion under physiological pH ($pK_a = 5.4$) [1]. The evolutionary loss of uricase, an enzyme that metabolizes uric acid to the more soluble product allantoin, brought about the accumulation of uric acid in plasma and the ability of these species to maintain the blood pressure whereas standing up during postural evolution [2]. Speculative advantages of the accumulation of uric acid in plasma include antioxidant protection, decreased incidence of cancer, ability to survival under low dietary salt and increased intelligence [3–5]. Uric acid is an excellent electron donor (one-electron reduction potential = 0.59 V, pH 7.0, $HU^{\cdot-}$, H^+ / $UH_2^{\cdot-}$) and because of its high concentration in plasma (50 – 420 μM) is

considered to be quantitatively the main antioxidant in this fluid [6]. The antioxidant properties of uric acid are attributed to the ability of chelating transition metal ions, scavenging oxidants such as hydroxyl radical, hypochlorous acid (HOCl), singlet oxygen and free radicals in proteins [3,7–9]. In agreement to this, low levels of uric acid have been associated with neurodegenerative disorders such as Parkinson disease, multiple sclerosis, optic neuritis, and Alzheimer disease [10].

In contrast to these beneficial effects, the increase in serum uric acid (hyperuricemia) is associated with inflammatory disorders. The deposition of monosodium urate crystals activates inflammasome [11,12] and induces the formation of neutrophils extracellular traps (NETs) a process known as NETosis [13]. The crystals also stimulate NETs aggregation, which is particularly relevant for resolution of inflammation [13]. Even in the absence of crystals, soluble uric acid can prime

Abbreviations: ABAH, 4-aminobenzoic acid hydrazide; dHL-60, differentiated human promyelocytic leukemia cells; DHE, dihydroethidium; DTNB, 5,5'-dithiobis-2-nitrobenzoic acid; GSH, glutathione; GSSG, glutathione disulfide; 2-OH-E⁺, 2-hydroxyethidium; PMA, phorbol myristate acetate; SOD, superoxide dismutase; TNB, 2-nitro-5-thiobenzoate; UA, uric acid

* Correspondence to: Instituto de Química (IQUSP), Universidade de São Paulo, Avenida Prof. Lineu Prestes, 748, bloco 10, sala 1001 CEP 05508-000, São Paulo, SP, Brazil.

E-mail address: flaviam@iq.usp.br (F.C. Meotti).

<https://doi.org/10.1016/j.freeradbiomed.2018.08.011>

Received 19 March 2018; Received in revised form 9 August 2018; Accepted 11 August 2018

Available online 16 August 2018

0891-5849/ © 2018 Elsevier Inc. All rights reserved.

mononuclear immune cells enhancing the pro-inflammatory effect of Toll-like receptors ligands [14], increasing the expression of monocyte chemoattractant protein-1 (MCP-1) [15,16], recruiting neutrophils [12,17] and inducing NETs [18]. Differently from monosodium urate crystals, no evidence for NET aggregation has been described for soluble uric acid and thus, the resolution of inflammation may be disrupted in this case. Unsurprisingly, serum levels of uric acid are associated with kidney disorder, hypertension, endothelial dysfunction and cardiovascular disease [19,20] and a causal role for uric acid has been proposed.

Markedly, uric acid has dual anti and pro-oxidant property. In spite of the antioxidants effects, uric acid can indirectly increase the oxidative status by stimulating NADPH oxidase to produce superoxide [21–24]. In addition, a direct pro-oxidant effect of uric acid is expected when it undergoes one-electron oxidation generating free radical intermediates that might trigger a free radical chain reaction [25–31]. As a result, uric acid has been reported to increase oxidative damage and inactivate enzymes sensitive to oxidative stress [26,32–35]. The reaction of urate free radical intermediate with other free radical species is expected to terminate the free radical chain reaction but might not mitigate the oxidative stress. For instance, the fast reaction between urate free radical and superoxide ($8 \times 10^8 \text{ M}^{-1} \text{ s}^{-1}$) [36] generates the strong oxidant urate hydroperoxide [27–29,37,38].

The production of urate free radical and urate hydroperoxide is likely relevant in inflammatory conditions since one-electron oxidation of uric acid efficiently occurs by the pro-inflammatory enzymes myeloperoxidase and lactoperoxidase catalysis [27–29]. In this same inflammatory milieu, the activation of the NADPH oxidase provides substantial amount of superoxide to the formation of urate hydroperoxide. Urate free radical is very reactive and reacts indiscriminately with biomolecules. However, urate hydroperoxide is less reactive and oxidizes selectively cysteine and methionine [28] and may have a relevant role in redox signaling [37]. Since uric acid is widespread in human fluids, urate hydroperoxide can be formed in any site of inflammation and might represent a novel oxidant generated during cell respiratory burst. Therefore, this study was designed to identify whether urate hydroperoxide is indeed formed by inflammatory cells and how the oxidation of uric acid affects the overall redox balance in these cells.

2. Materials and methods

2.1. Cell culture

Human promyelocytic leukemic cells (HL-60) (BCRJ, RJ, Brazil) were maintained in RPMI 1640 medium (Sigma) containing bovine fetal serum (20%), streptomycin (100 $\mu\text{g}/\text{mL}$) and penicillin (100 U/ mL), in a humidified atmosphere at 37 °C with CO₂ (5%). HL-60 cells were differentiated (dHL-60) by the addition of dimethyl sulfoxide (DMSO; 1.3%) in the RPMI-1640 medium supplemented with bovine fetal serum (10%), streptomycin (100 $\mu\text{g}/\text{mL}$) and penicillin (100 U/ mL) for four days. To perform the experiments the cells were centrifuged (350 $\times g$ for 10 min) and the supernatant discarded. The pellet was washed with sterile saline (NaCl 0.9%) and centrifuged again, under the conditions mentioned above. Cells were suspended in PBS/glucose (10 mM phosphate buffer pH 7.4, 137 mM NaCl, 1 mM CaCl₂, 0.5 mM MgCl₂, 1 g/L glucose) or in PBS/glucose containing DTPA (penta-acetic acid diethylenetriamine, 100 μM). Before each experiment, the cytochrome *c* assay was performed to test superoxide production and confirm HL-60 differentiation.

2.2. Oxygen consumption

Oxygen consumption by dHL-60 cells was evaluated by polarography using Clark's electrode (Oroboros Oxygraph-2 k; Innsbruck, Austria). Two milliliters of 1×10^6 cells /mL PBS/glucose were placed

in a closed chamber at 37 °C under continuous agitation (300 rpm). After 5 min of baseline O₂ measurement, uric acid (0.2 mM) or vehicle (NaOH 0.4 mM) were added and the cells were activated with Phorbol 12-myristate 13-acetate (PMA, 100 ng/mL). The concentration of O₂ was monitored for 40 min.

2.3. Assessment of superoxide production by formation of 2-hydroxyethidium (2-OH-E⁺)

dHL-60 (2×10^6 cells) were incubated with 50 μM DHE, uric acid (0.05–0.5 mM) and 4-aminobenzoic acid hydrazide (ABAH, 50 μM) in PBS/glucose and activated with 100 ng/mL PMA for 30 min at 37 °C. After this time cells were pelleted at 400 $\times g$ for 10 min at 4 °C and the supernatants (60 μL) were separated in a Phenomenex Synergi column Polar-RP 80 A, (4 μm , 150 \times 4.6 mm) coupled to a high performance liquid chromatography (HPLC; Shimadzu, Tokyo, Japan). The HPLC system was equipped with two pumps LC-20AT, fluorescence detector RF-10AxL, UV absorbance detector SPD-20A and a system controller CBM20A. The mobile phase was 10% acetonitrile in 0.1% TFA/H₂O (solvent A) and 60% acetonitrile in 0.1% TFA/H₂O (solvent B) with a 0.6 mL/min flow rate. The compounds were eluted with a gradient of 40% solvent B for 5 min and linear increase to 100% solvent B within 25 min. This was kept for 10 min. The return to initial condition was linear over 5 min and it was allowed to equilibrate for 6 min. The 2-OH-E⁺ peak at $\lambda_{\text{ex}} = 480 \text{ nm}$, $\lambda_{\text{em}} = 580 \text{ nm}$ were integrated and plotted against a standard curve. The standard solution of 2-OH-E⁺ was prepared as described before [39]. Briefly, DHE (50 μM) was oxidized by xanthine/xanthine oxidase system (1 mM xanthine with 100 $\mu\text{g}/\text{mL}$ xanthine oxidase) in 10 mM phosphate buffer pH 7.4 containing DTPA (100 μM) at 37 °C for 30 min in the dark. Aliquots of this reaction were injected in the HPLC under the conditions described above, the 2-OH-E⁺ was collected and freeze-dried. The obtained residue was suspended in DMSO and therefore the absorbance was measured at pH 7.4 for proper deprotonation [40]. 2-OH-E⁺ concentration was calculated by the its molar absorption coefficient $\epsilon_{475 \text{ nm}} = 1.2 \times 10^4 \text{ M}^{-1} \cdot \text{cm}^{-1}$ [41]. All the procedures above have been performed under minimal light exposure.

2.4. Hypochlorous acid production

Measurement of hypochlorous acid (HOCl) production by dHL-60 was performed by oxidation of 2-nitro-5-thiobenzoate (TNB) [42]. dHL-60 cells (1×10^6) were suspended in PBS/glucose with taurine (15 mM) and uric acid (0; 0.1; 0.2 and 0.5 mM). A work solution of uric acid (10 mM) was completely dissolved in 20 mM NaOH. Cells were activated with PMA (100 ng/mL) and incubated at 37 °C for 1 or 2 h. Samples were centrifuged at 350 $\times g$ for 10 min and a five-fold dilution of the supernatant was incubated with 80 μM TNB by 15 min in the dark. The oxidation of TNB to the colorless DTNB (5,5'-dithiobis-2-nitrobenzoic acid) by taurine chloramine was measured at 412 nm and quantified using TNB molar absorption coefficient ($\epsilon_{412 \text{ nm}} = 14,200 \text{ M}^{-1} \cdot \text{cm}^{-1}$). Since two TNB are consumed to form one DTNB per taurine chloramine, the molar absorption coefficient was multiplied by two, i.e, 28,400 $\text{M}^{-1} \cdot \text{cm}^{-1}$ [42].

2.5. Detection of urate hydroperoxide and hydroxyisourate in dHL-60 and purified peripheral blood neutrophils by LC/MS/MS

Human neutrophils were isolated from the blood of healthy donors by histopaque centrifugation, dextran sedimentation and hypotonic lysis of red cells [43]. After isolation, neutrophils were suspended in PBS/glucose/DTPA (100 μM). Cultured dHL-60 were washed with sterile saline and suspended in PBS/glucose, DTPA (100 μM). An aliquot of cells (1×10^6) was always tested to evaluate the respiratory burst by the reduction of cytochrome *c* just before the experiments. Average rate of superoxide production was $4.69 \pm 0.98 \mu\text{M}/\text{min}$ in neutrophils and

$2.46 \pm 0.18 \mu\text{M}/\text{min}$ in dHL-60.

dHL-60 cells or neutrophils (5×10^6) were incubated with uric acid (0.2 or 0.5 mM) and stimulated by the addition of 100 ng/mL PMA in the absence or presence of SOD (80 $\mu\text{g}/\text{mL}$). After 30 min of incubation, samples were pelleted by centrifugation at $1400 \times g$ (1 min at 4°C). The supernatant was diluted in 60% acetonitrile and 50 μL was immediately injected into the LC/MS/MS. To investigate any artefactual production of urate hydroperoxide during sample preparation or LC/MS/MS flow through, 0.2 mM uric acid-1,3- $^{15}\text{N}_2$ (Sigma Aldrich, Germany) was added at the end of the reaction and the mass transitions of this isotope were monitored. The analysis was performed in a 6600 Triple-TOF mass spectrometer (Sciex, CA) coupled with electrospray ionization source (ESI), operated in negative ion mode. The detection was performed using four different mass transitions for urate hydroperoxide and hydroxyisourate. The collision energy was 15 eV for urate hydroperoxide, 20 eV for hydroxyisourate and -80 V for DP. The source temperature was 350°C and the spray voltage was set at 4500 V. Urate hydroperoxide was synthesized as described previously by our group [28] and the MS/MS spectrum of this standard solution was used as reference to the detection of products in cells. The chromatographic method was developed in a Nexera UPLC system (Shimadzu; Kyoto) using a TSK-Gel amide-80 (4.6×150 mm, $3 \mu\text{m}$ particle size) (Tosoh Bioscience; Tokyo, Japan). The mobile phase was 10 mM ammonium acetate pH 6.8 (solvent A) and acetonitrile (solvent B). The separation was performed in isocratic mode using 60% solvent B for 20 min with flow rate of 0.2 mL/min at 25°C .

2.6. Quantification of hydroxyisourate in dHL-60 cells

dHL-60 cells (5×10^6) were incubated for 30 min in PBS/glucose, DTPA (100 μM) in the absence or presence of uric acid (0.2–0.5 mM) at 25°C in a total volume of 100 μL . Cells were activated with PMA (100 ng/mL) and pelleted at $1470 \times g$, for 1 min at 4°C . The supernatants were filtered in a 0.22 μm membrane and diluted in acetonitrile (40 μL reaction: 60 μL acetonitrile); a total of 50 μL was injected into the LC system. Hydroxyisourate, product of the reduction of urate hydroperoxide, was analyzed in a Shimadzu HPLC system (Tokyo, Japan) using the modified method described by Patricio et al. [28]. The products were separated in a TSK-Gel amide-80 (4.6×150 mm, $3 \mu\text{m}$ particle size) (Tosoh Bioscience; Tokyo, Japan). The mobile phase was 10 mM ammonium acetate pH 6.8 (solvent A) and acetonitrile (solvent B). The separation was performed in an isocratic mode using 60% of solvent B for 20 min with flow rate of 0.2 mL/min at 25°C . The LC system was coupled to a diode array (SPD M20A, DAD) and fluorescence detector (RF-20A, Shimadzu, Japan). Hydroxyisourate was monitored by absorption at 302 nm and by fluorescence ($\lambda_{\text{ex}} = 302$ nm, $\lambda_{\text{em}} = 385$ nm). The absorbance peak area was integrated and plotted against a standard curve of hydroxyisourate ranging from 6.25 to 100 μM . The standard solution of hydroxyisourate was obtained from the incubation of urate hydroperoxide with methionine (1:4). Concentration of hydroxyisourate was normalized by the rate of superoxide production as $1 \mu\text{M} \text{min}^{-1}$.

2.7. Quantification of GSH and GSSG by LC/MS/MS system

dHL-60 cells (5×10^6) were incubated with different concentrations of uric acid (0.05, 0.1, 0.2 or 0.5 mM) in PBS/glucose in a total volume of 180 μL . Cells were activated with PMA (100 ng/mL) for 30 min and then 18 μL extraction buffer (20%TCA; 10 mM DTPA) plus 2 μL internal standard (N-acetyl cysteine, 0.2 mg/mL) were added. This mixture was incubated on ice for 15 min followed by a vortex agitation for 45 s and again incubated on ice for 15 min. Sample pH was adjusted to 2.0 by mixing with 200 μL of mobile phase A (0.75 mM ammonium formate, 0.01% formic acid, 1% methanol) and cellular debris were subsequently pelleted by centrifugation at $5000 \times g$ for 10 min. Supernatants were collected and injected into the LC-MS/MS system

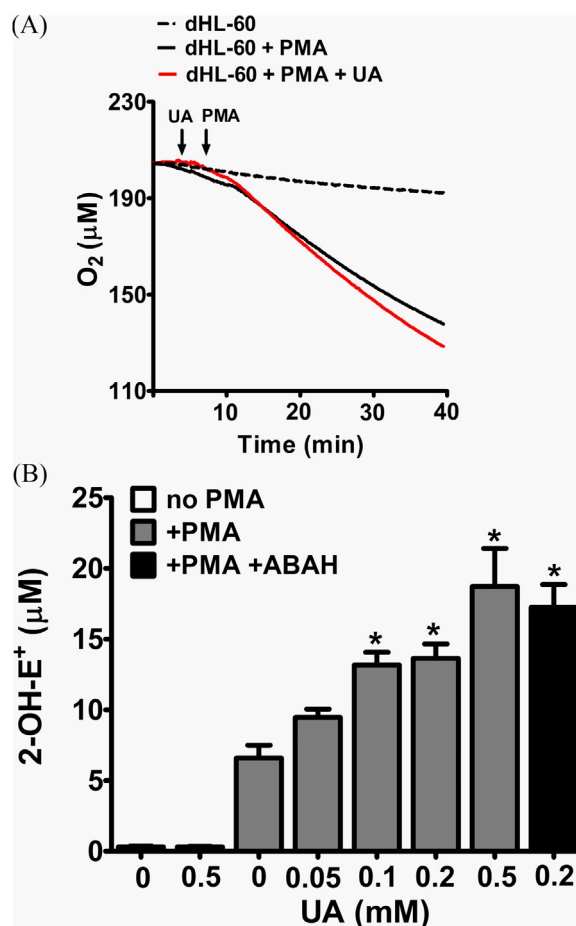


Fig. 1. Uric acid increases oxygen consumption (A) and superoxide production during respiratory burst in dHL-60. (A) O_2 concentration (μM) in dHL-60 cells (2×10^6) was monitored by a Clark electrode within an interval of 40 min. The baseline O_2 consumption was evaluated for 5 min. After baseline measurement, uric acid (UA, 0.2 mM) was added and it was followed by the addition of 100 ng/mL PMA. The arrows indicate the moment of addition of each compound. (B) dHL-60 cells (2×10^6) were incubated with DHE (50 μM), uric acid (0–0.5 mM), 4-aminobenzoic acid hydrazide (ABAH, 50 μM) and activated with PMA (100 ng/mL). After 30 min of incubation at 37°C in PBS/glucose, the supernatants were separated in a HPLC system and the 2-OH- E^+ peaks ($\lambda_{\text{ex}} = 480$ nm, $\lambda_{\text{em}} = 580$ nm) were integrated and plotted against a standard curve. Data represent the mean \pm S.E.M of three independent experiments. Statistical analyses were performed by one-way ANOVA followed by Newman-Keuls post-hoc test, * $p < 0.05$ from PMA-activated group without uric acid.

operated in positive ion mode [44].

GSH and GSSG were quantified by LC-MS/MS according to Carrol and collaborators [44] with minor modifications. The analysis was performed in a 6600 Triple-TOF mass spectrometer (Sciex, CA) coupled with electrospray ionization source (ESI), operated in the positive mode. The post-acquisition MRM-like data was used for quantification of GSH $[\text{M-H}]^+$ (m/z 308.0911 \rightarrow 179.0462), GSSG $[\text{M-H}]^+$ (m/z 613.1592 \rightarrow 355.0741), GSSG $[\text{M-H}]^{++}$ (m/z 307.0863 \rightarrow 177.0328) and internal standard NAC (m/z 164.0 \rightarrow 76.0215). The collision energies used for each compound were 22 eV for GSH; 32 eV for GSSG; 25 eV for NAC and 80 eV for DP (declustering potential). The source temperature was 450°C and the spray voltage was set to 5500 V. The chromatographic method was developed in a Nexera UHPLC system (Shimadzu, Kyoto, Japan) using a Kinetex C18 analytical column (100 mm \times 2.10 mm, $2.6 \mu\text{m}$) (Phenomenex, Torrance, CA, USA) eluted with a mobile phase of 0.75 mM ammonium formate/0.01% formic acid/1% methanol (solvent A) and methanol (solvent B) at 0.2 mL/min.

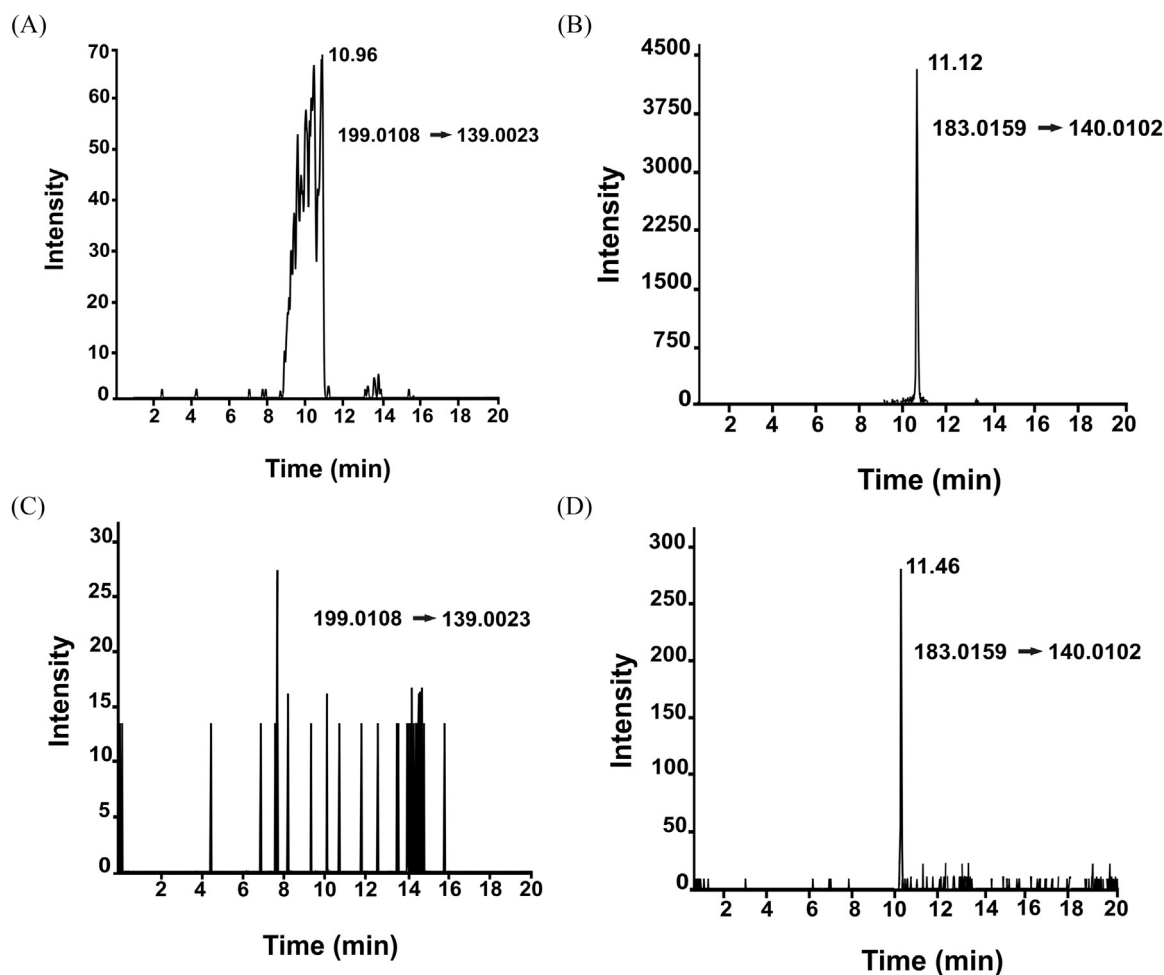


Fig. 2. Detection of urate hydroperoxide and hydroxyisourate produced by dHL-60 cells. dHL-60 cells (5×10^6) were incubated with uric acid (0.2 mM) and activated with PMA during 30 min at 25 °C. After centrifugation, supernatant was injected into the LC/MS/MS. Urate hydroperoxide (A) and hydroxyisourate (B) were identified by the chromatogram peaks using their respective mass transitions m/z 199.0108 \rightarrow 139.0023 ($\pm 5 \times 10^{-3}$ Da) and m/z 183.0159 \rightarrow 140.0102 ($\pm 5 \times 10^{-3}$ Da) in absence (A, B) or presence (C, D) of SOD (80 μ g/mL).

Elution was started with 1% solvent B, held for 5 min and followed by a gradient step to 80% from 5 to 6 min, maintained at 80% for 4 min and restored to 1% from 10 to 11 min. After this time, the column was equilibrated up to 20 min. The column temperature was set at 25 °C and injection volume was 10 μ L. Data were obtained using MultiQuant software (3.0, Sciex). GSH and GSSG concentrations were obtained by the ratios GSH/NAC and GSSG/NAC plotted against calculated by standard curve (0.16 – 3.25 μ M for GSH and 8.16 – 163 nM for GSSG).

2.8. Statistical analysis

The data are expressed as the mean \pm standard error (SEM) of at least three independent experiments. All data passed the normality test (D'Agostino & Pearson omnibus normality test) and were analyzed by one-way analysis of variance (ANOVA) followed by Newman-Keuls multiple range when appropriate. Results with $p < 0.05$ were considered to be significant.

3. Results

Activation of dHL-60 with PMA induced the respiratory burst with an increase in oxygen consumption (Fig. 1A) and superoxide production (Fig. 1B). As demonstrated in Fig. 1B, activation of dHL-60 cells with PMA greatly increased superoxide production and it was further increased by uric acid. Inhibition of myeloperoxidase by ABAH did not

alter uric acid effect. These results are in agreement with previous findings that demonstrated that uric acid is able to increase superoxide production in different type of cells [21,22,24].

During the respiratory burst, the dismutation of superoxide to hydrogen peroxide keeps up the production of hypochlorous acid by myeloperoxidase in neutrophils and dHL-60. We had previously demonstrated that myeloperoxidase also oxidizes uric acid generating urate free radical and that the combination of this free radical with superoxide generates the oxidant urate hydroperoxide [27,28]. Therefore, urate hydroperoxide is expected to be produced in the inflammatory milieu. However, the detection of this oxidizing agent in cells and tissues is a challenge because urate hydroperoxide rapidly reacts with thiol-peroxidases [37] and can also be reduced by glutathione and methionine [28]. In a previous study, we had settled the detection of urate hydroperoxide by mass spectrometry using a cell-free system [28]. The specific mass transitions of urate hydroperoxide from a standard solution are presented in the Supplem Fig. S1. In the present investigation, we confirmed that urate hydroperoxide is formed during the respiratory burst by monitoring these specific mass transitions in dHL-60 cells activated with PMA (Fig. 2A and Supplem Fig. S2). Fig. 2A shows the spectra of the most intense mass transition peak m/z 199.0108 \rightarrow 139.0023. Because of the reducing environment in cells, a much higher signal was identified for the product of urate hydroperoxide reduction, the hydroxyisourate, mass transition m/z 183.0159 \rightarrow 140.0102 (Fig. 2B). The addition of SOD in dHL-60 completely

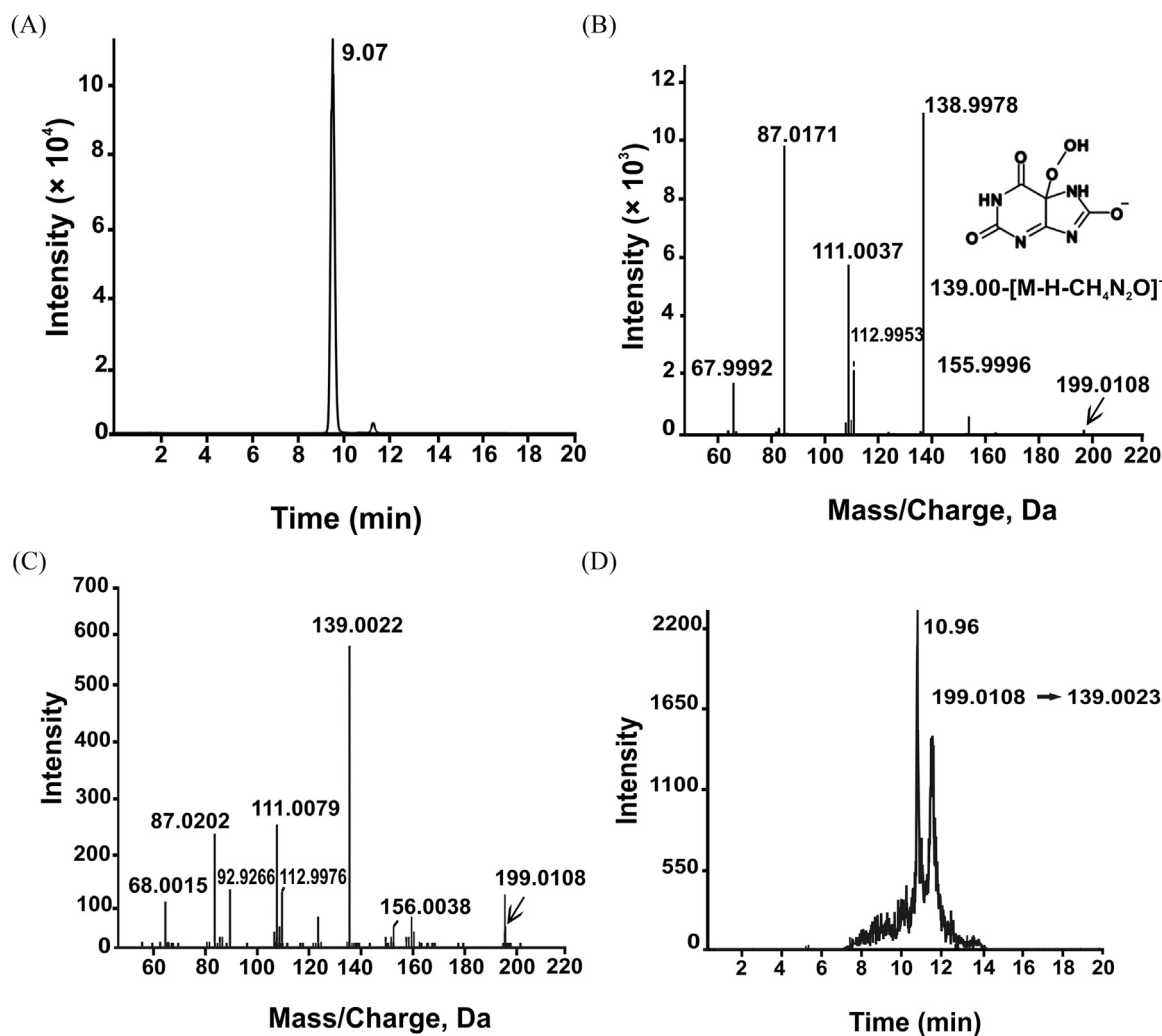


Fig. 3. Spectra of urate hydroperoxide and hydroxyisourate from a standard solution and from activated peripheral blood neutrophils. The standard solutions was synthesized as previously described [28] and injected into the LC/MS/MS for detection of urate hydroperoxide ion chromatogram in (A) and MS/MS in (B) or hydroxyisourate ion chromatogram in (E) and MS/MS in (F). Purified blood neutrophils (5×10^6) were incubated with 0.2 mM uric acid and activated with 100 ng/mL PMA for 30 min at 25 °C. After centrifugation supernatants were injected onto the LC/MS/MS and the fragmentation pattern of total m/z 199.0108 ion (C) and urate hydroperoxide mass transition m/z 199.0108 \rightarrow 139.0023 ($\pm 5 \times 10^{-3}$ Da) (D) were monitored. Fragmentation pattern of total m/z 183.0157 ion (G) and hydroxyisourate mass transition and m/z 183.0159 \rightarrow 140.0102 ($\pm 5 \times 10^{-3}$ Da) (H).

abolished urate hydroperoxide signal (Fig. 2C and Supplem Fig. S3) and decreased by 10-fold the hydroxyisourate signal (Fig. 2D), confirming the dependence on superoxide in the formation of urate hydroperoxide and hydroxyisourate [28]. The formation of urate hydroperoxide was completely dependent on the activation of cells (Supplem Fig. S3) and none artefactual urate hydroperoxide is formed by sample preparation or during LC/MS/MS analysis (Supplem Fig. S4).

Urate hydroperoxide and hydroxyisourate were also detected in blood neutrophils. Fig. 3 compares the fragmentation patterns of urate hydroperoxide (Fig. 3A and B) and hydroxyisourate (Fig. 3E and F) standard solutions and the PMA-activated neutrophil (Fig. 3C and G). Of relevance, both urate hydroperoxide (Fig. 3D and Supplem Fig. S5) and hydroxyisourate (Fig. 3H) presented a much more intense signal in blood neutrophils than in dHL-60 cells. As in dHL-60, the formation of urate hydroperoxide in neutrophils was largely dependent on the presence of superoxide and on the cell activation with PMA Suppl. Fig. S6).

Differently from urate hydroperoxide that rapidly reacts with reducing agents, hydroxyisourate accumulates in cells and can be well detected by HPLC. Therefore, we quantified the amount of hydroxyisourate as an indirect quantification of urate hydroperoxide. Five millions of dHL-60 cells produced micromolar range of hydroxyisourate

within 30 min. Because the respiratory burst in dHL-60 varied among different days of experiments, the results in Fig. 4A are expressed as the concentration of hydroxyisourate at a rate of superoxide production of $1 \mu\text{M min}^{-1}$. The production of hydroxyisourate was dependent on the concentration of uric acid and was totally dependent on myeloperoxidase activity (Fig. 4A). The addition of SOD decreased hydroxyisourate production but did not completely prevent it (Fig. 4A). In fact, the reaction of superoxide with urate free radical has a diffusion-limited rate of $8 \times 10^8 \text{ M}^{-1}\text{s}^{-1}$ and could not be completely abrogated by SOD. In addition, hydroxyisourate can also be formed by the hydration of dehydrourate, the product of urate free radical dismutation [27], i.e., a reaction independent of superoxide (Fig. 4A). Because the oxidation of uric acid to hydroxyisourate was dependent on myeloperoxidase (Fig. 4A) it should decrease the levels of HOCl in these cells. As expected, there was a gradual decrease in HOCl levels by increasing concentrations of uric acid (Fig. 4B).

Together these results show uric acid as a putative pro-oxidant that feeds the formation of urate free radical and urate hydroperoxide. However, uric acid can also contribute to a reducing environment by decreasing HOCl levels. To address the predominant effect, we assessed the GSH/GSSG ratio and thus, we could evaluate the overall redox

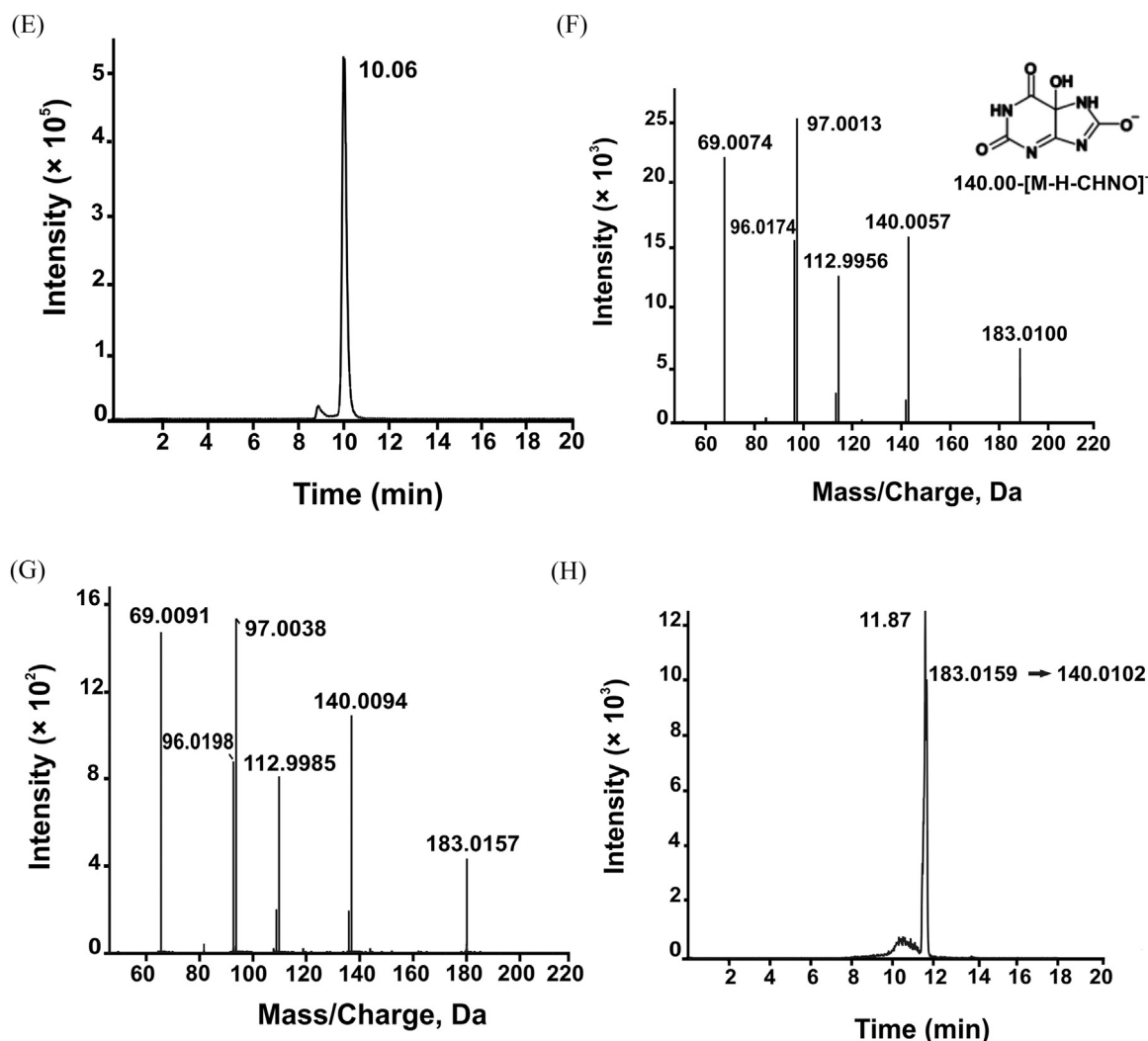


Fig. 3. (continued)

status of the cells in presence of uric acid. The activation of dHL-60 with PMA did not change GSH levels (Fig. 5A) but increased GSSG levels (Fig. 5B). The non-significant diminution in GSH levels after the respiratory burst is likely due to the large excess of this tripeptide in cells. Therefore, proper evaluation of redox balance is achieved by GSH/GSSG ratio rather than by their isolated measurements. As shown in the Fig. 5C, GSH/GSSG ratio was significantly decreased in PMA-activated dHL-60 cells. In addition, crescent concentrations of uric acid increased even more the GSSG levels (Fig. 5B) and, consequently, decreased GSH/GSSG ratio (Fig. 5C). These results suggest that the oxidation of uric acid in the inflammatory milieu overcomes the antioxidant effect and, overall, uric acid exerts a pro-oxidant effect in these cells.

4. Discussion

The dual role of uric acid in healthy and disease has been a matter of debate. Whilst some studies support a beneficial effect of uric acid by trapping transition metal ions, scavenging free radical in proteins, hydroxyl radical, hypochlorous acid, singlet oxygen, nitrogen dioxide radical, peroxynitrite and ozone [3,7–9,45,46], other studies revealed that the products of the reaction of uric acid with some of these species are not inert [25,26,30,31]. The protective role of uric acid has also been identified in vivo because low levels of uric acid were associated with neurodegenerative disorders in human and animal models [47–50]. Some points that support a beneficial antioxidant effect of uric acid: 1) the two-electron oxidation of uric acid generates allantoin that

is easily excreted [7]; 2) the one-electron oxidation of uric acid generates urate free radical, which can dismutate to yield allantoin and uric acid [27]. The antioxidant effect of uric acid also seems to be more relevant in presence of high levels of ascorbate. The lower reduction potential of ascorbate (one-electron $E^{0\prime} = 0.28$ V, Asc^{•-}, H⁺/Asc monoanion) [51] promotes reduction of urate free radical regenerating uric acid (second order rate constant 10^6 M⁻¹s⁻¹) [52]. Therefore, a protective effect of uric acid should be expected in tissues or species that contain high levels of ascorbate, e.g. human central nervous system and rodents.

In contrast, high levels of serum uric acid are associated with cardiovascular disease in humans [20,53–55]. This has been attributed to a pro-inflammatory effect of uric acid [16,17,19]. However, the exact mechanism on how uric acid affects vascular homeostasis is not fully understood. Uric acid is prone to oxidation in atheroma plaque [56,57] and, therefore, a direct association between uric acid oxidation and vascular damage has been suggested [20]. Of relevance, the oxidation of uric acid by peroxynitrite generates an aminocarbonyl radical, responsible by amplify lipid peroxidation of LDL [26] and this free radical has been detected in plasma [58]. In addition, other non-radical intermediates of urate oxidation by peroxynitrite were described to alkylate biomolecules [30]. The reactions with peroxynitrite are particularly relevant in the atheroma plaque, where the inflammatory cells produce superoxide and nitric oxide.

The atheroma plaque also contains the neutrophil heme-peroxidase, myeloperoxidase, favoring the oxidation of uric acid to urate free

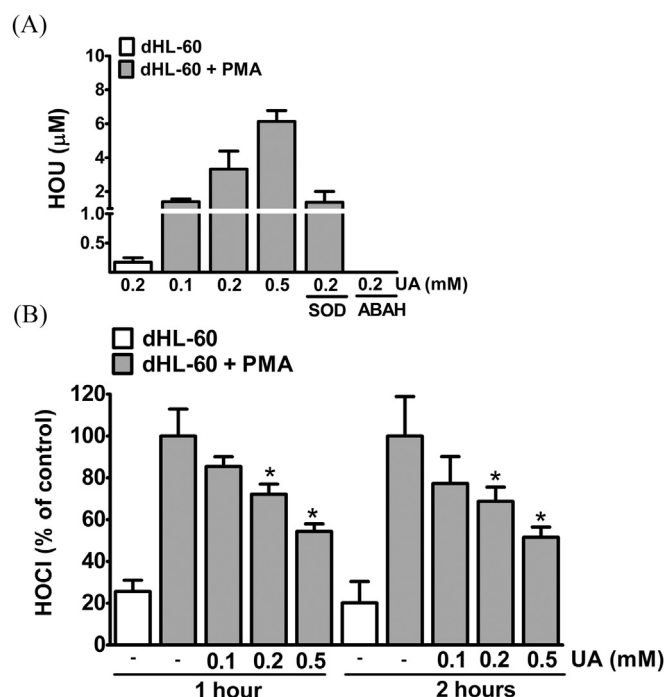


Fig. 4. : Quantification of hydroxyisourate and HOCl during respiratory burst in dHL-60 cells. (A) Cells (5×10^6) were incubated with different concentrations of uric acid and activated with PMA (100 ng/mL) during 30 min, the quantification of hydroxyisourate was performed by HPLC ($\lambda_{\text{HOU}} = 302 \text{ nm}$). Samples were also analyzed in presence of superoxide dismutase (SOD, 80 $\mu\text{g/mL}$) or the myeloperoxidase inhibitor 4-aminobenzoic acid hydrazide (ABAH, 50 μM). Chromatogram peaks were integrated and plotted against a hydroxyisourate standard curve. The concentrations were normalized by the rate of superoxide production of $1 \mu\text{M min}^{-1}$. (B) dHL-60 cells (1×10^6) were incubated with uric acid and activated with 100 ng/mL PMA for 1 and 2 h. Quantification of HOCl was performed by the oxidation of thionitrobenzoic acid (TNB, $\epsilon_{412 \text{ nm}} = 14,200 \text{ M}^{-1} \text{ cm}^{-1}$) to the colorless dithionitrobenzoic acid (DTNB). Values are mean \pm S.E.M of three independent experiments. Statistical analysis was performed by one-way ANOVA analysis of VARIANCE, followed by Newman-Keuls post-hoc test. * $p < 0.05$ from the group without uric acid.

radical and urate hydroperoxide (Fig. 6) [27,29]; both species are reactive and, therefore, hardly detected in the biological system. Urate free radical can undergo electron transference, dismutation or free radical combination whereas urate hydroperoxide can react with thiol proteins and low molecular antioxidants. Such a short half-live makes the assessment of these species in fluids, e.g. plasma, a challenge. Therefore, the oxidation of uric acid in biological systems has usually been assessed by the amount of allantoin, a more stable product than urate hydroperoxide and hydroxyisourate [20,27,59,60]. In fact, the oxidation of plasma uric acid by activated neutrophils or by inflammatory oxidants forms allantoin as the main product and parabanic acid, oxaluric and oxonic acid as minor products [7,27]. An exception seems to be the reaction with peroxyne, which generates triuret as the main yield [30]. In accordance with these evidences, previous studies quantified allantoin as a marker of uric acid oxidation in atheroma plaque and in fluids of patients with subclinical atherosclerosis, rheumatoid arthritis and cystic fibrosis [20,56,57,59,60].

We had previously demonstrated the formation of urate hydroperoxide in presence of myeloperoxidase and superoxide generating-system [27,28]. However, this is the first study that identified the production of urate hydroperoxide by inflammatory cells. This proves that the oxidation of uric acid during the respiratory burst generates an oxidant intermediate that, together with hypochlorous acid, peroxyne, superoxide and hydrogen peroxide, might exacerbate tissue

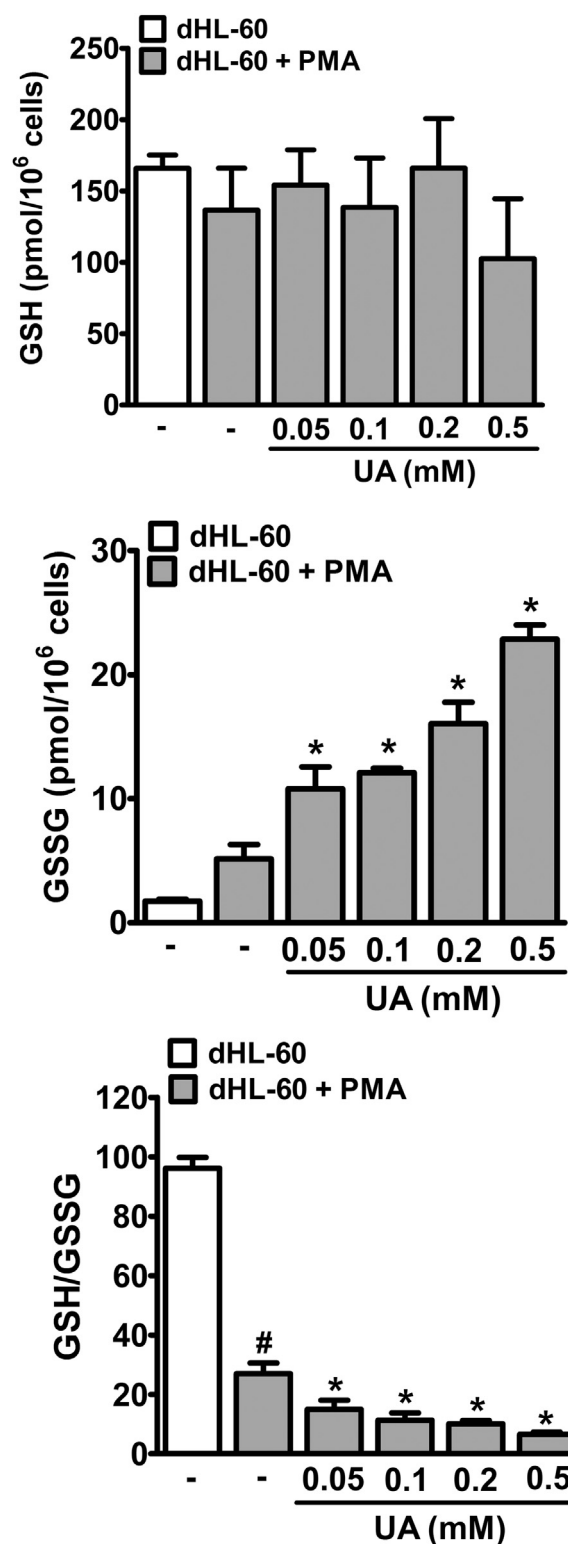


Fig. 5. Evaluation of overall oxidative status in dHL-60 cells by GSH and GSSG levels. Cells (5×10^6) were incubated with different concentrations of uric acid (0.05, 0.1, 0.2 or 0.5 mM) and activated with PMA (100 ng/mL) during 30 min at 37°C . Quantification was performed by LC/MS/MS using mass transition for GSH $[\text{M-H}]^+ (m/z 308.0911 \rightarrow 179.0462)$ and GSSG $[\text{M-H}]^+ : m/z 613.1592 \rightarrow 355.0741$ and $[\text{M-H}]^+ : m/z 307.0863 \rightarrow 177.0328$. Values are mean \pm S.E.M. of three independent experiments. Statistical analysis was performed by one-way ANOVA analysis of VARIANCE, followed by Newman-Keuls post-hoc test, * $p < 0.05$ compared with group in absence of uric acid and # $p < 0.05$ compared with group in absence of PMA.

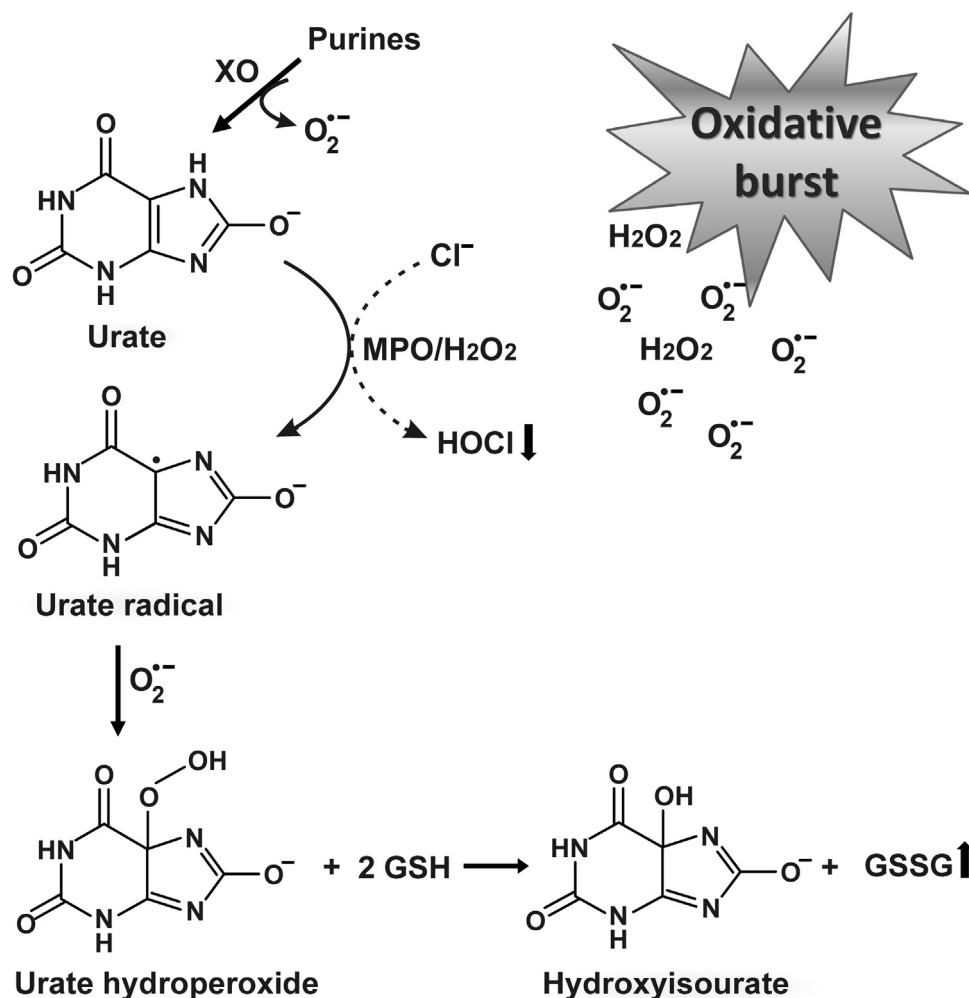


Fig. 6. Oxidation of uric acid in the respiratory burst. Uric acid is produced by the oxidation of xanthine and hypoxanthine by xanthine oxidoreductase (XO). The oxidative burst generates superoxide ($O_2^{\bullet -}$) and hydrogen peroxide (H_2O_2). The latter is used by myeloperoxidase (MPO) to oxidize chloride to hypochlorous acid (HOCl). Alternatively, MPO oxidizes urate to urate free radical, decreasing the production of HOCl. Urate free radical combines with superoxide to generate urate hydroperoxide. Urate hydroperoxide oxidizes glutathione to glutathione disulfide, increasing the overall oxidative status of the cell.

damage and homeostasis imbalance. Urate hydroperoxide can oxidize cell surface thiol-protein or diffuse into the intracellular milieu to rapidly oxidize thiol-peroxidases [37]. It can also oxidize glutathione but at a much lower rate [28]. Since the extracellular ratio of GSH/GSSG and of other low molecular weight thiol antioxidants is much lower than the intracellular one [61,62], these antioxidants unlikely contribute to the extracellular clearance of urate hydroperoxide. Additionally, albumin is much more abundant than the low molecular weight thiol antioxidants and is expected to be a more relevant extracellular target [63]. However, urate hydroperoxide oxidizes albumin at a low rate constant ($20 \pm 3.7 M^{-1} s^{-1}$) (unpublished data), which increases the chances of urate hydroperoxide diffusion.

Uric acid significantly increased superoxide production, indicating an indirect pro-oxidant effect of uric acid. Previous studies had already demonstrated that soluble uric acid induced the membrane assemblage of NADPH and superoxide production in differentiated adipocytes and leucocytes [15,21,22,24]. However, the exact mechanism by which uric acid increases superoxide production remains to be investigated.

The oxidation of uric acid by inflammatory cells decreased HOCl production because of the competition between uric acid and chloride for myeloperoxidase (Fig. 6) [24,27]. In addition, uric acid has been described as a direct scavenger of HOCl [7]. Therefore, it is hard to predict the overall redox state of the cell in presence of uric acid. Our results demonstrated that uric acid significantly decreased GSH/GSSG

and, therefore, a pro-oxidant effect overcame the antioxidant properties of uric acid. In agreement, a pro-oxidant effect of uric acid has been demonstrated in different models of inflammation in cells and in vivo [21–24,64]. Noteworthy, alterations in the redox balance have been associated with regulation of cytokines release and modulation of signaling pathways that might contribute to inflammation [65–67].

In summary, this study reveals the pro-oxidant effect of uric acid in inflammatory conditions. The respiratory burst triggered by NADPH oxidase activation feeds the production of hydrogen peroxide for the myeloperoxidase-catalyzed oxidation of uric acid to urate free radical. In addition, uric acid generates a cyclic process because it increased superoxide production in cells. Urate free radical combines with superoxide to generate urate hydroperoxide and both products can oxidize glutathione (Fig. 6). Therefore, this study identified, for the first time, the production of a novel uric acid-derivative oxidizing agent in inflammatory cells and opens up a new insight into the mechanisms by which uric acid propagates tissue damage in inflammatory-related conditions.

Acknowledgments

This study was supported by Fundação de Amparo a Pesquisa do Estado de São Paulo (FAPESP): CEPID Redoxoma 2013/07937-8; Young Investigator 2011/18106-4 and Conselho Nacional de Desenvolvimento

Científico e Tecnológico (CNPq) 472105/2012-4. R.P.S, J.P.P.B., E.S.P and L.A.C.C. receive scholarship from FAPESP. The authors thank colleagues of CEPID-Redoxoma network for all discussion concerning this investigation and Prof. Alicia Kowaltowski for assistance in oxygraph experiments.

Appendix A. Supplementary material

Supplementary data associated with this article can be found in the online version at doi:10.1016/j.freeradbiomed.2018.08.011.

References

- [1] A.F. Wright, I. Rudan, N.D. Hastie, H. Campbell, A 'complexity' of urate transporters, *Kidney Int* 78 (2010) 446–452.
- [2] X.W. Wu, D.M. Muzny, C.C. Lee, C.T. Caskey, Two independent mutational events in the loss of urate oxidase during hominoid evolution, *J. Mol. Evol.* 34 (1992) 78–84.
- [3] B.N. Ames, R. Cathcart, E. Schwiers, P. Hochstein, Uric acid provides an antioxidant defense in humans against oxidant- and radical-caused aging and cancer: a hypothesis, *Proc. Natl. Acad. Sci. USA* 78 (1981) 6858–6862.
- [4] S. Watanabe, D.H. Kang, L. Feng, T. Nakagawa, J. Kanellis, H. Lan, M. Mazzali, R.J. Johnson, Uric acid, hominoid evolution, and the pathogenesis of salt-sensitivity, *Hypertension* 40 (2002) 355–360.
- [5] M. Oda, Y. Satta, O. Takenaka, N. Takahata, Loss of urate oxidase activity in hominoids and its evolutionary implications, *Mol. Biol. Evol.* 19 (2002) 640–653.
- [6] M.G. Simic, S.V. Jovanovic, Antioxidant mechanisms of uric acid, *J. Am. Chem. Soc.* 111 (1989) 5778–5782.
- [7] H. Kaur, B. Halliwell, Action of Biologically-Relevant Oxidizing Species Upon Uric-Acid - Identification of Uric-Acid Oxidation-Products, *Chem.-Biol. Interact.* 73 (1990) 235–247.
- [8] B.F. Becker, Towards the physiological function of uric acid, *Free Radic. Biol. Med.* 14 (1993) 615–631.
- [9] A.S. Domazou, H. Zhu, W.H. Koppenol, Fast repair of protein radicals by urate, *Free Radic. Biol. Med.* 52 (2012) 1929–1936.
- [10] M.K. Kutzung, B.L. Firestein, Altered uric acid levels and disease states, *J. Pharmacol. Exp. Ther.* 324 (2008) 1–7.
- [11] F. Martinon, Mechanisms of uric acid crystal-mediated autoinflammation, *Immunol. Rev.* 233 (2010) 218–232.
- [12] H. Kono, C.J. Chen, F. Ontiveros, K.L. Rock, Uric acid promotes an acute inflammatory response to sterile cell death in mice, *J. Clin. Invest* 120 (2010) 1939–1949.
- [13] C. Schauer, C. Janko, L.E. Munoz, Y. Zhao, D. Kienhofer, B. Frey, M. Lell, B. Manger, J. Rech, E. Naschberger, et al., Aggregated neutrophil extracellular traps limit inflammation by degrading cytokines and chemokines, *Nat. Med.* 20 (2014) 511–517.
- [14] T.O. Crisan, M.C. Cleophas, M. Oosting, H. Lemmers, H. Toenhake-Dijkstra, M.G. Netea, T.L. Jansen, L.A. Joosten, Soluble uric acid primes TLR-induced proinflammatory cytokine production by human primary cells via inhibition of IL-1Ra, *Ann. Rheum. Dis.* (2015).
- [15] W. Baldwin, S. McRae, G. Marek, D. Wymer, V. Pannu, C. Baylis, R.J. Johnson, Y.Y. Sautin, Hyperuricemia as a mediator of the proinflammatory endocrine imbalance in the adipose tissue in a murine model of the metabolic syndrome, *Diabetes* 60 (2011) 1258–1269.
- [16] J. Kanellis, S. Watanabe, J.H. Li, D.H. Kang, P. Li, T. Nakagawa, A. Wamsley, D. Sheikh-Hamad, H.Y. Lan, L. Feng, et al., Uric acid stimulates monocyte chemoattractant protein-1 production in vascular smooth muscle cells via mitogen-activated protein kinase and cyclooxygenase-2, *Hypertension* 41 (2003) 1287–1293.
- [17] Y. Shi, Caught red-handed: uric acid is an agent of inflammation, *J. Clin. Invest* 120 (2010) 1809–1811.
- [18] Y. Arai, Y. Nishinaka, T. Arai, M. Morita, K. Mizugishi, S. Adachi, A. Takaori-Kondo, T. Watanabe, K. Yamashita, Uric acid induces NADPH oxidase-independent neutrophil extracellular trap formation, *Biochem Biophys. Res Commun.* 443 (2014) 556–561.
- [19] R.J. Johnson, D.H. Kang, D. Feig, S. Kivlighn, J. Kanellis, S. Watanabe, K.R. Tuttle, B. Rodriguez-Iturbe, J. Herrera-Acosta, M. Mazzali, Is there a pathogenic role for uric acid in hypertension and cardiovascular and renal disease? *Hypertension* 41 (2003) 1183–1190.
- [20] M.S. Santana, K.P. Nascimento, P.A. Lotufo, I.M. Benseaor, F.C. Meotti, Allantoin as an independent marker associated with carotid intima-media thickness in sub-clinical atherosclerosis, *Braz. J. Med Biol. Res* 51 (2018) e7543.
- [21] Y.Y. Sautin, T. Nakagawa, S. Zhariok, R.J. Johnson, Adverse effects of the classic antioxidant uric acid in adipocytes: nadph oxidase-mediated oxidative/nitrosative stress, *Am. J. Physiol. Cell. Physiol.* 293 (2007) C584–C596.
- [22] M.J. Thomas, Urate causes the human polymorphonuclear leukocyte to secrete superoxide, *Free Radic. Biol. Med.* 12 (1992) 89–91.
- [23] Y.Y. Sautin, R.J. Johnson, Uric acid: the oxidant-antioxidant paradox, *Nucleosides Nucleotides Nucleic Acids* 27 (2008) 608–619.
- [24] L.A.C. Carvalho, J. Lopes, G.H. Kaihama, R.P. Silva, A. Bruni-Cardoso, R.L. Baldini, F.C. Meotti, Uric acid disrupts hypochlorous acid production and the bactericidal activity of HL-60 cells, *Redox Biol.* 16 (2018) 179–188.
- [25] K.R. Maples, R.P. Mason, Free-Radical metabolite of Uric-acid, *J. Biol. Chem.* 263 (1988) 1709–1712.
- [26] C.X. Santos, E.I. Anjos, O. Augusto, Uric acid oxidation by peroxynitrite: multiple reactions, free radical formation, and amplification of lipid oxidation, *Arch. Biochem. Biophys.* 372 (1999) 285–294.
- [27] F.C. Meotti, G.N. Jameson, R. Turner, D.T. Harwood, S. Stockwell, M.D. Rees, S.R. Thomas, A.J. Kettle, Urate as a physiological substrate for myeloperoxidase: implications for hyperuricemia and inflammation, *J. Biol. Chem.* 286 (2011) 12901–12911.
- [28] E.S. Patricio, F.M. Prado, R.P. da Silva, L.A. Carvalho, M.V. Prates, T. Dadamos, M. Bertotti, P. Di Mascio, A.J. Kettle, F.C. Meotti, Chemical Characterization of Urate Hydroperoxide, A Pro-oxidant Intermediate Generated by Urate Oxidation in Inflammatory and Photoinduced Processes, *Chem. Res. Toxicol.* 28 (2015) 1556–1566.
- [29] A. Seidel, H. Parker, R. Turner, N. Dickerhof, I.S. Khalilova, S.M. Wilbanks, A.J. Kettle, G.N. Jameson, Uric acid and thiocyanate as competing substrates of lactoperoxidase, *J. Biol. Chem.* 289 (2014) 21937–21949.
- [30] C. Gersch, S.P. Pali, W. Imaram, K.M. Kim, S.A. Karumanchi, A. Angerhofer, R.J. Johnson, G.N. Henderson, Reactions of peroxynitrite with uric acid: formation of reactive intermediates, alkylated products and triuret, and in vivo production of triuret under conditions of oxidative stress, *Nucleosides Nucleotides Nucleic Acids* 28 (2009) 118–149.
- [31] W. Imaram, C. Gersch, K.M. Kim, R.J. Johnson, G.N. Henderson, A. Angerhofer, Radicals in the reaction between peroxynitrite and uric acid identified by electron spin resonance spectroscopy and liquid chromatography mass spectrometry, *Free Radic. Biol. Med.* 49 (2010) 275–281.
- [32] V.W. Bowry, R. Stocker, Tocopherol-Mediated Peroxidation - the Prooxidant Effect of Vitamin-E on the Radical-Initiated Oxidation of Human Low-Density-Lipoprotein, *J. Am. Chem. Soc.* 115 (1993) 6029–6044.
- [33] P. Filipe, J. Haigle, J. Freitas, A. Fernandes, J.C. Maziere, C. Maziere, R. Santos, P. Morliere, Anti- and pro-oxidant effects of urate in copper-induced low-density lipoprotein oxidation, *Eur. J. Biochem.* 269 (2002) 5474–5483.
- [34] O.I. Aruoma, B. Halliwell, Inactivation of alpha 1-antitrypsinase by hydroxyl radicals. The effect of uric acid, *FEBS Lett.* 244 (1989) 76–80.
- [35] K.J. Kittridge, R.L. Willson, Uric-Acid Substantially Enhances the Free Radical-Induced Inactivation of Alcohol-Dehydrogenase, *FEBS Lett.* 170 (1984) 162–164.
- [36] R. Santos, L.K. Patterson, P. Filipe, P. Morliere, G.L. Hug, A. Fernandes, J.C. Maziere, Redox reactions of the urate radical/urate couple with the superoxide radical anion, the tryptophan neutral radical and selected flavonoids in neutral aqueous solutions, *Free Radic. Res.* 35 (2001) 129–136.
- [37] L.A.C. Carvalho, D.R. Truzzi, T.S. Fallani, S.V. Alves, J.C. Toledo Jr, O. Augusto, L.E.S. Netto, F.C. Meotti, Urate hydroperoxide oxidizes human peroxiredoxin 1 and peroxiredoxin 2, *J. Biol. Chem.* 292 (2017) 8705–8715.
- [38] M.R. Clausen, K. Huvaere, L.H. Skibsted, J. Stagsted, Characterization of peroxides formed by riboflavin and light exposure of milk. detection of urate hydroperoxide as a novel oxidation product, *J. Agric. Food Chem.* 58 (2010) 481–487.
- [39] H. Zhao, J. Joseph, H.M. Fales, E.A. Sokoloski, R.L. Levine, J. Vasquez-Vivar, B. Kalyanaram, Detection and characterization of the product of hydroethidine and intracellular superoxide by HPLC and limitations of fluorescence, *Proc. Natl. Acad. Sci. USA* 102 (2005) 5727–5732.
- [40] J. Zielonka, H. Zhao, Y. Xu, B. Kalyanaram, Mechanistic similarities between oxidation of hydroethidine by Fremy's salt and superoxide: stopped-flow optical and EPR studies, *Free Radic. Biol. Med.* 39 (2005) 853–863.
- [41] J. Zielonka, J. Vasquez-Vivar, B. Kalyanaram, The confounding effects of light, sonication, and Mn(III)TBAP on quantitation of superoxide using hydroethidine, *Free Radic. Biol. Med.* 41 (2006) 1050–1057.
- [42] A.J. Kettle, C.C. Winterbourn, Assays for the chlorination activity of myeloperoxidase, *Methods Enzymol.* 233 (1994) 502–512.
- [43] A. Boyum, Isolation of mononuclear cells and granulocytes from human blood. Isolation of mononuclear cells by one centrifugation, and of granulocytes by combining centrifugation and sedimentation at 1 g, *Scand. J. Clin. Lab Invest Suppl.* 97 (1968) 77–89.
- [44] D. Carroll, D. Howard, H. Zhu, C.M. Paumi, M. Vore, S. Bondada, Y. Liang, C. Wang St, D.K. Clair, Simultaneous quantitation of oxidized and reduced glutathione via LC-MS/MS: an insight into the redox state of hematopoietic stem cells, *Free Radic. Biol. Med.* 97 (2016) 85–94.
- [45] G.L. Squadrito, R. Cueto, A.E. Splenser, A. Valavanidis, H. Zhang, R.M. Uppu, W.A. Pryor, Reaction of uric acid with peroxynitrite and implications for the mechanism of neuroprotection by uric acid, *Arch. Biochem Biophys.* 376 (2000) 333–337.
- [46] C.E. Cross, P.A. Motchnik, B.A. Bruener, D.A. Jones, H. Kaur, B.N. Ames, B. Halliwell, Oxidative damage to plasma constituents by ozone, *FEBS Lett.* 298 (1992) 269–272.
- [47] S. Zoccollella, I.L. Simone, R. Capozzo, R. Tortelli, A. Leo, E. D'Errico, G. Logroscino, An exploratory study of serum urate levels in patients with amyotrophic lateral sclerosis, *J. Neurol.* 258 (2011) 238–243.
- [48] D. Keizman, M. Ish-Shalom, S. Berliner, N. Maimon, Y. Vered, I. Artamonov, J. Tsehor, B. Nefussy, V.E. Drory, Low uric acid levels in serum of patients with ALS: further evidence for oxidative stress? *J. Neurol. Sci.* 285 (2009) 95–99.
- [49] D.C. Hooper, S. Spitsin, R.B. Kean, J.M. Champion, G.M. Dickson, I. Chaudhry, H. Koprowski, Uric acid, a natural scavenger of peroxynitrite, in experimental allergic encephalomyelitis and multiple sclerosis, *Proc. Natl. Acad. Sci. USA* 95 (1998) 675–680.
- [50] D.C. Hooper, G.S. Scott, A. Zborek, T. Mikheeva, R.B. Kean, H. Koprowski, S.V. Spitsin, Uric acid, a peroxynitrite scavenger, inhibits CNS inflammation, blood-CNS barrier permeability changes, and tissue damage in a mouse model of multiple sclerosis, *FASEB J.* 14 (2000) 691–698.

- [51] N.H. Williams, J.K. Yandell, Reduction of oxidized cytochrome c by ascorbate ion, *Biochim. Et. Biophys. Acta* 810 (1985) 274–277.
- [52] B. Halliwell, J.M. Gutteridge, *Free Radicals in Biology and Medicine*, Fourth edn, Oxford University Press Inc., New York, 2007.
- [53] H. Wang, D.R. Jacobs Jr., A.L. Gaffo, M.D. Gross, D.C. Goff Jr., J.J. Carr, Longitudinal association between serum urate and subclinical atherosclerosis: the Coronary Artery Risk Development in Young Adults (CARDIA) study, *J. Intern Med* 274 (2013) 594–609.
- [54] M. Gur, R. Yilmaz, R. Demirbag, N. Aksoy, Relation of serum uric acid levels with the presence and severity of angiographic coronary artery disease, *Angiology* 59 (2008) 166–171.
- [55] M. Gur, D.Y. Sahin, Z. Elbasan, G.Y. Kalkan, A. Yildiz, Z. Kaya, B. Ozaltun, M. Cayli, Uric acid and high sensitive C-reactive protein are associated with subclinical thoracic aortic atherosclerosis, *J. Cardiol.* 61 (2013) 144–148.
- [56] I. Ciari, L. Terzuoli, B. Porcelli, M.G. Coppola, E. Marinello, Antioxidant status and purine bases in carotid artery plaque, *Nucl. Nucl. Nucl.* 27 (2008) 624–627.
- [57] L.M.E. Terzuoli, C. Felici, B. Frosi, C. Setacci, M. Giubbolini, B. Porcelli, Purine bases and atheromatous plaque, *Int J. Immun. Pharmacol.* 17 (2004) 31–33.
- [58] J. Vasquez-Vivar, A.M. Santos, V.B. Junqueira, O. Augusto, Peroxynitrite-mediated formation of free radicals in human plasma: epr detection of ascorbyl, albumin-thiyl and uric acid-derived free radicals, *Biochem J.* 314 (Pt 3) (1996) 869–876.
- [59] N. Dickerhof, R. Turner, I. Khalilova, E. Fantino, P.D. Sly, A.J. Kettle, C.F. Arest, Oxidized glutathione and uric acid as biomarkers of early cystic fibrosis lung disease, *J. Cyst. Fibros.* 16 (2017) 214–221.
- [60] L.K. Stamp, R. Turner, I.S. Khalilova, M. Zhang, J. Drake, L.V. Forbes, A.J. Kettle, Myeloperoxidase and oxidation of uric acid in gout: implications for the clinical consequences of hyperuricaemia, *Rheumatology* 53 (2014) 1958–1965.
- [61] A. Andersson, A. Isaksson, L. Brattstrom, B. Hultberg, Homocysteine and other thiols determined in plasma by HPLC and thiol-specific postcolumn derivatization, *Clin. Chem.* 39 (1993) 1590–1597.
- [62] M.A. Mansoor, A.M. Svardal, P.M. Ueland, Determination of the in vivo redox status of cysteine, cysteinylglycine, homocysteine, and glutathione in human plasma, *Anal. Biochem.* 200 (1992) 218–229.
- [63] S. Carballal, R. Radi, M.C. Kirk, S. Barnes, B.A. Freeman, B. Alvarez, Sulfenic acid formation in human serum albumin by hydrogen peroxide and peroxynitrite, *Biochemistry* 42 (2003) 9906–9914.
- [64] T.T. Braga, M.F. Forni, M. Correa-Costa, R.N. Ramos, J.A. Barbutto, P. Branco, A. Castoldi, M.I. Hiyane, M.R. Davanzo, E. Latz, et al., Soluble uric acid activates the NLRP3 inflammasome, *Sci. Rep.* 7 (2017) 39884.
- [65] S. Salzano, P. Checconi, E.M. Hanschmann, C.H. Lillig, L.D. Bowler, P. Chan, D. Vaudry, M. Mengozzi, L. Coppo, S. Sacre, et al., Linkage of inflammation and oxidative stress via release of glutathionylated peroxiredoxin-2, which acts as a danger signal, *Proc. Natl. Acad. Sci. USA* 111 (2014) 12157–12162.
- [66] S.C. Trevelin, C.X. dos Santos, R.G. Ferreira, L.D. Lima, R.L. Silva, C. Scavone, R. Curi, J.C. Alves, T.M. Cunha, P. Roxo, et al., Apocynin and Nox2 regulate NF-kappa B by modifying thioredoxin-1 redox-state, *Sci. Rep.* 6 (2016).
- [67] D. Han, M.D. Ybanez, S. Ahmadi, K. Yeh, N. Kaplowitz, Redox regulation of tumor necrosis factor, *Signal. Antioxid. Redox Sign* 11 (2009) 2245–2263.

CHAPTER 2

**Oxidation of Uric Acid Promotes Modifications in Plasma Albumin in
Patients with Heart Failure**

**Railmara P. da Silva^{1,2}, Nicholas J. Magon¹, Anna P. Pilbrow³, A. Mark Richards³,
Flavia C. Meotti² and Anthony J. Kettle¹**

¹*Centre for Free Radical Research, Department of Pathology and Biomedical Science,
University of Otago, Christchurch, Christchurch, New Zealand*

²*Departamento de Bioquímica, Instituto de Química, Universidade de São Paulo,
São Paulo, Brazil*

ABSTRACT

Urate is a reductant and may act as an antioxidant. However, its oxidation products have the potential to exacerbate oxidative stress. Here we show that modification of serum albumin by products from urate oxidation is associated with poor outcome in patients with heart failure. We used mass spectrometry to identify twenty tryptic peptides from human serum albumin that were modified after incubation with a reaction system containing xanthine oxidase, myeloperoxidase, hypoxanthine and uric acid. All the modified peptides contained a lysine residue with a 140 Da mass addition from urate oxidation derived-product, a process we have named oxidative uratylation. We developed a single-reaction monitoring mass spectrometry method to quantify four of the uratylated tryptic peptides from plasma albumin of patients with heart failure and diabetes. The uratylated peptides were significantly elevated in plasma of patients with heart failure and diabetes, and positively correlated with myeloperoxidase and allantoin – the final stable product of urate oxidation. This modification on albumin was associated with death or heart failure. In conclusion, we showed that urate is more oxidized in patients suffering heart failure and that the presence of uratylated serum albumin could be a valuable marker in cardiovascular disease. The strong association between uratylated serum albumin and worst outcome in heart failure patients suggests that uric acid could contribute to the pathology of this disease. Together, these clinical and mechanistic studies support a role for uric acid in vascular inflammatory process.

1. INTRODUCTION

Uric acid is the end product of purine metabolism in humans and primates and it is found predominantly as urate under physiological pH ($pK_a = 5.4$) [1]. High levels of urate in plasma can reflect a decrease in its excretion, increased of generation or both events [2]. A contributor to increased urate levels is the higher activity of xanthine oxidase. This enzyme produces urate from xanthine and hypoxanthine [3]. In this case, the production of superoxide by xanthine oxidase associates urate generation with oxidative stress.

Urate has a low one-electron reduction potential (reduction potential = 0.59 V, pH 7.0, $HU^{\cdot-} + H^+ / UH_2^{\cdot-}$), which gives the ability to donate electrons [4]. Because of this chemical feature and since it is found at high concentrations in plasma (50 – 400 μM), urate is considered the main antioxidant in plasma [5, 6]. In spite of that, the one-electron oxidation of uric acid by free radicals [7] and by heme-peroxidases, as myeloperoxidase (MPO), generates urate free radical, which can initiate a free radical chain reaction [8, 9]. Myeloperoxidase contributes to host defense by production of bactericidal oxidants, such as hypochlorous acid, and elevated levels of myeloperoxidase in circulation are associated with inflammatory disease and increased oxidative stress [10-12].

The urate free radical formed by myeloperoxidase or other peroxidases can combine with superoxide, also abundant in the inflammatory milieu, to form urate hydroperoxide, a more stable intermediate than urate free radical, but with powerful oxidant capacity [13, 14]. This product can react with biological targets being reduced to 5-hydroxyisourate [15]. When urate radical loses a second electron dehydrourate is generated. This product can be slowly hydrolyzed to 5-hydroxyisourate that through a series reaction, breaks down to allantoin [9, 15, 16].

The presence of allantoin in several inflammatory diseases, including cardiovascular disease [17], rheumatoid arthritis [18], gout [19], diabetes [20] and cystic fibrosis [21] indicates that

urate is oxidized in these situations. Furthermore, several studies suggest an association between myeloperoxidase and cardiovascular disease [11, 22, 23]. One of the most important mechanisms linking inflammation, oxidative stress and cardiovascular disease is triggered by myeloperoxidase-derived oxidant products [24, 25]. These numerous reactive products, including those from urate, can initiate lipid peroxidation and promote post-translational modifications in proteins [7, 26-29].

More recently, our group demonstrated that urate-derived intermediates can form adducts with a 140-Da mass addition with amino groups in proteins, occurring mainly on lysine residues and on the α -amino of the N-terminal, a process called uratylation [30]. This is clinically relevant because urate and its oxidation products may contribute to vascular damage and inflammation [31-36].

In this study we sought a robust and convincing evidence that oxidation products of uric acid are involved in the pathogenesis of cardiovascular disease. For this purpose, we investigated the mechanism of formation of urate-derived adducts on albumin and the associated outcome in patients with heart failure and diabetes. We found that the amount of uratylated peptides was significantly elevated in plasma of these patients and were correlated with myeloperoxidase, supporting a role for uric acid in inflammatory process.

2. EXPERIMENTAL PROCEDURES

2.1 Materials

Bovine milk xanthine oxidase (XO), human serum albumin, bovine erythrocyte superoxide dismutase (SOD), bovine liver catalase (CAT), Hank's balanced saline solution (HBSS, 8264) were purchased from Sigma (St Louis, MO, USA) and trypsin (sequence grade, Promega, Madison, USA). Human myeloperoxidase (MPO; $\epsilon_{430\text{nm}}$ per heme = $89,000 \text{ M}^{-1}\text{cm}^{-1}$) was purchased from Planta Naturstoffe VertriebsGmbH (Austria). AZM 198 was from AstraZeneca [28].

2.2 Quantification of Urate Hydroperoxide by Ferrous Oxidation Xylenol Orange (FOX) assay.

Urate hydroperoxide was quantified by the oxidation of ferrous iron in the presence of xylenol orange. Urate was incubated with myeloperoxidase (100 nM), xanthine oxidase (0.025 U/mL or 0.0125) and hypoxanthine (200 μM) in 50 mM phosphate buffer, pH 7.4. After 30 min at 22 °C, the reaction was stopped with catalase (100 $\mu\text{g/mL}$) and an aliquot (20 μL) was diluted in 200 μL 10 mM ammonium acetate, pH 6.8 plus 80 μL FOX reagent. The composition of the FOX reagent was xylenol orange (30 mg), ferrous ammonium sulfate (39 mg) and sorbitol (7.3 g) in 100 mL of 0.2 M sulfuric acid [9]. The samples were left at room temperature for at least 40 min before reading the absorbance at 560 nm using a microplate reader. Concentrations were determined from a hydrogen peroxide (H_2O_2) standard curve as described by Patricio et al 2015 [15]. Hydrogen peroxide solution was prepared using $\epsilon_{240\text{nm}} = 43.6 \text{ M}^{-1} \text{ cm}^{-1}$. Results are expressed as hydrogen peroxide equivalents. The activity of xanthine oxidase was determined by measuring the rate of superoxide-dependent reduction of cytochrome c assay [37].

2.3 Reaction of oxidized urate with human serum albumin

Uric acid was prepared in water at pH 11 and then immediately diluted to 500 μM in phosphate buffer (pH 7.4) to minimize auto-oxidation. Urate (200 μM) was incubated with human serum albumin (0.5 mg/mL), myeloperoxidase (100 nM), xanthine oxidase (0.025 U/mL or 0.012 U/mL) and hypoxanthine (200 μM) during 1h at 37°C in phosphate buffer (50 mM, pH 7.4) or Hank's balanced saline solution (HBSS). When used, superoxide dismutase was added at 20 $\mu\text{g}/\text{mL}$. The reaction was stopped with allopurinol (100 μM) and 50 μg of serum albumin were collected of reaction mixed for digestion and then analysed for urate-derived adducts on tryptic peptides by LC/MS.

a. Detection of urate-derived adducts on human serum albumin

To identify urate-derived adducts on lysine residues from serum albumin, the protein was digested with trypsin as described previously with modifications[38]. Albumin (50 μg) was denatured with 100 mM ammonium bicarbonate solution containing 6 mM guanidinium chloride for 30 min at 25°C and shaking (400 rpm). After incubation, the volume was completed to 1 mL with ammonium bicarbonate solution (100 mM) followed by DTT (5 mM) and reacted for another hour at 37°C before alkylation with iodoacetamide (15 mM, 30 min in the dark, at 25°C, 400 rpm). After alkylation, DTT (2 mM) was added for 15 min at 25°C to scavenger iodoacetamide. Finally, trypsin was added at a ratio of 1:40 (w/w) and incubated at 37°C. After 4 hours a second dose of trypsin (1:80, w/w) was added and incubated at 37°C overnight. Samples were lyophilized and the tryptic peptides were resuspended with formic acid 0.1% in water and separated on a Jupiter Proteo 90A column (150 \times 2 mm, 4 μm ; Phenomenex) with water (A) and acetonitrile (B) (both containing 0.1% formic acid) as mobile phase and column temperature at 40°C. The gradient started at 2% acetonitrile and changed to 95% over 45 min at 0.2 mL/min. The peptides were detected by a Thermo Velos Pro mass spectrometer using double-play method and 20% of collisional energy. Proteome Discoverer (Thermo) software was used for identification of the peptides.

b. Quantification of urate-derived adducts on tryptic peptides of albumin

A semi-quantitative method was developed to quantify uratylation (K-140 Da) on four different Lys (Table S1) from human serum albumin. After reaction, 50 μg protein was collected and digested as described above. The peptides (20 μg) were injected onto an Ultimate 3000 HPLC (Thermo, Waltham, MA) and separated on a Jupiter Proteo 90A column (150 \times 2 mm, 4 μm ; Phenomenex) with water (A) and acetonitrile (B) (both containing 0.1% formic acid) and flow rate of 0.2 mL/min. The elution started with 2% of acetonitrile, held for 7 min, followed by a gradient step to 40% up to 24 min, maintained at 40% for 2 min and restored to 2% over 2 min. The column was equilibrated up to 32 min. The column temperature was set at 40°C. The peptides were identified by a Sciex 4000 QTRAP mass spectrometer (Framingham, MA) using positive enhanced product ion (EPI). For SRM method the mass transition (m/z precursor \rightarrow m/z fragment) for each modified peptide and its respective unmodified peptide was set as described in the Table S1. The ion spray was set to 5 kV, the nebulizer gas to 20 psi, and the interface heater to 400°C. The parameters used to each peptide are shown in table S1. For EPI, the collisional energy was 30%, declustering potential was 50V and with 10V collisional energy spread. These parameters were applied for all ions. Peptides were identified using mass software. All SRM data were processed using MultiQuant with the MQL algorithm for peak integration. Automatic peak detection was used, but all integrated peaks were manually inspected to ensure correct peak detection and integration. For quantification, the area of the most intense mass transition (m/z precursor \rightarrow m/z fragment) of each peptide was divided by the area of TYETTLEK peptide $[\text{M}+3\text{H}]^+$ 476.23 \rightarrow 723.33). Both exact ions fragment and retention time were used to guarantee proper peptide identification.

2.4 Formation of uratyated peptides by the products of uric acid photo-oxidation

Urate was oxidized as previously described by Patricio et al, 2015 [15]. Briefly, urate (10 mM) solution was prepared in 20 mM NaOH, and riboflavin was diluted in sodium phosphate buffer (10 mM; pH 6) containing 100 μ M of DPTA (Diethylenetriaminepentaacetic acid). The reaction was carried out in a 340 mm diameter well, with a total volume of 4 mL sodium phosphate buffer (10 mM; pH 6.8), urate (1.5 mM) and riboflavin (40 μ M) under UV light. The light source was equipped with six lamps, 15 mW (GE.) The reaction was performed at controlled temperature between 5°C and 10°C with continuous mixing for 10 min in the absence or presence of SOD (200 μ g/mL) in sodium phosphate buffer (10 mM; pH 6.8). After the reaction, urate hydroperoxide was quantified by FOX assay in the presence of catalase (100 μ g/mL) to remove hydrogen peroxide from the. Urate hydroperoxide (100 - 200 μ M) was incubated with albumin (0.5 mg/mL) in phosphate buffer (50 mM; pH 7.4) for 30 min at 22°C. The reaction was stopped by filtration using ultra Amicon filters (10 kDa). To test the effect of urate hydroperoxide reduction products, the peroxide was incubated with methionine (2 mM) for 15 min and then with albumin. After reaction, 50 μ g albumin was collected and digested with trypsin. The tryptic peptides VFDEFK⁴⁰²PLVEEPQNLIK, LAK³⁷⁵TYETTLEK, FK³⁶DLGEENFK and NLGK⁴⁵⁶VGSK containing urate-derived adducts and their respective unmodified peptides were quantified as described above.

Alternatively, urate hydroperoxide and hydroxyisourate were separated in a preparative HPLC (Shimadzu, Tokyo, Japan) through a TSK-Gel Amide column (10 μ m; 21.5 mm \times 30 cm, TOSOH Bioscience, Tokyo, Japan), mobile phase of 30% ammonium acetate (10 mM, pH 6.8) and 70% acetonitrile, with constant flux of 6 mL/min in an isocratic mode during 30 minutes. The excess of acetonitrile from urate hydroperoxide or hydroxyisourate samples was evaporated with inert gas as described by Mineiro et al, 2020 [39]. Urate hydroperoxide concentration was measured by its absorbance at 308 nm ($\epsilon_{308\text{nm}} = 6,540 \text{ M}^{-1}.\text{cm}^{-1}$) and by Ferrous Oxidation Xylenol Orange (FOX) as previously described [15]. Hydroxyisourate

concentration was estimated using the molar extinction coefficient at 308nm of urate hydroperoxide.

After purification, the reaction of albumin with urate hydroperoxide or hydroxyisourate was performed as described above. Fifty micrograms of albumin were digested and the peptides (10 μ g) were injected into an ultra-high performance liquid chromatography (UHPLC Nexera, Shimadzu, Kyoto, Japan) and separated on a Jupiter Proteo 90A column (150 \times 2 mm, 4 μ m; Phenomenex) using the gradient method described above. The analyses were performed by a ESI-Q-TOFMS (Triple TOF[®] 6600, Sciex, Concord, US), operating in the positive mode. For SRM method, the mass transition (m/z precursor \rightarrow m/z fragment) of each modified peptide and its respective unmodified peptide was set as described on table S1. The ion spray was set to 5.5 kV, curtain gas set at 25 psi, nebulizer and heater gases at 50 psi and interface heater 450°C.

All SRM data were processed using MultiQuant with the MQL algorithm for peak integration as described above. For quantification, the area of the most intense mass transition (m/z precursor \rightarrow m/z fragment) of each peptide was divided by the area of TYETTLEK peptide [$M+3H$]⁺ 476.23 \rightarrow 723.33). Both exact ions fragment and retention time were used to guarantee proper peptide identification.

2.5 Quantification of urate-derived adducts on serum albumin from patients with heart failure and diabetes

Human plasma was obtained from ten healthy donors (3 women and 7 men, 30-63 years old) and from patients admitted to the Christchurch Hospital (Christchurch, New Zealand) with heart failure accordance to the Framingham and European Society of Cardiology Criteria [40]. The admitted patients were registered at the Christchurch Heart Failure Registry as described by Cameron et al 2006 [41]. A randomly selected subgroup of diabetic patients with heart failure who were considered fit at the discharge by the attending medical team was subsequently followed-up to investigate levels of plasma protein carbonyls, as a marker of oxidative stress.

Then, we measured uratyated peptides in 68 patients with heart failure and type-2 diabetes. Plasma proteins (10 μ L) were diluted in 290 μ L phosphate buffer (50 mM, pH 7.4) and 50 μ g of protein were collected and digested as described above. The peptides (20 μ g) were injected onto an Ultimate 3000 HPLC (Thermo, Waltham, MA) and separated on a Jupiter Proteo 90A column (150 \times 2 mm, 4 μ m; Phenomenex) with water (A) and acetonitrile (B) (both containing 0.1% formic acid) in a flow rate of 0.2 mL/min. The elution started with 2% acetonitrile for 7 min, followed by a gradient step to 40 % up to 24 min, maintained at 40% for 2 min and restored to 2% over 2 min. The column was equilibrated up to 32 min. The column temperature was set at 40°C. The modified peptides were identified by a Sciex 4000 Q TRAP mass spectrometer (Framingham, MA) using single reaction monitoring (SRM) as the parameters described above. For quantification, the area of the most intense mass transition (m/z precursor \rightarrow m/z fragment) of each peptide was divided by the area of TYETTLEK peptide $[M+3H]^+$ 476.23 \rightarrow 723.33). Both exact ions fragment and retention time were used to guarantee proper peptide identification.

2.6 Quantification of myeloperoxidase and allantoin

Myeloperoxidase and allantoin in plasma of patients with heart failure and diabetes were determined by ELISA and liquid chromatography tandem mass spectrometry using stable isotope dilution (LC/MS/MS), respectively, as described previously [21, 42].

2.7 Statistical Analysis

Analyses of the adducts on human serum albumin generated by the reaction system with enzymes or urate hydroperoxide synthesized by UV light were carried out by ANOVA-analysis of Variance using Newman-Keuls Multiple Comparison Test. Analyses of the adducts on human serum albumin in clinical samples were carried out as non-parametric test (Test t)

Mann-Whitney test two-tailed. For all data, the level of significant was set when $p < 0.05$. The correlation coefficient r and p -value of a Pearson r correlation are shown in the figure legend.

2.8 Correlation between uratylated peptides and death or heart failure events in non-diabetic patients

A total of 100 patients were selected to cover the spectrum of heart failure severity (20 samples in each ascending quintile of NT-proBNP). We divided patients in two different situations during the follow-up: 1) death event only and 2) heart failure or death event combined. Overall, mean age was 74 (SD 11) years, gender was 78% male, ethnicity was 99% European. Years of follow up were up to 5.3 in death event (median follow-up 2.9 years, range 0.01 – 5.3 years, total of 29 events) and up to 2 years in heart failure or death event (total of 41 events). Data from all sites were collected in standardized and entered into a central electronic database sustained in Singapore and New Zealand (NZ) as described by Lam and collaborators [43]. Multivariate analysis was performed using a step-wise Cox proportional hazards model to determine independent association between uratylated peptides and death or heart failure events. All statistical analyses were performed using SAS version 9.4 (SAS Institute Inc., Cary, NC, USA) software. A $p < 0.05$ was considered significant.

3. RESULTS

3.1 Oxidation of urate by myeloperoxidase/xanthine oxidase/hypoxanthine system and by photo-oxidation

During inflammation urate is oxidized by myeloperoxidase forming urate free radical, which rapidly reacts with superoxide [13, 14] to form urate hydroperoxide. To establish the production of urate hydroperoxide and other urate-derived intermediates from this reaction, urate was oxidized by myeloperoxidase using xanthine oxidase and hypoxanthine as the source of superoxide and hydrogen peroxide. The activity of xanthine oxidase was determined by measuring the superoxide-dependent rate of cytochrome *c* reduction [37] and a flux of 14 $\mu\text{M}/\text{min}$ superoxide was used. The enzymatic system produced around 15 μM urate hydroperoxide and it was dependent on superoxide and myeloperoxidase (**Figure S1A**). From this point, we used this system in the presence of albumin to identify uratylation on lysine residues in albumin.

Urate also was oxidized by type 1 photo-oxidation. Since this system also produces H_2O_2 , the levels of urate hydroperoxide were measured after addition of catalase (**Figure S1B**). The addition of SOD during UV irradiation decreased urate hydroperoxide formation, confirming that it depends on superoxide, as described before [15]. Furthermore, the decrease in superoxide is supposed to increase the dismutation of urate free radicals, favouring the production of dehydrourate and the recovering of urate [9]. Dehydrourate undergoes hydrolyses to form 5-hydroxyisourate (**Figure 1**). Likewise, addition of methionine (2 mM) completely reduced urate hydroperoxide (**Figure S1B**) and an increase in 5-hydroxyisourate is expected.

This system was used to confirm whether urate hydroperoxide and its reduction product, 5-hydroxyisourate would form adducts with a 140-Da mass addition on serum albumin as previously purposed by Turner et al, 2018 [28].

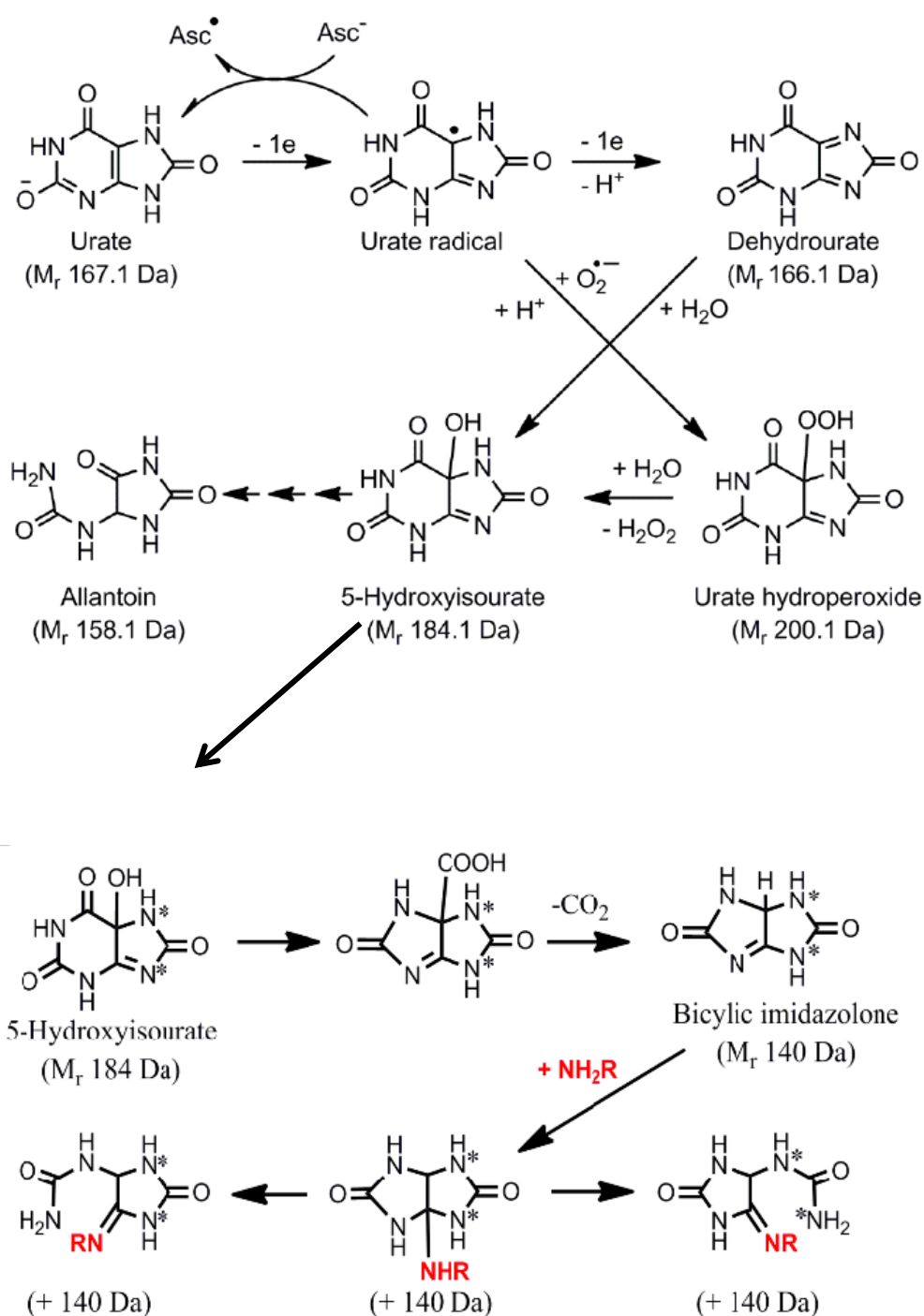


Figure 1: Schematic formation of products from uric acid oxidation (adapted from Turner et al [28]). One-electron oxidation of urate generates the urate radical that, if not reduced back to urate (by ascorbate, Asc, for instance), can be further oxidized to dehydrourate or react with superoxide to produce urate hydroperoxide. Both of these products hydrolyse to 5-hydroxyisourate that through a series of reactions breaks down to allantoin. Alternatively, 5-hydroxyisourate breaks down to the bicyclic imidazolone that adds to an amino group (NH_2R) to yield the stable 140-Da adduct [30].

3.2 Urate-derived intermediates from myeloperoxidase catalysed reaction modify lysine residues in human serum albumin

Urate was oxidized by myeloperoxidase in the presence of albumin, xanthine oxidase and hypoxanthine. The tryptic peptides were analysed by LC-MS/MS and the lysine adducts with 140 Da mass addition were identified. The adducts were detected in different peptides in the absence or presence of SOD and chloride (**Figure 2**). In general, these adducts were more consistently found in absence of chloride and SOD (**Table 1**). No adducts were detected in the absence of xanthine oxidase or myeloperoxidase (not shown). These results demonstrated that oxidation of urate generates stable adducts in plasma albumin. In spite of the physiological concentrations of chloride (Hank's based solution), there was still a significant amount of adducts in peptides. From here, we chose four different peptides that did not contain the easily oxidizable amino acids cysteine, methionine and tryptophan for relative quantification using single reaction monitoring (SRM).

Table 1. Urate-derived intermediates modified lysine residues in human serum albumin.

Modified peptides on lysine from human serum albumin (K -140)	Number of positive detections (maximun 4)			
	Incubation in phosphater buffer		Incubation in Hank's based solution	
	Full system	Full system+SOD	Full system	Full system+SOD
LDELRDEG K ²¹⁴ ASSAK	++++	+	+++	+++
NYAE K ³⁴⁷ DVFLGMFLYEYAR	++++	+++	+	
NLG K ⁴⁵⁶ VG S K ⁴⁶⁰ CCK	++++	++	++	+
NLG K ⁴⁵⁶ VGSK	++++	+++	+++	+++
AT K ⁵⁶⁵ EQLK	+++	++	+	+
L A K ³⁷⁵ TYETTLEK	++++	+++	+++	++++
AF K ²³⁶ AWAVAR	++++	+	+	
L K ²²³ CASLQK	++++	+++	++++	
F K ³⁶ DLGEENFK	++++	++++	+	++++
RHPYFYAPELLFF A K ¹⁸³ R	+++	+++	++++	+++

HPYFYAPELLFFAK ¹⁸³ R	+++	+++	+++	+
K ¹⁶¹ YLVEIAR	++++	+++	+++	+++
K ⁵⁴⁹ QTALVELVK	++++	+++	++	+++
K ⁴³⁸ VPQVSTPTLVEVSR	++++	++++	++	++++
LKECCEK ³⁰⁵ PLLEK	++	+++		
QNCELFEQLGEYK ⁴²⁶ FQNALLVR	++++	+++	+++	++++
EFNAETFTFHADICTLSEK ⁵⁴³ ER	++++	++++	++++	++++
VFDEFK ⁴⁰² PLVEEPQNLIK	+++	+	++++	++++

Urate was oxidized in the presence of myeloperoxidase (100 nM), xanthine oxidase (0.025 U/mL), hypoxanthine (200 μ M) and human serum albumin (0.5 mg/mL), for 1h at 37°C in phosphate buffer (50 mM, pH 7.4) or Hank's balanced saline solution (HBSS) in absence or presence of SOD (20 μ g/mL). The reaction was stopped with allopurinol (100 μ M). Tryptic peptides were detected by a Thermo Velos Pro mass spectrometer using double play and positive mode. Modified lysine with a mass addition of 140 Da (**K**) are red bold. Adducts were identified using Proteome Discoverer (Thermo) software. The data are from four independent experiments. (+) Positive detections, maximum 4 times.

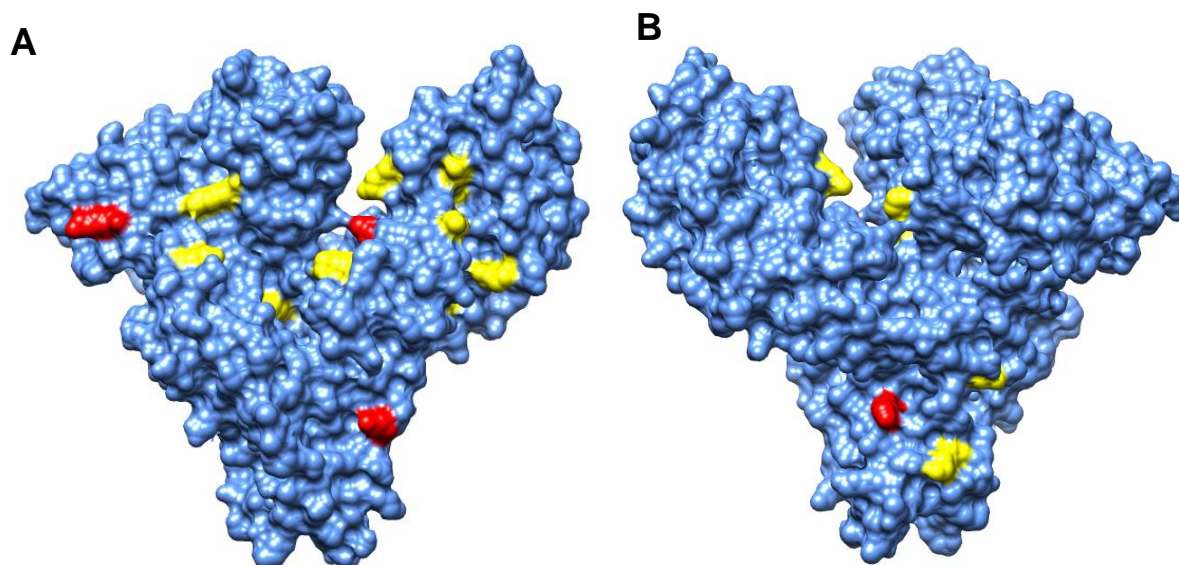


Figure 2: Schematic representation of urate-derived adducts on albumin (A) front and (B) back. Peptides containing urate adducts in lysine (red and yellow colour) were found in the global structure based on peptide identification by mass spectrometry. Peptides which uratylation were quantified are red coloured. Crystal structure drawn using Chimera 1.10.1 program (Protein Data Bank code 6hsc).

3.3 Fragmentation pattern and single reaction monitoring of the urate modified and the respective unmodified peptides.

Fragmentation spectra of LAK³⁷⁵TYETTLEK, NLGK⁴⁵⁶VGSK, FK³⁶DLGEENFK and VFDEFK⁴⁰²PLVEEPQNLIK peptides containing urate-derived adducts with a mass addition of 140 Da (red label) and their unmodified TYETTLEK, NLGK, DLGEENFK and VFDEFKPLVEEPQNLIK peptides are shown in **Figure 3 and 4** respectively. For quantification, the mass transition of the most intense ion fragments in the modified (y_5^+ ; a_2^+ ; y_8^+ ; y_6^+ in LAK³⁷⁵TYETTLEK, NLGK⁴⁵⁶VGSK, FK³⁶DLGEENFK and VFDEFK⁴⁰²PLVEEPQNLIK, respectively) or unmodified peptides (y_6^+ ; y_3^+ ; y_6^+ ; y_{15}^{2+} in TYETTLEK, NLGK, DLGEENFK and VFDEFKPLVEEPQNLIK, respectively) were chosen. The mass transitions of peptides are presented in chromatograms (**Figure 5**) and in the **Table S1**. The chromatograms show a specific retention time and the specific ion fragment had a good signal/noise ratio (**Figure 5**).

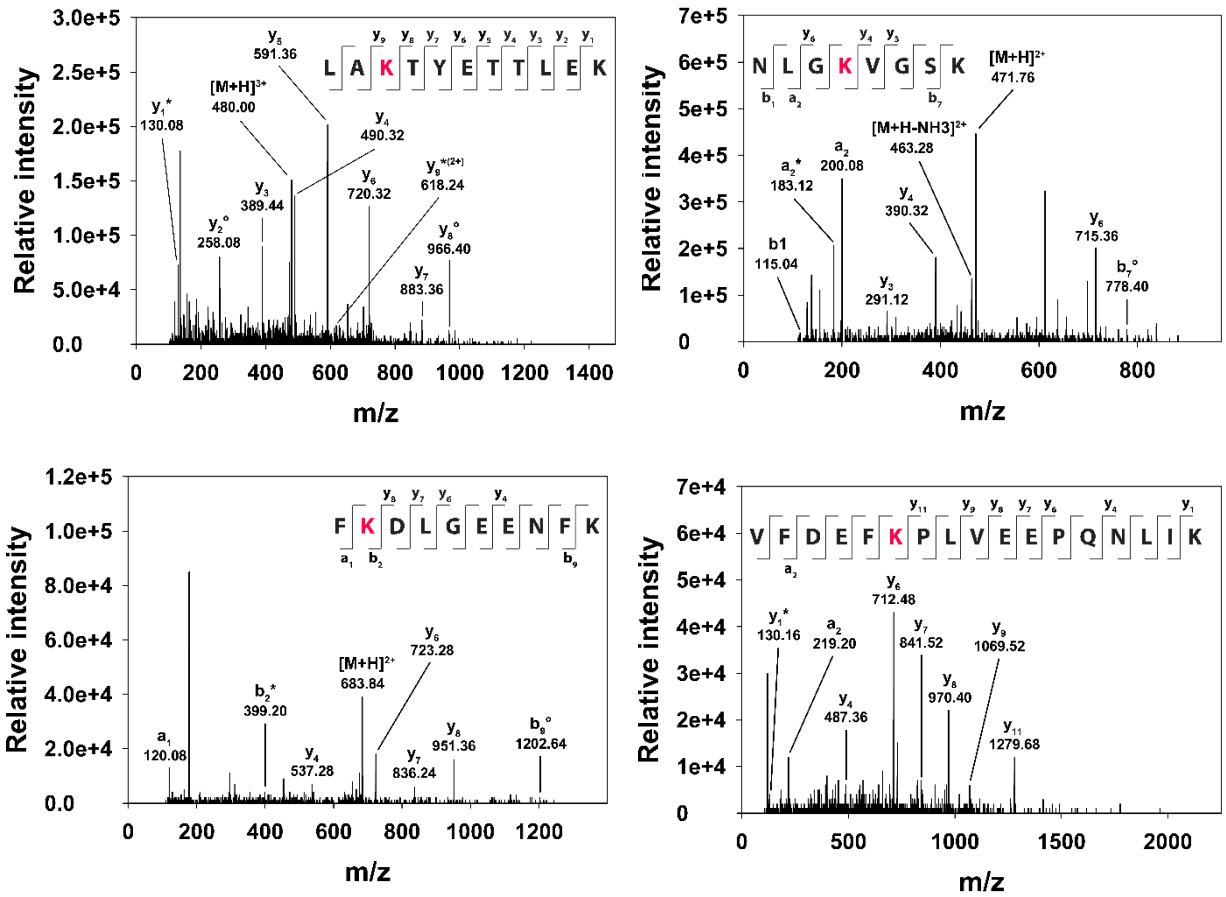


Figure 3. Fragmentation pattern of uratylated peptides from human serum albumin. Urate was oxidized in the presence of myeloperoxidase (100 nM), xanthine oxidase (0.025 U/mL), hypoxanthine (200 μ M) and human serum albumin (0.5 mg/mL) for 1h at 37°C in phosphate buffer (50 mM, pH 7.4). The reaction was stopped with allopurinol (100 μ M). Four tryptic peptides with a mass addition of 140 Da on lysine residues (K) were monitored by a Sciex 4000 Q TRAP mass spectrometer using positive enhanced product ion (EPI) mode. Adducts were identified using mass software.

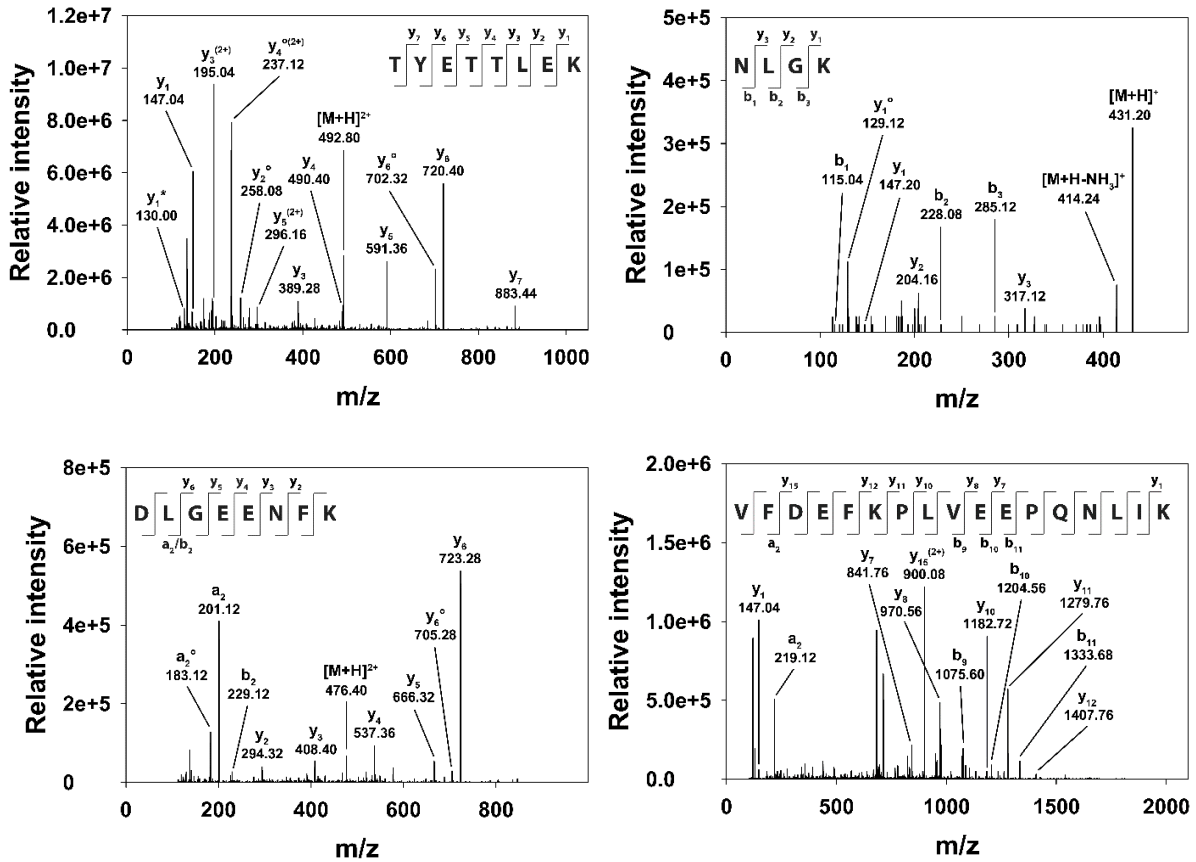


Figure 4. Fragmentation pattern of unmodified peptides from human serum albumin. Urate was oxidized in the presence of myeloperoxidase (100 nM), xanthine oxidase (0.025 U/mL), hypoxanthine (200 μ M) and human serum albumin (0.5 mg/mL), during 1h at 37°C in phosphate buffer (50 mM, pH 7.4). The reaction was stopped with allopurinol (100 μ M). Four tryptic peptides of unmodified peptides were monitored by a Sciex 4000 Q TRAP mass spectrometer using positive enhanced product ion (EPI) mode. Adducts were identified using mass software.

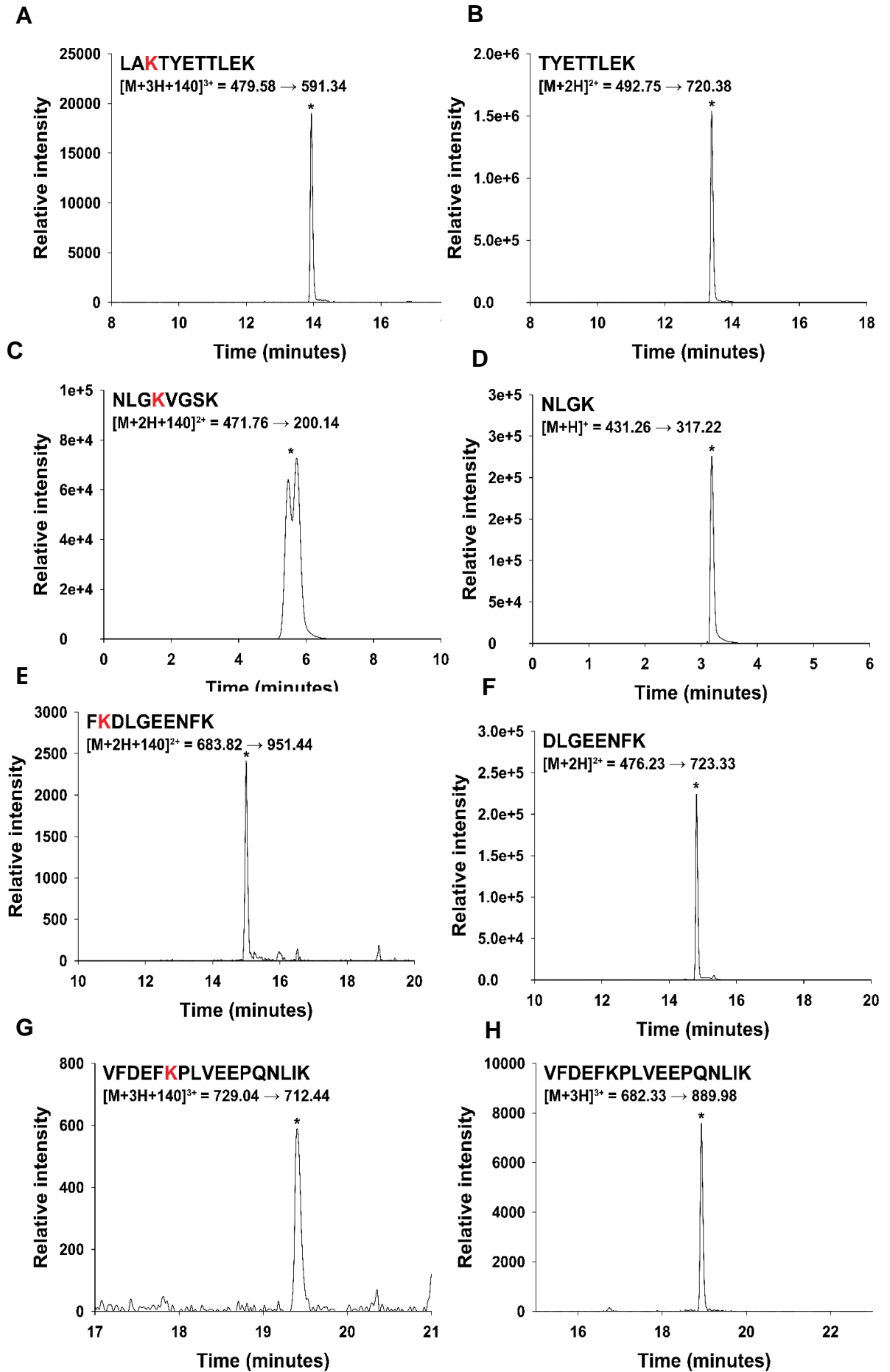


Figure 5. Single reaction monitoring of peptides from human serum albumin containing modified and unmodified lysine residues. Urate was oxidized in the presence of myeloperoxidase (100 nM), xanthine oxidase (0.025 U/mL), hypoxanthine (200 μ M) and human serum albumin (0.5 mg/mL), for 1h at 37°C in phosphate buffer (50 mM, pH 7.4). The reaction was stopped with allopurinol (100 μ M). The mass transition of four tryptic peptides with a mass addition of 140 Da on lysine residues (**K**- A; C; E; G) and their respective unmodified peptides (B; D; F; H) were monitored in a Sciex 4000 Q TRAP mass spectrometer using positive mode.

3.4 Quantification of uratylation using different oxidation systems

In an attempt to establish the mechanism for the formation of these modified peptides, the system was performed in two different xanthine oxidase concentrations and in the presence of SOD or AZM 198 (inhibitor of myeloperoxidase). The relative abundance of the four modified peptides increased substantially in the presence of a complete system, i.e., xanthine oxidase plus hypoxanthine and myeloperoxidase (**Figure 6**). Uratylation was fully prevented by myeloperoxidase inhibitor AZM. An increment in xanthine oxidase did not further increase uratylation, showing that the rate of superoxide production is not limiting at 12 mU/mL xanthine oxidase. SOD slightly increased uratylation. Presumably, the rate of superoxide dismutation to hydrogen peroxide is limiting and formation of others urate-derived intermediates are as important as urate hydroperoxide in the formation of adducts (**Figure 6**). To investigate this hypothesis, urate was oxidized by an UV system in the absence or presence SOD to generate urate hydroperoxide and 5-hydroxyisourate predominantly.

Incubation of urate with riboflavin, a photosensitizer, under UV irradiation generates mainly urate hydroperoxide [15]. Addition of this solution to albumin increased the amount of two modified peptides, LA**K**³⁷⁵TYETTL**EK**, NLG**K**⁴⁵⁶VGSK (**Figure 7**). Uratylation decreased after reduction of urate hydroperoxide by methionine but increased when SOD was present during photo-oxidation. It was unforeseen since in both conditions, presence of methionine and SOD, a predominance of the same product, 5-hydroxyisourate, is expected. In the former, 5-

hydroxyisourate is a result from urate hydroperoxide reduction and in the latter it is from the dismutation of urate free radical followed by hydration of the dehydrourate [15, 44]. This suggests that adduct formation does not depend on a direct reaction of urate hydroperoxide with lysine but rather from its decomposition products.

To further pursue the difference in the results in presence of methionine and SOD the photo-oxidation was performed but instead to incubate this full system with albumin, the products urate hydroperoxide and 5-hydroxyisourate were separated in a preparative HPLC beforehand. Incubation of albumin with the isolated urate hydroperoxide formed substantial amount of the modified peptides (**Figure 8**). Similar to the previous data, the 5-hydroxyisourate obtained in presence of SOD further increased total modified peptides. In opposite, the 5-hydroxyisourate obtained from the spontaneous decay of urate hydroperoxide was less efficient to form adducts (**Figure 8**). Together, these results suggest that the 5-hydroxyisourate generated from the reduction of urate hydroperoxide, either spontaneously or by methionine, and that yielded by the dismutation of urate free radical and hydration of dehydrourate can have different chemical structure and reactivity. This characteristic can cause different interactions with albumin and consequently to alter the ability to uratylated the protein.

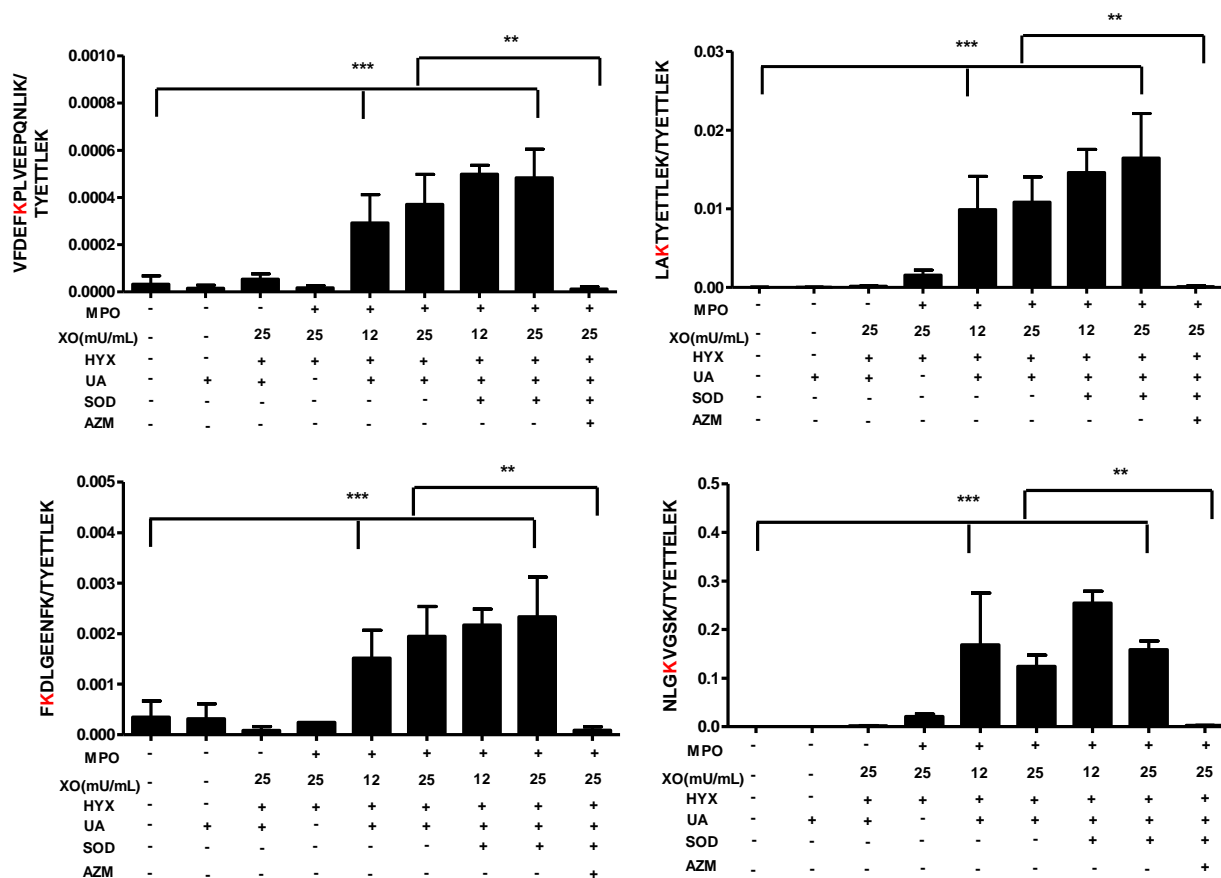


Figure 6. Uratylation on lysine residues from human serum albumin is dependent on myeloperoxidase activity. Urate (UA, 400 μ M) was oxidized by myeloperoxidase (100 nM)/xanthine oxidase (XO)/hypoxanthine (HYX, 200 μ M) system in the presence of SOD (100 μ g/mL) or AZM (inhibitor of MPO, 10 μ M), for 1h at 37°C in phosphate buffer (50 mM; pH 7.4) containing human serum albumin (0.5 mg/mL). The reaction was stopped with allopurinol (100 μ M). Using single reaction monitoring MS (SRM), four peptides: VFDEFK⁴⁰²PLVEEPQNLIK (A), LAK³⁷⁵TYETTLEK (B), FK³⁶DLGEENFK (C) and NLGK⁴⁵⁶VGSK (D), containing uratylation modification, a mass addition of 140 Da, on lysine (K) and TYETTLEK (unmodified peptide) from albumin were measured by Qtrap 4000 mass spectra. All SRM data were processed using MultiQuant. Data are mean \pm S.D of three independent experiments. Significant difference (**, $p < 0.01$; ***, $p < 0.0001$) were determined by one-way ANOVA using Newman Keuls post-test.

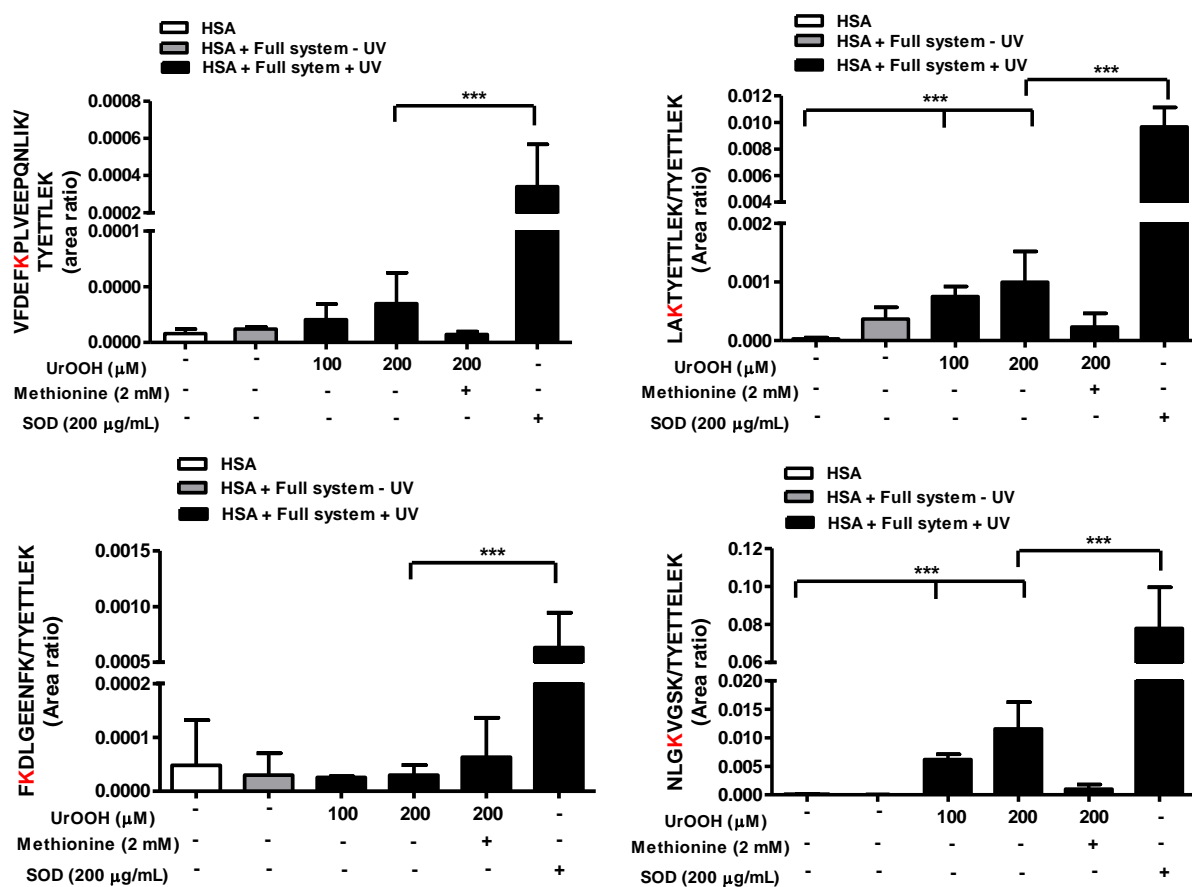


Figure 7. Uratylation on lysine residues from human serum albumin in a photo-oxidation system.

Urate was oxidized by photo-oxidation system for 10 min in phosphate buffer (10 mM; pH 6). Urate hydroperoxide (UrOOH) concentration was assessed by FOX assay in the presence of catalase (CAT, 100 μg/mL). Albumin (HSA, 0.5 mg/mL) was incubated with the full system containing urate hydroperoxide (UrOOH, 100 or 200 μM) for 30 min at 25 °C. Methionine (2 mM) was added just before albumin and incubated for 5 min at 22 °C. SOD was added in the reaction mixture during the irradiation. Using single reaction monitoring (SRM), four peptides containing the uratylation, a mass addition of 140 Da on lysine (K) and TYETTLEK (unmodified peptide) from albumin were measured by Qtrap 4000 mass spectrum. Data are mean ± S.D of the area of modified peptides normalized by the unmodified peptide (TYETTLEK) of three independent experiments. Significant difference (***, p < 0.0001) were determined by one-way ANOVA using Newman Keuls post test.

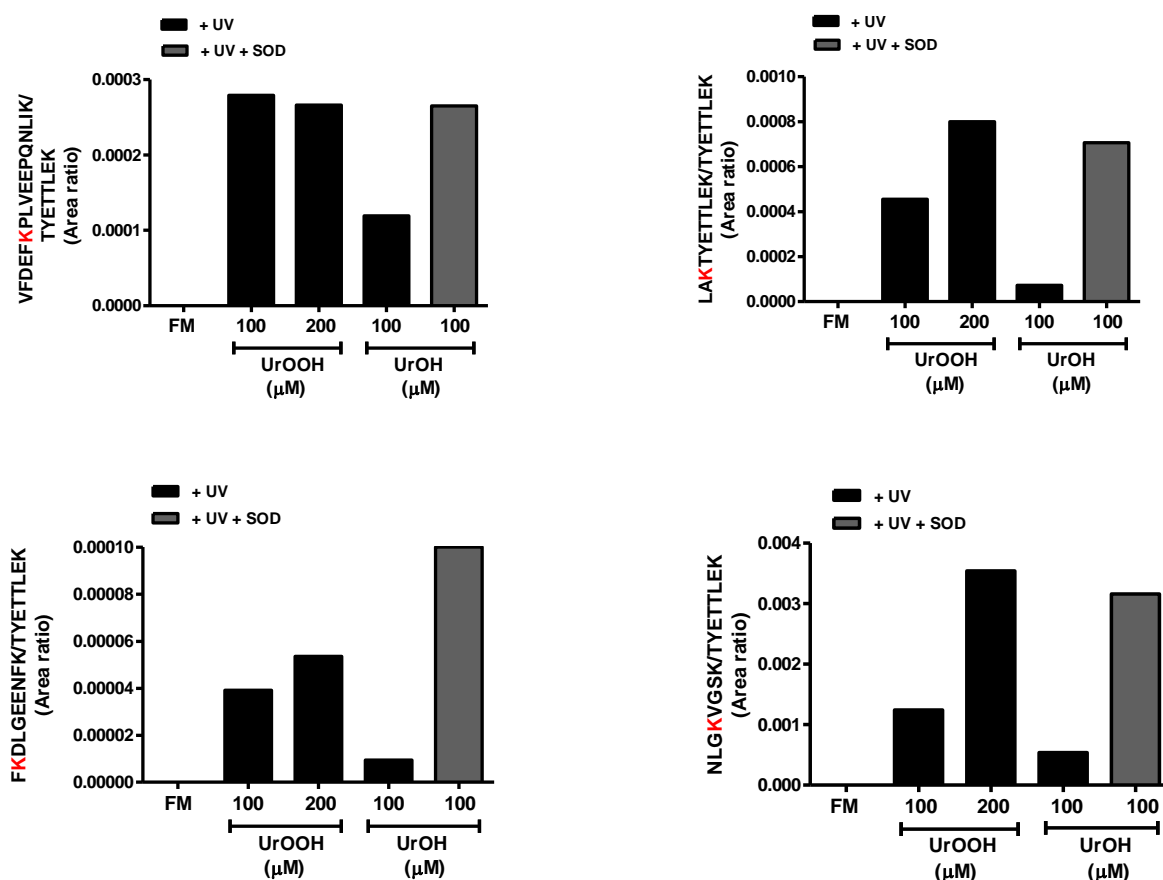


Figure 8. Urate hydroperoxide and hydroxyisourate increase uratylation on lysine residues from human serum albumin. Urate was oxidized by photo-oxidation for 10 min in phosphate buffer (10 mM; pH 6). Urate hydroperoxide (UrOOH) and hydroxyisourate (UrOH) were isolated in a preparative HPLC. Hydroxyisourate was isolated from a reaction in the absence (dark gray bar) or in the presence of SOD (100 μg/mL, black bar). UrOOH and UrOH concentrations were measured by their absorbance at 308 nm ($\epsilon_{308\text{nm}} = 6,540 \text{ M}^{-1}\text{cm}^{-1}$) and by FOX and incubated with albumin (0.5 mg/mL) for 30 min at 25°C. Using single reaction monitoring MS (SRM), four peptides containing the uratylation, a mass addition of 140 Da on lysine (K) and TYETTLEK (unmodified peptide) were identified by QTOF 6600 mass spectrum. Data is the area of the modified peptides normalized by the unmodified peptide (TYETTLEK) of one experiment.

3.6 Uratylation of albumin is elevated in plasma of patients with heart failure and diabetes

The next step was to evaluate whether uratylation on lysine residues from serum albumin would be correlated with heart failure and diabetes. The plasma of ten healthy donors and 68

patients with heart failure and diabetes were analysed. The modified (**Figure 9**) and unmodified (**Figure S2**) peptides were readily detected by their specific mass transition and retention time.

For quantification, the area under the curve from each modified peptide was divided by the TYETTLEK peptide (unmodified peptide). There was a significant increase in the uratylated VFDEFK⁴⁰²PLVEEPQNLIK ($p < 0.03$), NLGK⁴⁵⁶VGSK ($p < 0.015$) and LAK³⁷⁵TYETTLEK ($p < 0.0003$) peptides from patients with heart failure and diabetes comparing to healthy donors (**Figure 10**). In addition, uratylated peptides were significantly correlated among each other (**Table 3**), with allantoin and myeloperoxidase but not with uric acid (**Table 4**). Plasma allantoin was also strongly correlated with myeloperoxidase and uric acid. All together, these results support a role for uric acid oxidation in cardiovascular disease and the uratylation of albumin as a biomarker in heart failure.

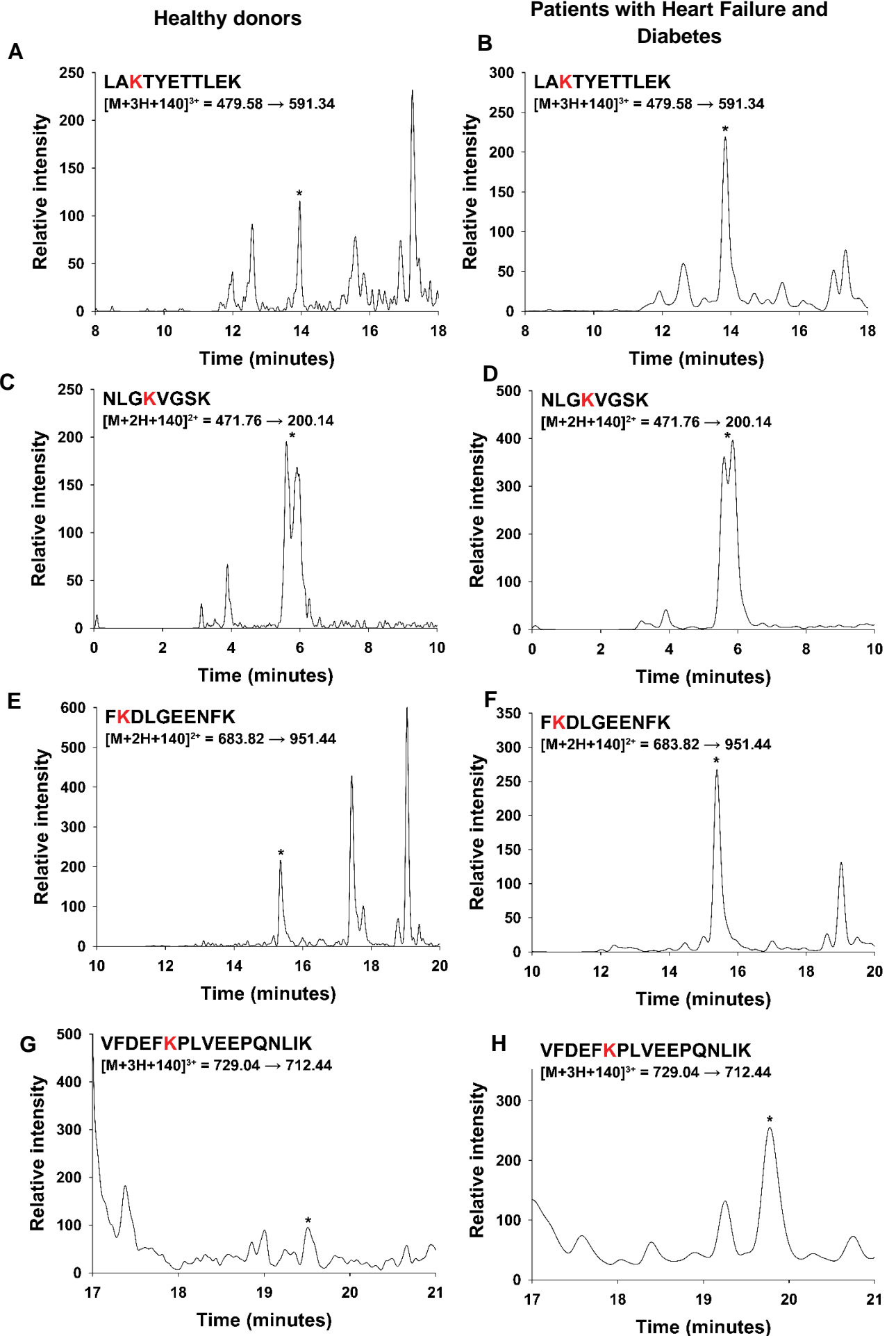


Figure 9. Detection of uratylation on lysine residues of serum albumin from healthy donors and patients with heart failure and diabetes. Protein from plasma (10 μ L) of healthy donors or patients with heart failure and diabetes were denatured, reduced (5 mM, DTT), alkylated (15 mM, IAM) and digested with trypsin. Then, the mass transition of four tryptic peptides with a mass addition of 140 Da in lysine residues (**K**) were monitored in healthy donors (A; C; E. G) and in patients with heart failure and diabetes (B; D; F; G). The retention time was used to confirm the specificity of the identified ions.

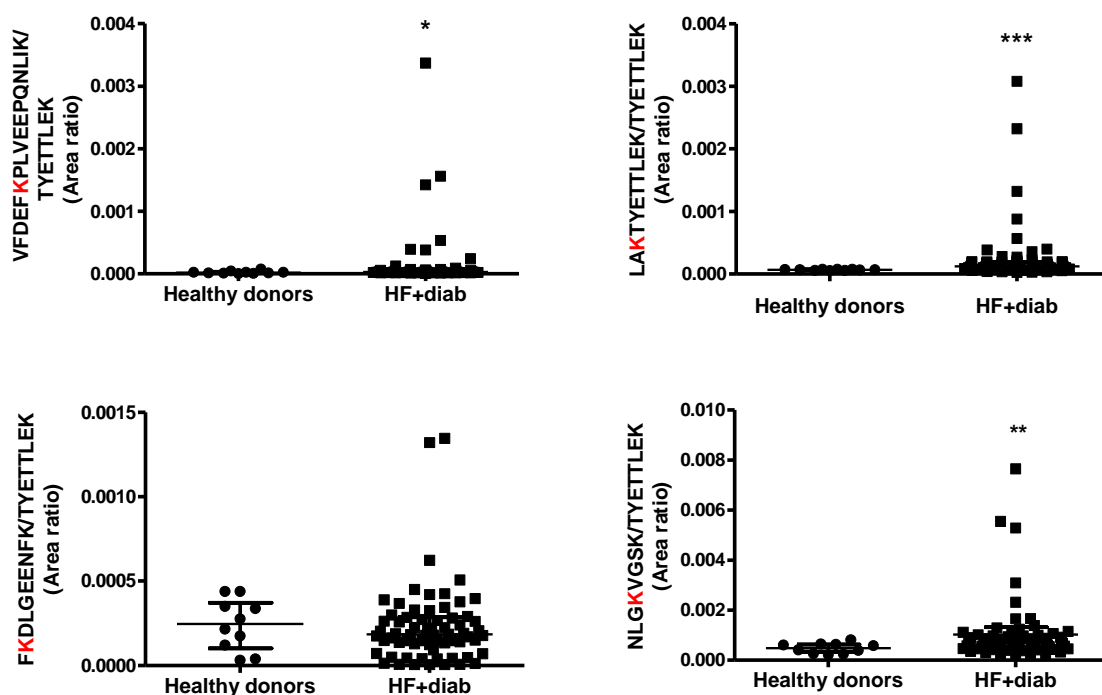


Figure 10. Uratylation of albumin is elevated in plasma of patients with heart failure and diabetes (HF+diab). Protein from plasma (10 μ L) of healthy donors (n=10) or patients with heart failure and diabetes (n=68) were denatured, reduced (5 mM, DTT), alkylated (15 mM, IAM) and digested with trypsin. Using SRM method, the mass transition of four tryptic peptides with a mass addition of 140 Da on lysine residues (**K**) and their respective unmodified peptides of albumin were assessed. All SRM data were processed using MultiQuant. The data are plotted as the area of the modified peptide divided by the unmodified peptide TYETTLEK. Plots show individual points and median with interquartile range. Significant difference was determined by non-parametric analyses using Mann Whitney and two-tailed p value (*p < 0.03; **p < 0.015; ***p < 0.0003).

Table 3. Pearson's correlation between uratylated peptides in serum albumin from patients with heart failure and diabetes.

Pearson correlation	LAKTYETTLEK/TYETTLEK		NLGKVGSK/TYETTLEK	
	r	p	r	p
LAKTYETTLEK/TYETTLEK (area ratio)			0.7799	< 0.0001
NLGKVGSK/TYETTLEK (area ratio)	0.7799	< 0.0001		
VFDEFKPLVEEPQNLIK/TYETTLEK (area ratio)	0.8293	< 0.0001	0.8709	< 0.0001
FKDLGEENFK/TYETTLEK (area ratio)	0.6656	< 0.0001	0.6492	< 0.0001
Pearson correlation	VFDEFKPLVEEPQNLIK/TYETTLEK		FKDLGEENFK/TYETTLEK	
	r	p	r	p
LAKTYETTLEK/TYETTLEK (area ratio)	0.8293	< 0.0001	0.6656	< 0.0001
NLGKVGSK/TYETTLEK (area ratio)	0.8709	< 0.0001	0.6492	< 0.0001
VFDEFKPLVEEPQNLIK/TYETTLEK (area ratio)			0.8041	< 0.0001
FKDLGEENFK/TYETTLEK (area ratio)	0.8041	< 0.0001		

The result is presented as the area ratio (modified peptide/unmodified TYETTLEK peptide).

Table 4. Pearson's correlation between uratylated peptides from serum albumin with myeloperoxidase, allantoin and uric acid of patients with heart failure and diabetes.

Pearson correlation	MPO (ng/mL)		Allantoin (μM)		Uric acid (μM)	
	r	p	r	p	r	p
LAKTYETTLEK/TYETTLEK (area ratio)	0.3232	0.0071	0.3983	0.0005	0.0931	0.2394
NLGKVGSK/TYETTLEK (area ratio)	0.3544	0.0030	0.4898	< 0.0001	0.2793	0.0153
VFDEFKPLVEEPQNLIK/TYETTLEK (area ratio)	0.3054	0.0113	0.4650	< 0.0001	0.1866	0.0766
FKDLGEENFK/TYETTLEK (area ratio)	0.3453	0.0039	0.5670	< 0.0001	0.1088	0.2038
MPO (ng/mL)			0.4508	< 0.0001	0.1513	0.1221
Allantoin (μM)	0.4508	< 0.0001			0.3059	0.0083

Area ratio of the modified peptides divided by the unmodified (TYETTLEK) peptide. The correlations were calculated using Pearson test and p value one tailed. Myeloperoxidase was measured by ELISA using a monoclonal antibody. Allantoin was analysed by mass spectrometry and uric acid was measured using HPLC with UV detection at 293 nm [45].

3.7 Uratylation is associated with heart failure and death

Next, we investigated whether uratylated peptides from albumin would correlate with a worst outcome in patients with heart failure. The cumulative survival was performed using Kaplan-Meier survival. Kaplan–Meier survival curves for N-terminal pro-brain natriuretic peptide (NT-proBNP, a marker of cardiac death and hospitalization for heart failure [46]), allantoin and modified peptides were compared between above and below median (high and low risk groups) using log-rank tests. The known biomarker in cardiovascular events NT-proBNP had a significant difference between the above and below median in death events (p=0.001) and when heart failure and death were combined (p=0.001), which validates the

model of analyses (**Figure 11**). The modified peptide LAK³⁷⁵TYETTLEK also had a significant difference between the above and below median either at death events ($p=0.049$) or heart failure and death ($p=0.027$). Allantoin had a very strong significant difference in death events ($p=0.006$) but not in heart failure and death ($p=0.143$) (**Figure 11**). These results demonstrated that uratylated peptides could be useful predictors of death and heart failure along with allantoin and other known biomarkers

Multivariate analyses were performed using a Cox regression model to correlate the markers with death (follow up 5.3 years, 29 events) and heart failure or death (follow up 2 years, 41 events). Cox regression was also used to determine independent associations between markers of oxidative stress and the risk factors: age, gender, ethnicity and NT-proBNP. A potential bivariate correlation was found between NT-proBNP and death ($p < 0.001$) and heart failure and death ($p < 0.001$) as well. Both uratylated peptides LAKTYETTLEK and NLGKVGSK were correlated with death ($p=0.004$ and $p=0.012$) and heart failure and death events together ($p=0.022$ and $p=0.006$). The levels of allantoin were strongly correlated with death only ($p < 0.001$) but not with heart failure and death event together ($p=0.103$).

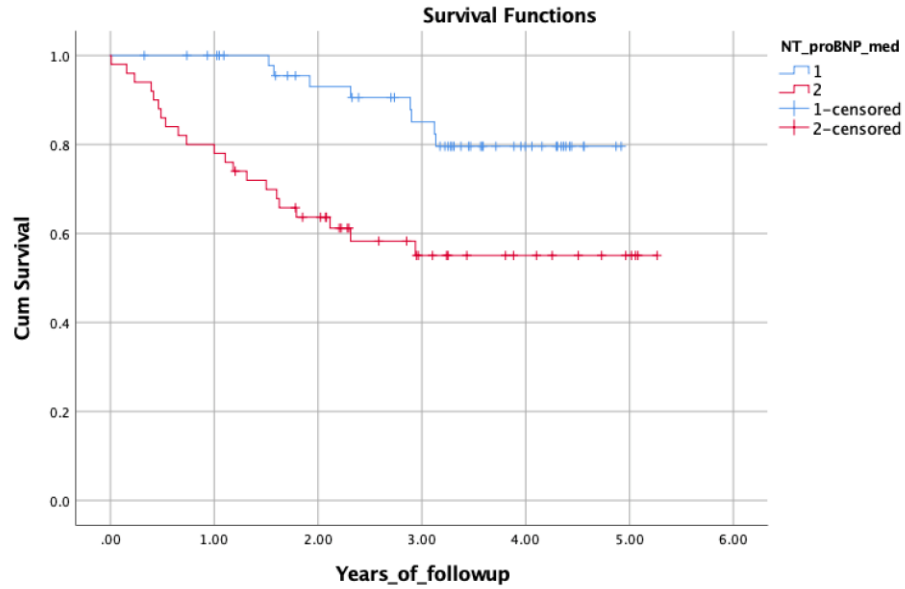
When we analysed the associations between allantoin, modified peptides or unmodified peptides and risk factors, we found a significant correlation of allantoin with NT-proBNP ($p=0.016$), age ($p=0.001$) and ethnicity (99 % European, $p=0.038$). The albumin modified peptides were not correlated with age, gender and NT-proBNP.

These data demonstrated, for the first time, that uratylation on lysine from albumin is strongly associated with heart failure and death event. These positive and significant correlations corroborate the increase in uratylated peptides in patients with heart failure and diabetes compared to healthy controls.

In conclusion, we have demonstrated that oxidation products of urate are formed in cardiovascular disease and can react with albumin to yield covalent adducts. The modification

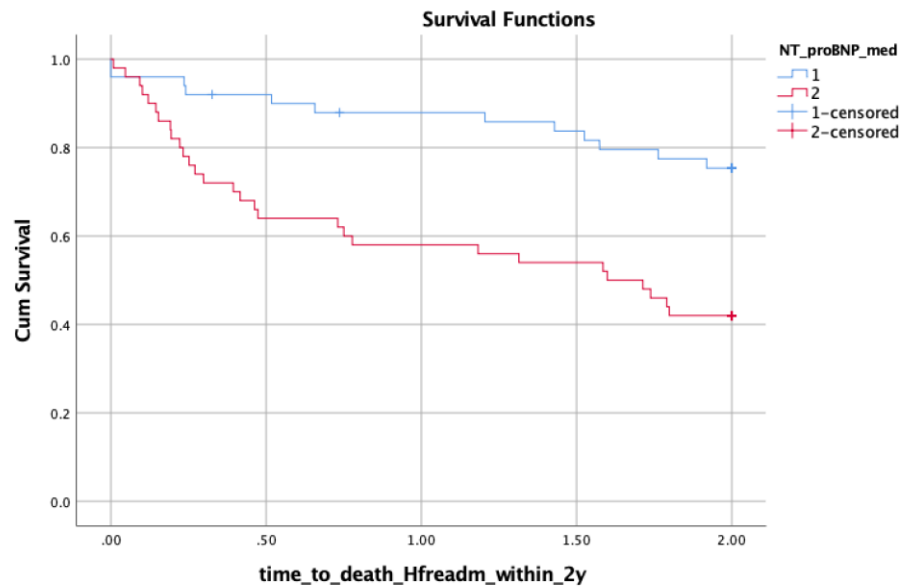
of albumin can alter protein function and contribute to vascular disease. This could explain, at least in part, the relationship between uric acid and cardiovascular disease.

NT-proBNP Death



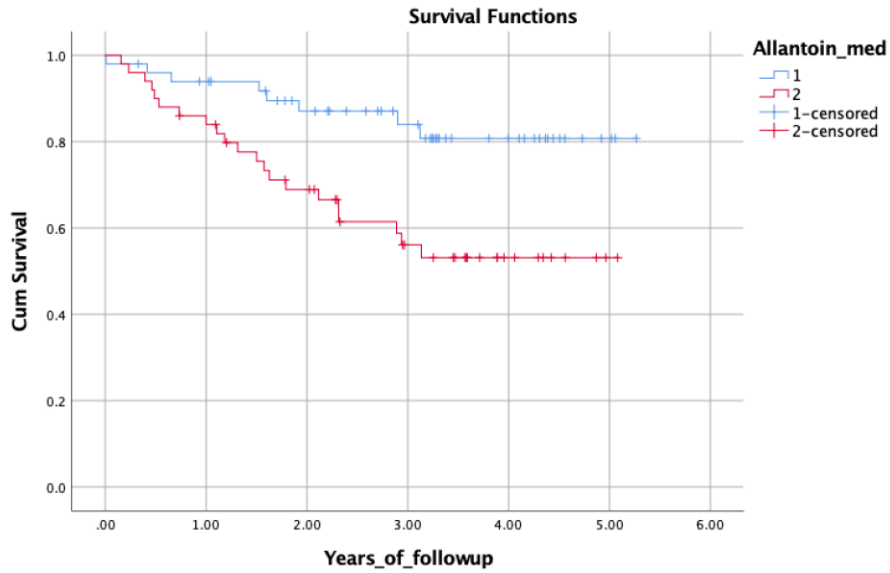
Log rank $p=0.001$
Cox reg. $p<0.001$

NT-proBNP HF death



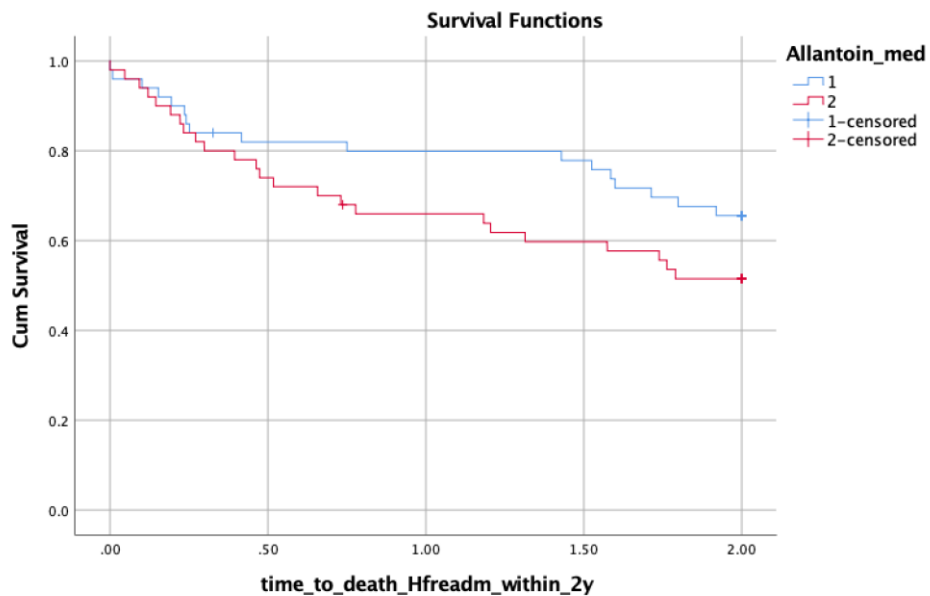
Log rank $p<0.001$
Cox reg. $p<0.001$

Allantoin Death



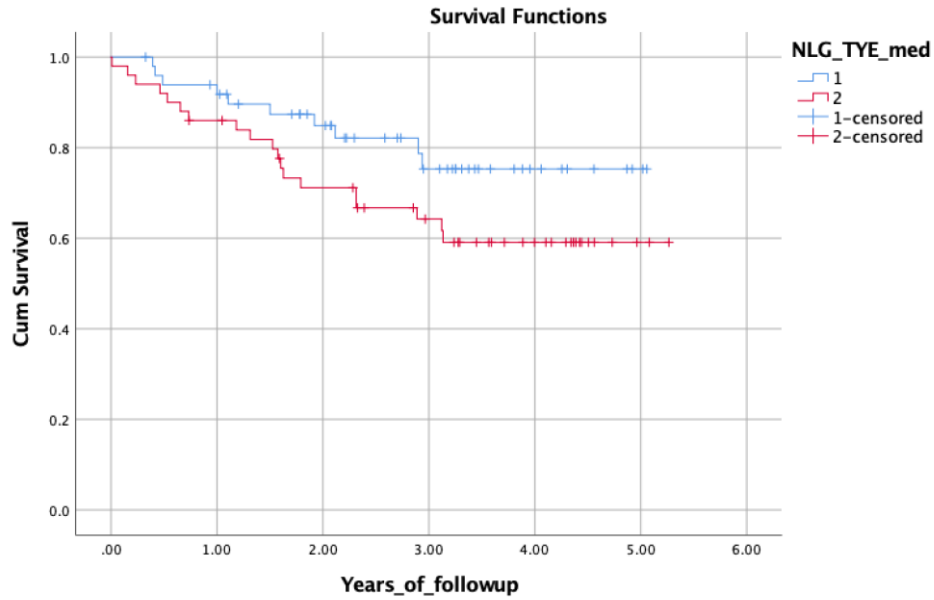
Log rank $p=0.006$
Cox reg. $p<0.001$

Allantoin HF or death



Log rank $p=0.143$
Cox reg. $p=0.103$

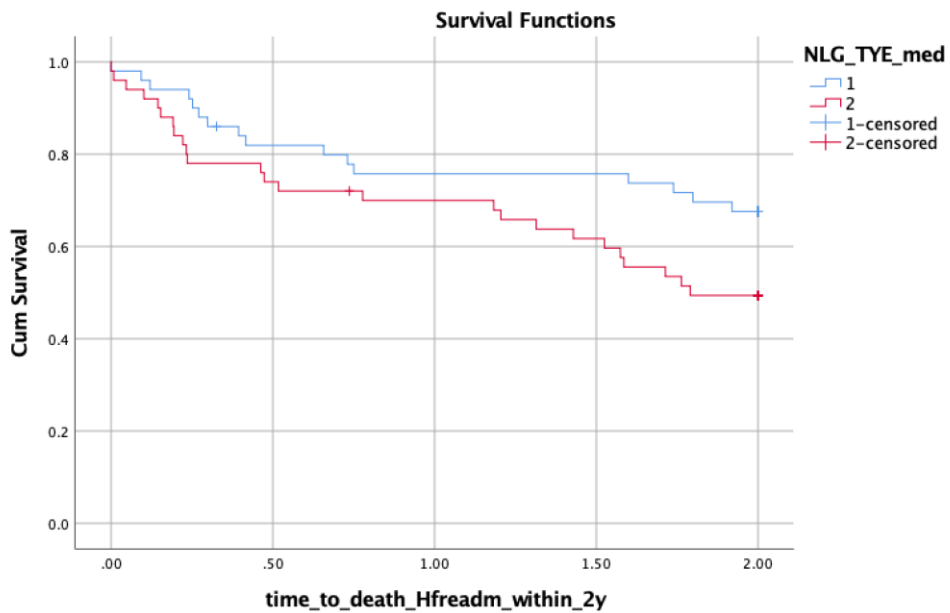
NLGKVGSK/TYETTLEK Death



Log rank $p=0.103$

Cox reg. $p=0.012$

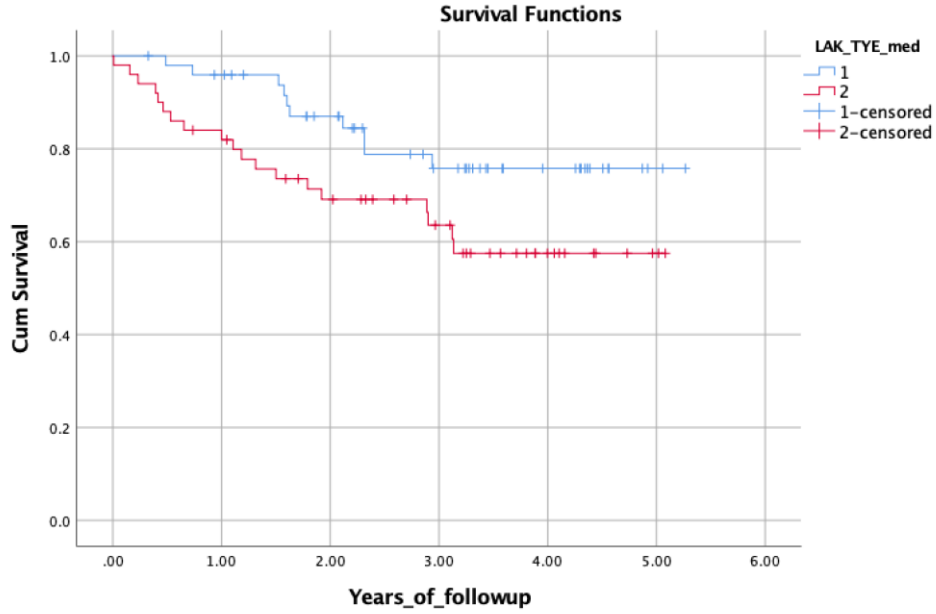
NLGKVGSK/TYETTLEK HF or death



Log rank $p=0.066$

Cox reg. $p=0.006$

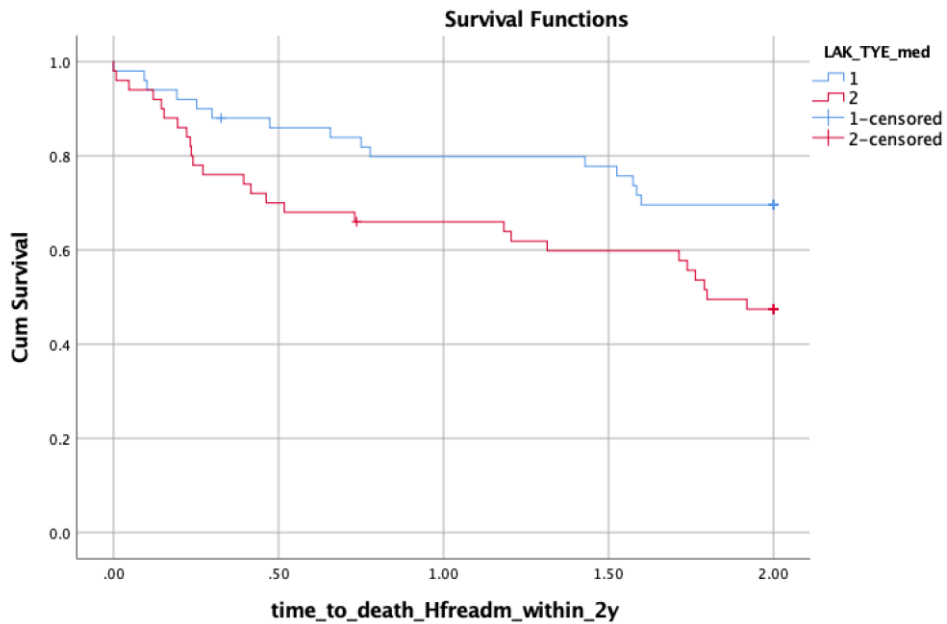
LAKTYETTLEK/TYETTLEK Death



Log rank p=0.049

Cox reg. p=0.004

LAKTYETTLEK/TYETTLEK HF or death



Log rank p=0.027

Cox reg. p=0.022

Figure 11. Uratylated peptides are correlated with death or heart failure and death events together (HF or death). A total of 100 patients were studied to cover the spectrum of HF severity. In those recruited, N-terminal pro-brain type natriuretic peptide (NT-proBNP), allantoin and two uratylated albumin peptides (**K + 140 Da**) were evaluated. Data of death events were available for all patients. The patients in death events were followed for up to 5.3 years and the patients within HF and death events group were followed for up to 2 years. Time to death was summarized using the standard Kaplan–Meier survival statistics for NT-proBNP, allantoin and uratylated peptides. For Kaplan-Meier analyses, the parameters were split above and below-median: 2 = above median, 1 = below median. Comparison between the above and below median were performed by Log rank and were considered statistically different at a p value < 0.05. Multivariable Cox regression model was also used to estimate the correlation between the markers and death or heart failure and death together with p < 0.05.

4. DISCUSSION

In this investigation, we propose that oxidation of uric acid generates reactive intermediates that can form adducts on lysine residues of albumin. We demonstrated a sensitive single-reaction monitoring mass spectrometry method to detect four uratylated tryptic peptides from plasma albumin. Using this method, our results showed that uratylated peptides levels are elevated in patients with heart failure and diabetes and it correlates with lower survival of patients with heart failure.

In addition, our findings reinforce a pro-oxidant role of uric acid in spite of several studies demonstrating its antioxidant properties and ability to neutralize a range of oxidants [4, 47, 48]. Intermediates from uric acid oxidation can inactivate redox sensitive enzymes like alpha-1-antiproteinase, alcohol dehydrogenase and glyceraldehyde phosphate dehydrogenase [28, 49, 50]. For example, the intermediate in uric acid oxidation, urate hydroperoxide, is able to oxidize glutathione, peroxiredoxin (Prx1 and Prx2) and endothelial cell surface protein disulphide isomerase-A1 (PDI) in different cells [15, 39, 51]. In this context, urate oxidation may contribute to a redox imbalance toward a more oxidant environment and exert a role in redox signalling.

Here, we found that inhibition of myeloperoxidase completely prevented the increase in uratylated peptides, suggesting that the products generated during uric acid oxidation rather than uric acid itself induces uratylation. Therefore, the oxidizing role of uric acid becomes more evident when urate undergo one electron abstraction through heme-peroxidases, as myeloperoxidase, generating urate free radical [9]. The fate of urate free radical depends on the environment. When high levels of urate free radical are produced and no other reductant is nearby, two urate radicals react with each other in a one-electron transference producing dehydrourate and uric acid. Dehydrourate can be hydrated to form hydroxyisourate [16]. In opposite, in the presence of superoxide, as occur in inflammatory conditions, superoxide can quickly be added to urate free radical yielding urate hydroperoxide [9, 13, 14]. Therefore, it is

expected that in presence of SOD, urate free radical will predominantly dismutate to dehydrourate than to produce urate hydroperoxide.

Interestingly, our results show the hydroxyisourate generated from the dismutation of urate free radical followed by hydration of dehydrourate is much more reactive upon the ϵ amine from lysine residues than the hydroxyisourate originated from urate hydroperoxide reduction. It is possible that these two sources generate different isomers of hydroxyisourate with different reactivity towards albumin and further studies are on the way to identify it.

Oppositely to our results, SOD decreased the amount of uratylated peptides in plasma albumin incubated with activated neutrophils [28]. One possible explanation for this is the high amount of ascorbate in neutrophils [52]. Ascorbate can donate one-electron to urate free radical and diminish the formation of hydroxyisourate [53].

Myeloperoxidase is associated with progression of inflammation and cardiovascular disease [25, 34, 54] and we demonstrated that uratylated peptides of albumin correlate with myeloperoxidase levels in plasma of patients with heart failure and diabetes. Thus, oxidation of uric acid by myeloperoxidase and urate free radical formation could be an event preponderant during inflammation and an important mechanism by which uric acid causes tissue damage.

Modifications on albumin by hypochlorous acid causes increased expression of adhesion molecules in endothelial cells, a process that involves NADPH oxidase activation [55]. In patients undergoing dialysis, high levels of modified albumin independently correlate with increased oxidative stress markers and decreased vasodilation response [56]. These data support an endothelial damage caused by HOCl-modified albumin and could also mirror an effect of uratylated-albumin. In this context, the oxidative stress caused by uric acid could explain tissue damage, exacerbation of inflammation and, finally, the positive clinical correlation between uric acid levels and cardiovascular disease.

There are several clinical studies that demonstrated a positive correlation between plasma uric acid levels and the development of cardiovascular disease [57, 58]. In addition, there is an intense debate whether hyperuricemia is an independent risk factor or only reinforces others classical risk factors such as dyslipidemia and metabolic syndrome [58, 59]. Based on this and on previous findings from our group [31], urate oxidation rather than urate level itself is a stronger indicator for cardiovascular disease.

5. CONCLUSION

In conclusion, we showed that urate is oxidized during heart failure and that the presence of uratylated serum albumin could be a valuable marker in cardiovascular disease. The strong association between uratylated serum albumin and worst outcome in heart failure suggests that uric acid can contribute to the pathology of this disease. Together, these clinical and mechanistic studies support a role for uric acid in inflammatory process.

6. REFERENCES

1. Wright, A.F., et al., *A 'complexity' of urate transporters*. *Kidney Int*, 2010. **78**(5): p. 446-52.
2. So, A. and B. Thorens, *Uric acid transport and disease*. *J Clin Invest*, 2010. **120**(6): p. 1791-9.
3. Ekelund, U.E., et al., *Intravenous allopurinol decreases myocardial oxygen consumption and increases mechanical efficiency in dogs with pacing-induced heart failure*. *Circ Res*, 1999. **85**(5): p. 437-45.
4. Ames, B.N., et al., *Uric acid provides an antioxidant defense in humans against oxidant- and radical-caused aging and cancer: a hypothesis*. *Proc Natl Acad Sci U S A*, 1981. **78**(11): p. 6858-62.
5. Johnson, R.J. and B.A. Rideout, *Uric acid and diet--insights into the epidemic of cardiovascular disease*. *N Engl J Med*, 2004. **350**(11): p. 1071-3.
6. Becker, B.F., *Towards the physiological function of uric acid*. *Free Radic Biol Med*, 1993. **14**(6): p. 615-31.
7. Santos, C.X., E.I. Anjos, and O. Augusto, *Uric acid oxidation by peroxynitrite: multiple reactions, free radical formation, and amplification of lipid oxidation*. *Arch Biochem Biophys*, 1999. **372**(2): p. 285-94.
8. Maples, K.R. and R.P. Mason, *Free radical metabolite of uric acid*. *J Biol Chem*, 1988. **263**(4): p. 1709-12.
9. Meotti, F.C., et al., *Urate as a physiological substrate for myeloperoxidase: implications for hyperuricemia and inflammation*. *J Biol Chem*, 2011. **286**(15): p. 12901-11.
10. Davies, M.J., *Myeloperoxidase-derived oxidation: mechanisms of biological damage and its prevention*. *J Clin Biochem Nutr*, 2011. **48**(1): p. 8-19.
11. Winterbourn, C.C. and A.J. Kettle, *Redox reactions and microbial killing in the neutrophil phagosome*. *Antioxid Redox Signal*, 2013. **18**(6): p. 642-60.
12. Winterbourn, C.C. and A.J. Kettle, *Biomarkers of myeloperoxidase-derived hypochlorous acid*. *Free Radic Biol Med*, 2000. **29**(5): p. 403-9.
13. Silva, R.P., et al., *Identification of urate hydroperoxide in neutrophils: A novel pro-oxidant generated in inflammatory conditions*. *Free Radic Biol Med*, 2018. **126**: p. 177-186.
14. Santus, R., et al., *Redox reactions of the urate radical/urate couple with the superoxide radical anion, the tryptophan neutral radical and selected flavonoids in neutral aqueous solutions*. *Free Radic Res*, 2001. **35**(2): p. 129-36.
15. Patricio, E.S., et al., *Chemical Characterization of Urate Hydroperoxide, A Pro-oxidant Intermediate Generated by Urate Oxidation in Inflammatory and Photoinduced Processes*. *Chem Res Toxicol*, 2015. **28**(8): p. 1556-66.
16. Volk, K.J., R.A. Yost, and A. Brajter-Toth, *On-line electrochemistry/thermospray/tandem mass spectrometry as a new approach to the study of redox reactions: the oxidation of uric acid*. *Anal Chem*, 1989. **61**(15): p. 1709-17.
17. Seet, R.C., et al., *Oxidative damage in ischemic stroke revealed using multiple biomarkers*. *Stroke*, 2011. **42**(8): p. 2326-9.
18. Stamp, L.K., et al., *Myeloperoxidase and oxidative stress in rheumatoid arthritis*. *Rheumatology (Oxford)*, 2012. **51**(10): p. 1796-803.
19. Stamp, L.K., et al., *Myeloperoxidase and oxidation of uric acid in gout: implications for the clinical consequences of hyperuricaemia*. *Rheumatology (Oxford)*, 2014. **53**(11): p. 1958-65.
20. Chung, W.Y. and I.F. Benzie, *Plasma allantoin measurement by isocratic liquid chromatography with tandem mass spectrometry: method evaluation and application in oxidative stress biomonitoring*. *Clin Chim Acta*, 2013. **424**: p. 237-44.
21. Dickerhof, N., et al., *Oxidized glutathione and uric acid as biomarkers of early cystic fibrosis lung disease*. *J Cyst Fibros*, 2017. **16**(2): p. 214-221.
22. Baldus, S., et al., *Myeloperoxidase serum levels predict risk in patients with acute coronary syndromes*. *Circulation*, 2003. **108**(12): p. 1440-5.

23. Mocatta, T.J., et al., *Plasma concentrations of myeloperoxidase predict mortality after myocardial infarction*. J Am Coll Cardiol, 2007. **49**(20): p. 1993-2000.
24. Vita, J.A., et al., *Serum myeloperoxidase levels independently predict endothelial dysfunction in humans*. Circulation, 2004. **110**(9): p. 1134-9.
25. Ndrepepa, G., *Myeloperoxidase - A bridge linking inflammation and oxidative stress with cardiovascular disease*. Clin Chim Acta, 2019. **493**: p. 36-51.
26. Wilkie-Grantham, R.P., et al., *Myeloperoxidase-dependent lipid peroxidation promotes the oxidative modification of cytosolic proteins in phagocytic neutrophils*. J Biol Chem, 2015. **290**(15): p. 9896-905.
27. Podrez, E.A., H.M. Abu-Soud, and S.L. Hazen, *Myeloperoxidase-generated oxidants and atherosclerosis*. Free Radic Biol Med, 2000. **28**(12): p. 1717-25.
28. Turner, R., et al., *Conjugation of urate-derived electrophiles to proteins during normal metabolism and inflammation*. J Biol Chem, 2018. **293**(51): p. 19886-19898.
29. Magon, N.J., et al., *Oxidation of calprotectin by hypochlorous acid prevents chelation of essential metal ions and allows bacterial growth: Relevance to infections in cystic fibrosis*. Free Radic Biol Med, 2015. **86**: p. 133-44.
30. Turner, R., et al., *Conjugation of urate-derived electrophiles to proteins during normal metabolism and inflammation*. 2018. **293**(51): p. 19886-19898.
31. Santana, M.S., et al., *Allantoin as an independent marker associated with carotid intima-media thickness in subclinical atherosclerosis*. Braz J Med Biol Res, 2018. **51**(8): p. e7543.
32. Shi, Y., J.E. Evans, and K.L. Rock, *Molecular identification of a danger signal that alerts the immune system to dying cells*. Nature, 2003. **425**(6957): p. 516-21.
33. Strasak, A., et al., *Serum uric acid and risk of cardiovascular mortality: a prospective long-term study of 83,683 Austrian men*. Clin Chem, 2008. **54**(2): p. 273-84.
34. Nicholls, S.J. and S.L. Hazen, *Myeloperoxidase and cardiovascular disease*. Arterioscler Thromb Vasc Biol, 2005. **25**(6): p. 1102-11.
35. Kanellis, J., et al., *Uric acid stimulates monocyte chemoattractant protein-1 production in vascular smooth muscle cells via mitogen-activated protein kinase and cyclooxygenase-2*. Hypertension, 2003. **41**(6): p. 1287-93.
36. Lippi, G., et al., *The paradoxical relationship between serum uric acid and cardiovascular disease*. Clin Chim Acta, 2008. **392**(1-2): p. 1-7.
37. Beyer, W.F., Jr. and I. Fridovich, *Assaying for superoxide dismutase activity: some large consequences of minor changes in conditions*. Anal Biochem, 1987. **161**(2): p. 559-66.
38. Brennan, S.O., et al., *Unique albumin with two silent substitutions (540Thr-->Ala and 546Ala-->Ser): Insights into how albumin is recycled*. Clin Chim Acta, 2016. **457**: p. 125-9.
39. Mineiro, M.F., et al., *Urate hydroperoxide oxidizes endothelial cell surface protein disulfide isomerase-A1 and impairs adherence*. Biochim Biophys Acta Gen Subj, 2020. **1864**(3): p. 129481.
40. McKee, P.A., et al., *The natural history of congestive heart failure: the Framingham study*. N Engl J Med, 1971. **285**(26): p. 1441-6.
41. Cameron, V.A., et al., *Angiotensin type-1 receptor A1166C gene polymorphism correlates with oxidative stress levels in human heart failure*. Hypertension, 2006. **47**(6): p. 1155-61.
42. Chapman, A.L., et al., *Ceruloplasmin is an endogenous inhibitor of myeloperoxidase*. J Biol Chem, 2013. **288**(9): p. 6465-77.
43. Lam, C.S.P., et al., *Mortality associated with heart failure with preserved vs. reduced ejection fraction in a prospective international multi-ethnic cohort study*. Eur Heart J, 2018. **39**(20): p. 1770-1780.
44. Clausen, M.R., et al., *Characterization of peroxides formed by riboflavin and light exposure of milk. Detection of urate hydroperoxide as a novel oxidation product*. J Agric Food Chem, 2010. **58**(1): p. 481-7.

45. Kandar, R., P. Drabkova, and R. Hampl, *The determination of ascorbic acid and uric acid in human seminal plasma using an HPLC with UV detection*. J Chromatogr B Analyt Technol Biomed Life Sci, 2011. **879**(26): p. 2834-9.
46. Doehner, W., et al., *Uric acid and xanthine oxidase in heart failure - Emerging data and therapeutic implications*. Int J Cardiol, 2016. **213**: p. 15-9.
47. Kaur, H. and B. Halliwell, *Action of biologically-relevant oxidizing species upon uric acid. Identification of uric acid oxidation products*. Chem Biol Interact, 1990. **73**(2-3): p. 235-47.
48. Ford, E., M.N. Hughes, and P. Wardman, *Kinetics of the reactions of nitrogen dioxide with glutathione, cysteine, and uric acid at physiological pH*. Free Radic Biol Med, 2002. **32**(12): p. 1314-23.
49. Aruoma, O.I. and B. Halliwell, *Inactivation of alpha 1-antiproteinase by hydroxyl radicals. The effect of uric acid*. FEBS Lett, 1989. **244**(1): p. 76-80.
50. Kittridge, K.J. and R.L. Willson, *Uric acid substantially enhances the free radical-induced inactivation of alcohol dehydrogenase*. FEBS Lett, 1984. **170**(1): p. 162-4.
51. Carvalho, L.A.C., et al., *Urate hydroperoxide oxidizes human peroxiredoxin 1 and peroxiredoxin 2*. J Biol Chem, 2017. **292**(21): p. 8705-8715.
52. Winterbourn, C.C. and M.C. Vissers, *Changes in ascorbate levels on stimulation of human neutrophils*. Biochim Biophys Acta, 1983. **763**(2): p. 175-9.
53. Frei, B., R. Stocker, and B.N. Ames, *Antioxidant defenses and lipid peroxidation in human blood plasma*. Proc Natl Acad Sci U S A, 1988. **85**(24): p. 9748-52.
54. Anatoliotakis, N., et al., *Myeloperoxidase: expressing inflammation and oxidative stress in cardiovascular disease*. Curr Top Med Chem, 2013. **13**(2): p. 115-38.
55. Tang, D.D., et al., *Hypochlorite-Modified Albumin Upregulates ICAM-1 Expression via a MAPK-NF-kappaB Signaling Cascade: Protective Effects of Apocynin*. Oxid Med Cell Longev, 2016. **2016**: p. 1852340.
56. Kocak, H., et al., *Advanced oxidative protein products are independently associated with endothelial function in peritoneal dialysis patients*. Nephrology (Carlton), 2009. **14**(3): p. 273-80.
57. Wang, H., et al., *Longitudinal association between serum urate and subclinical atherosclerosis: the Coronary Artery Risk Development in Young Adults (CARDIA) study*. J Intern Med, 2013. **274**(6): p. 594-609.
58. Feig, D.I., D.H. Kang, and R.J. Johnson, *Uric acid and cardiovascular risk*. N Engl J Med, 2008. **359**(17): p. 1811-21.
59. White, J., et al., *Plasma urate concentration and risk of coronary heart disease: a Mendelian randomisation analysis*. Lancet Diabetes Endocrinol, 2016. **4**(4): p. 327-36.

7. SUPPLEMENTARY

Table S1. Mass spectrometer parameters in the single reaction monitoring of peptides from human serum albumin.

Modified Peptide (K -140 Da)	Charge	<i>m/z</i> (Precursor ion)	<i>m/z</i> (Fragment)	DP	CE (volts)
VFDEF K PLVEEPQNLIK	+ 3	729.04	712.44	120	38
LA K TYETTLEK	+ 3	479.58	591.34	50	30
F K DLGEENFK	+ 2	683.82	951.44	120	38
NLG K VGSK	+ 2	471.76	200.14	80	30

unmodified Peptide	Charge	<i>m/z</i> (Precursor ion)	<i>m/z</i> (Fragment)	DP	CE (volts)
VFDEFKPLVEEPQNLIK	+ 3	682.33	889.98	50	30
TYETTLEK	+ 2	492.75	720.38	50	30
DLGEENFK	+ 2	476.23	723.33	50	30
NLGK	+ 1	431.26	317.22	50	30

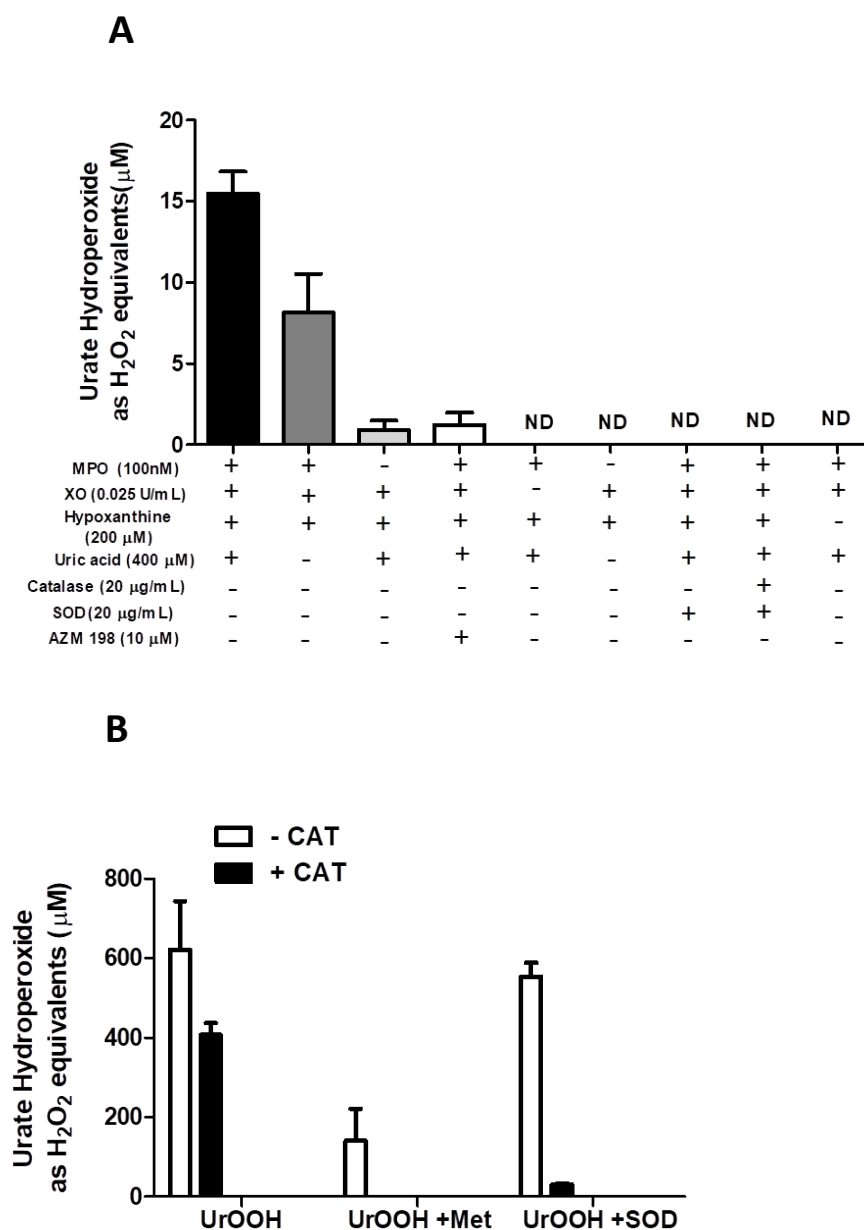


Figure S1. Synthesis of urate hydroperoxide by enzymes and by photo-oxidation. (A) Urate hydroperoxide was obtained by the oxidation of uric acid by myeloperoxidase (MPO) in presence of xanthine oxidase (XO) and hypoxanthine in phosphate buffer (50 mM; pH 7.4). (B) Urate hydroperoxide was produced using urate (1.5 mM) and riboflavin (40 µM) under UV radiation in the presence or absence of SOD (200 µg/mL) in phosphate buffer (10 mM; pH 6). Methionine (2 mM) was added after urate hydroperoxide production and incubated for 5 min at 22°C. The concentration of urate hydroperoxide was measured by FOX assay in the presence or absence of catalase (CAT, 100 µg/mL). Concentrations were determined from a standard curve with hydrogen peroxide (H₂O₂). Graphs represent mean ± SD of five (A) or two (B) independent experiments. ND: not detected.

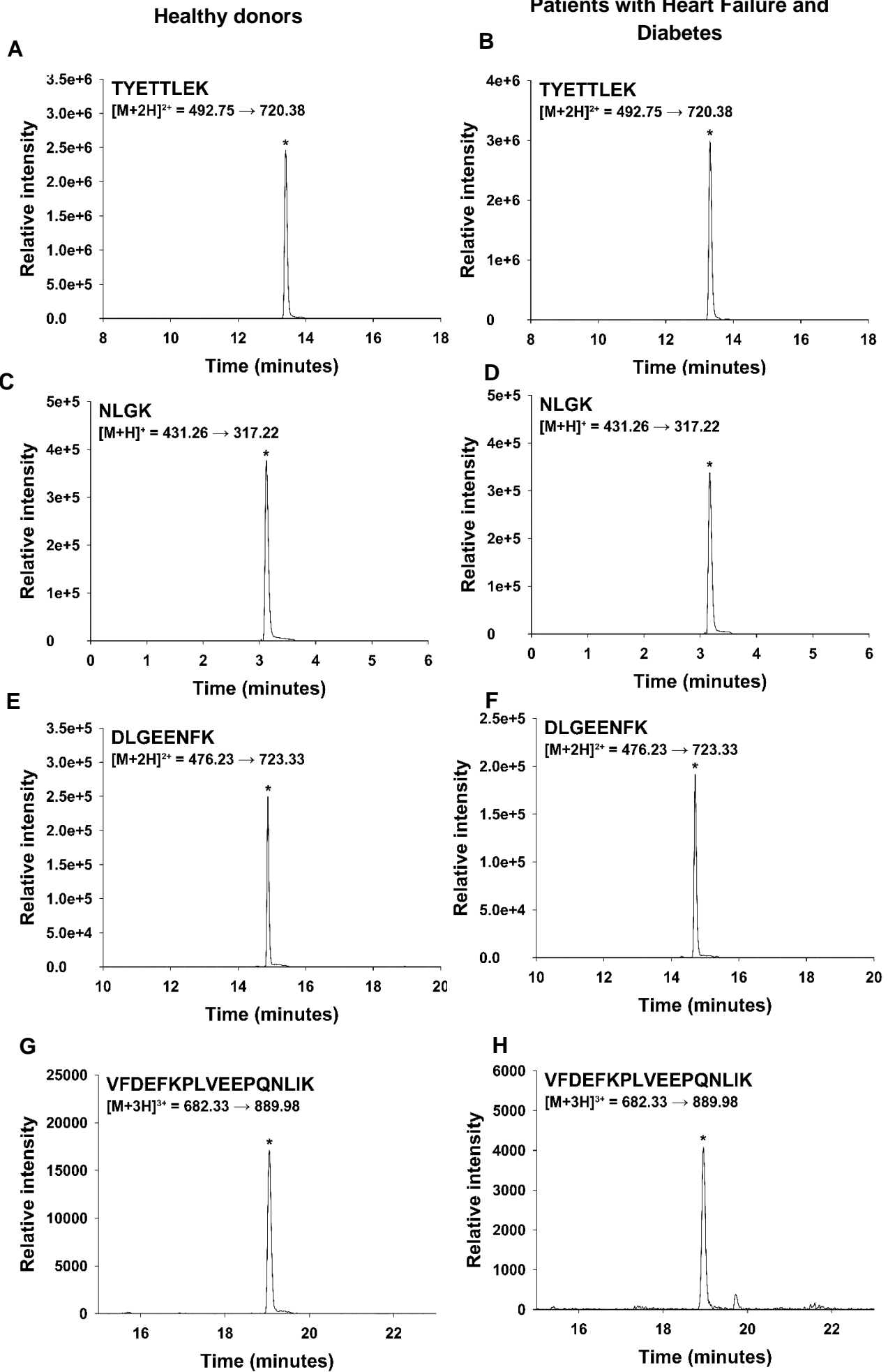


Figure S2. Detection of unmodified peptides of serum albumin from healthy donors and patients with heart failure and Diabetes (HF+diab). Protein from plasma (10 μ L) of healthy donors or patients with heart failure and diabetes were denatured, reduced (5 mM, DTT), alkylated (15 mM, IAM) and digested with trypsin. Then, the mass transition of four tryptic peptides in healthy donors (A; C; E. G) and in patients with heart failure and diabetes (B; D; F; G) were monitored. The retention time was used to confirm the specificity of the identified ions.

CHAPTER 3

**Uric Acid Promotes Oxidative Modification in Neutrophils and Plasma of
Septic Patients.**

Railmara P. da Silva^{1,2}, Marcos Yoshinaga¹, Anitra C. Carr², Anthony J. Kettle³

Flavia C. Meotti¹

*¹Departamento de Bioquímica, Instituto de Química, Universidade de São Paulo,
São Paulo, Brazil*

*²Nutrition in Medicine Research Group, Department of Pathology and Biomedical Science,
University of Otago, Christchurch, New Zealand*

*³Centre for Free Radical Research, Department of Pathology and Biomedical Science,
University of Otago, Christchurch, Christchurch, New Zealand*

ABSTRACT

The production of reactive intermediates in the oxidation of uric acid is an important event during the inflammatory oxidative burst. These intermediates can oxidize thiol proteins and react with plasma albumin to form covalent adducts. The oxidation of uric acid by neutrophils decreases the production of hypochlorous acid due to the competition between uric acid and chloride by myeloperoxidase and this disturbed the killing activity of these cells against *Pseudomonas aeruginosa*. However, the role of uric acid oxidation in sepsis or other infectious diseases has not been investigated. Moreover, the exact mechanisms on how uric acid could affect the inflammatory response in infection is still unknown. In this study, we investigated the oxidation of uric and its effects on protein and lipid profile in infectious process. Our results demonstrated that the oxidation of uric acid promoted the increase of urate-derived adducts in plasma albumin of septic patients and their levels were correlated with allantoin, the stable end product of uric acid oxidation. Allantoin was also significantly augmented in neutrophils infected with *Pseudomonas aeruginosa* in the presence of urate and its levels were directly dependent on the concentration of uric acid, on the activity of myeloperoxidase and in the activity of superoxide. Uric acid also increased the oxidation of glutathione in neutrophils infected with *Pseudomonas aeruginosa* and the glutathionylation of important proteins, such as calprotectin (S100A8). Interestingly, the oxidative power of uric acid induced an increase of triacylglycerols (TAGs) in neutrophils, modulating lipid profile in the infection process. Therefore, our data corroborated previous data reinforcing the pro-oxidant effect of uric acid in inflammatory and infection conditions and propose a causal role for uric acid in the progression of inflammatory-related diseases. The monitoring of allantoin and uratylated peptides from albumin can be a useful tool in the prognosis of infectious disease.

KEY WORDS: Uric acid, Neutrophils, *Pseudomonas aeruginosa*, Sepsis.

1. INTRODUCTION

Uric acid (7,9-dihydro-1H-purine-2,6,8(3H)-trione) is the end product of purine metabolism in humans and some primates and accumulates in their plasma at higher concentrations than in other mammals [1]. The repression of the enzyme that decomposes uric acid, uricase, was thought to be an evolutionary advantage, because uric acid is a facile electron donor, and so, a good antioxidant [2, 3]. In spite of being considered the main antioxidant in plasma, the one-electron oxidation of uric acid by free radicals or heme-peroxidases generates urate free radical [4-6], which can trigger a free radical chain reaction.

Uric acid exacerbates inflammation and is associated with hypertension, nephritis, gout and atherosclerosis [7-12]. This metabolite can increase cellular oxidative damage by inducing superoxide production through NADPH oxidase (NOX) [13, 14] and amplify lipoperoxidation after reaction with peroxynitrite decomposition products [4]. In addition, uric acid can act as a DAMP (damage-associated molecular pattern) activating inflammatory cells [15], the recruitment of neutrophils [16], formation of NETs (neutrophil extracellular traps) and precipitation of crystals in the joints [17]. Despite these evidences, the exact mechanism on how soluble uric acid activates inflammatory cells is still unknown.

A previous study showed that uric acid is an important substrate for the pro-inflammatory enzyme myeloperoxidase [6], a peroxidase released from neutrophils and responsible for the synthesis of hypochlorous acid, an important microbicide [18, 19]. We have demonstrated that the oxidation of uric acid by myeloperoxidase generates the highly reactive intermediate urate free radical. In this same inflammatory environment, urate free radical combines with superoxide to generate another strong oxidant, urate hydroperoxide [20, 21]. This is particularly relevant at the inflammatory site, e.g. atheroma plaque or in infections, where there are plenty amount of inflammatory peroxidases, superoxide, hydrogen peroxide and uric acid.

In a recent study, we showed that the oxidation of uric acid by myeloperoxidase disrupted the formation of hypochlorous acid and dampened the killing activity of inflammatory cells against *Pseudomonas aeruginosa*, an opportunistic resistant bacteria involved in hospital infection and in cystic fibrosis [22]. This data was further supported by clinical studies that revealed a positive correlation between uric acid levels, its oxidation and worse outcome in patients with cystic fibrosis infected with *Pseudomonas aeruginosa* [23]. Additionally, other authors have found a positive correlation between plasma uric acid and a worse prognosis in sepsis, a severe infection associated with organ dysfunction that induces a high mortality [24-27].

Parallel to the disruption in hypochlorous acid formation, the oxidation of uric acid and subsequent formation of urate free radical and urate hydroperoxide maintains a pro-oxidant environment which may further exacerbate inflammation. The products of uric acid oxidation form stable adducts in lysine residues of plasma albumin [28], altering its native structure. In addition, urate hydroperoxide oxidizes thiols in glutathione [20], peroxiredoxins [29] and protein disulfide isomerase (PDI) [30]. The oxidation of extracellular surface PDI from endothelial cells by urate hydroperoxide impaired cellular adherence [30] and could contribute to alterations in vascular homeostasis

Together, these clinical and mechanistic studies support a role for uric acid in inflammatory and infectious processes. However, the correlation between the oxidation of uric acid and sepsis or other infectious diseases has not been investigated so far. In this study, we show that oxidation of uric acid leads to the formation of urate-derived adducts in plasma albumin of patients with sepsis, contributes to protein glutathionylation, increase in glutathione disulphide and alters lipid profile in neutrophils infected with *Pseudomonas aeruginosa*. Therefore, our data opens up a new insight into the mechanisms by which uric acid can propagate oxidative stress in infectious disease.

2. MATERIALS AND METHOD

2.1. Clinical samples

The ill patients were admitted to the Christchurch Hospital ICU, Christchurch, New Zealand (December 2015–August 2016) [31]. All procedures involving human individuals were approved by the New Zealand Southern Health and Disability Ethics Committee. The ill patients aged ≥ 18 years admitted to the Christchurch Hospital ICU were fit, except for those patients who did not survive up to 72 hours or when the consent form could not be obtained. The criteria to include patients in the septic group were: receiving intravenous antimicrobial therapy for infection, receiving ≥ 5 $\mu\text{g}/\text{min}$ of noradrenaline or adrenaline, evidence of organ dysfunction based on the Sequential Assessment of Organic Failure (SOFA) score by at least one of them: respiratory function (ratio of partial arterial oxygen pressure and inspired oxygen fraction $[\text{PaO}_2/\text{FiO}_2] < 300$), liver function (bilirubin > 33 $\mu\text{mol}/\text{L}$), coagulation (platelets $< 100 \times 10^9/\text{L}$) and renal function (creatinine > 171 $\mu\text{mol}/\text{L}$)[32]. The number of septic patients admitted were eighteen ($n=18$) and the number of donors healthy were ten ($n=10$).

2.2. Human cell culture

Human leukemic cells of myeloid origin (HL-60; BCRJ, RJ, Brazil) were maintained in RPMI 1640 culture medium, supplemented with fetal bovine serum (FBS 20%), streptomycin (100 $\mu\text{g}/\text{mL}$) and penicillin (100 U/mL), in humidified atmosphere at 37°C and 5% CO_2 . The desired concentration of HL-60 cells was differentiated into neutrophils (dHL-60) by the addition of dimethyl sulfoxide (1.3% DMSO) in the same culture medium, but supplemented with only 10% FBS. The cells were kept in this medium for 4 days, under the same temperature and atmosphere conditions mentioned. To carry out the experiments, the cells were washed once with PBS/glucose (10 mM phosphate buffer; 137 mM NaCl, 1 mM CaCl_2 , 0.5 mM MgCl_2 ,

1 g/L glucose). Subsequently, cell suspension was centrifuged for 10 min at 1400 rpm, the supernatant was discarded and cells were suspended in PBS/glucose for the experiments.

Purified neutrophils were isolated from human blood (healthy donors) by histopaque density gradient centrifugation and sedimentation with dextran [32]. The experiments with blood neutrophils were previously approved by the ethical committee (CEPSH-ICB1435/18). After purification, neutrophils were suspended in PBS/glucose and the reduction of cytochrome *c* was taken after cells activation with phorbol 12-myristate 13-acetate (PMA, 100 ng/mL). The rate of superoxide production was around 2.5 and 5 $\mu\text{M}/\text{min}$ per million cells for dHL-60 and blood neutrophils, respectively.

2.3. Bacterial cell culture

Pseudomonas aeruginosa (strain PA14) were cultured in Luria-Bertani (LB) medium overnight at 37°C under 200 rpm agitation. After this period, they were diluted in 1 mL LB medium to $\text{OD}_{600\text{nm}} = 0.1$ and incubated at 37°C again until reaching stationary phase, (approximately 5 h). Afterwards the bacteria were centrifuged at $1700 \times g$ for 10 min and the pellet was suspended in PBS/glucose (1 mL).

The infection assays with purified peripheral blood neutrophils were performed with opsonized *Pseudomonas aeruginosa*. The bacteria (1×10^9) were opsonized in 10% inactivated autologous serum for 20 min at 37°C. After that, the bacterial were centrifuged at $1700 \times g$ for 5 min and washed with PBS. The experiments with inflammatory cells in the presence or absence of uric acid were performed using multiplicity of infection 10 (MOI 10).

2.4. Quantification of allantoin in plasma

Allantoin from plasma of healthy donors and septic patients was measured by liquid chromatography tandem mass spectrometry using stable isotope dilution (LC/MS/MS), as described

previously [33]. Control samples were also prepared to discard allantoin artefacts from sample preparation as described by Turner et al 2012 [33].

2.5. Quantification of urate-derived adducts on human serum albumin in patients with sepsis

To identify and quantify urate-derived adducts in lysine residues from serum albumin, the protein was digested with trypsin as described in the previous paper of this thesis. Plasma protein (50 µg) was denatured with 100 mM ammonium bicarbonate solution containing 6 mM guanidinium chloride for 30 min at 25°C and shaking (400 rpm). After incubation, the plasma proteins were reduced by DTT (5 mM) for one hour at 37°C before alkylation with iodoacetamide (15 mM, 30 min in the dark, at 25°C, shaking 400 rpm). After alkylation, DTT (2 mM) was added to scavenge iodoacetamide (15 min at 25°C). Finally, trypsin was added to a ratio of 1:40 (w/w) and incubated at 37°C. After 4 hours a second dose of trypsin (1:80, w/w) was added and incubated at 37°C overnight. Samples were lyophilized and the tryptic peptides were resuspended with formic acid 0.1% in water. The peptides (20 µg) were injected onto an Ultimate 3000 HPLC (Thermo, Waltham, MA) and separated on a Jupiter Proteo 90A column (150 × 2 mm, 4 µm; Phenomenex) with water (A) and acetonitrile (B) (both containing 0.1% formic acid) in a flow rate of 0.2 mL/min. The elution started with 2% acetonitrile held for 7 min, followed by a gradient step to 40% up to 24 min, maintained at 40% for 2 min and restored to 2% over 2 min. The column was equilibrated up to 32 min. The column temperature was set at 40°C. The peptides were identified by a Sciex 4000 QTRAP mass spectrometer (Framingham, MA) using positive enhanced product ion (EPI) mode to fragment peptides for sequence identification or single reaction monitoring (SRM) for semi-quantification. In the SRM method the mass transition (m/z precursor → m/z fragment) was used for each unmodified peptide and peptides containing the mass addition of 140 Da on the lysine (K). For the **LAK³⁷⁵TYETLEK** and **NLGK⁴⁵⁶VGSK** peptides, the mass transition were, respectively,

$[M+3H+140]^{3+}$ 479.58 \rightarrow 591.34 and $[M+2H+140]^{2+}$ 471.76 \rightarrow 200.14. The ion spray was set to 5 kV, the nebulizer gas to 20 psi, and the interface heater to 400°C. The parameters used to each peptide are shown in the table S1. For EPI, the collisional energy was 30%, declustering potential was 50V and with collisional energy spread was 10V, and these parameters were applied for all ions. All SRM data were processed using MultiQuant with the MQL algorithm for peak integration. Automatic peak detection was used, but all integrated peaks were manually inspected to ensure correct peak detection and integration. For quantification, the area of the most intense mass transition (m/z precursor \rightarrow m/z fragment) of each modified peptide was divided by the area of **TYETTLEK** peptide $[M+2H]^{2+}$ 476.23 \rightarrow 723.33. Both exact ion fragments and retention time were used to guarantee proper peptide identification.

2.6. Quantification of allantoin in human neutrophils infected with *Pseudomonas aeruginosa* (PA14)

Purified neutrophils (3×10^6) were infected with *Pseudomonas aeruginosa* (MOI 10) and incubated with uric acid (0.2 mM or 0.5 mM) in the absence or presence of superoxide dismutase (SOD, 100 μ g/mL) in PBS/glucose containing DTPA (100 μ M), for 30 min at 37°C. After incubation, the cells were lysed with 2% TCA and 60% acetonitrile containing the internal standard allantoin- $^{13}\text{C}_2^{15}\text{N}_4$ (1.66 μ M). The samples were vortexed for 30 seconds and then centrifuged at $1700 \times g$ for 1 min at 4°C. The supernatant was filtered (PTFE filter 0.22 μ m) and injected into the LC system coupled to a Q-TOF mass spectrometer (6600 Triple-TOF; AB Sciex), electrospray ionization source (ESI), that was operating in the negative mode. The method used was described by Turner et al, 2012 with modifications [33]. The fragments were obtained through collision energy (-20 V) and -80 V of DP (declustering potential) for all analytes. The source temperature was 350°C and the spray voltage was adjusted to 4500 V. The chromatographic method was developed on a UPLC system from Nexera (Shimadzu, Kyoto) using a UPLC BEH Amide 1.7 μ M (2.1 \times 100 mm, Acquity Waters). The mobile phase was 10

mM ammonium acetate pH 6.8 (solvent A) and acetonitrile (solvent B). The separation was carried out in a gradient mode: 0-1 min: 90% B; 1-2 min: 50% B; 2-8 min: 50% B; 9-15 min: 90% B, with a flow rate of 0.2 mL/min and an injection volume of 10 μ L, the column was maintained at 25°C. The quantification of allantoin was corrected by the internal standard: allantoin/allantoin- $^{13}\text{C}_2^{15}\text{N}_4$ ratio through the mass transition analysis for allantoin, m/z 157.0367 \rightarrow 114.0309 and allantoin- $^{13}\text{C}_2^{15}\text{N}_4$, m/z 163.0316 \rightarrow 118.0209 and plotted against a standard curve. A second fragment (m/z 157.0367 \rightarrow 97.053) and retention time were used to confirm allantoin detection.

2.7. Quantification of 2-hidroxiethidium (2-OH-E⁺)

Purified peripheral blood neutrophils (2×10^6) were incubated with DHE (Dihydroethidium, 50 μ M), uric acid (0.05 - 0.5 mM) and 4-aminobenzoic acid hydrazide (ABAH, 50 μ M) in PBS/glucose containing DTPA (100 μ M) and activated with opsonized *Pseudomonas aeruginosa* (2×10^7) for 60 min at 37°C. After incubation, cells were pelleted at $400 \times g$ for 10 min at 4°C and the supernatants were collected. Due to phagocytosis, the neutrophils were lysed and the intracellular content was also analysed as described by Zielonka et al., 2008 [34]

The samples (60 μ L) were injected into the high performance liquid chromatography system (HPLC; Shimadzu, Tokyo, Japan) and the analytes were separated on a Phenomenex Synergi Polar-RP 80 A column, (4 μ m, 150 \times 4.6 mm). The HPLC system was equipped with two LC-20AT pumps, an RF-10AxL fluorescence detector and a CBM20A system controller. The mobile phase was 10% acetonitrile in 0.1% TFA/H₂O (solvent A) and 60% acetonitrile in 0.1% TFA/H₂O (solvent B) with a flow rate of 0.6 mL/min. The compounds were eluted with a gradient of 40% solvent B for 5 min and linear increase to 100% solvent B in 25 min. This was maintained for 10 min. The return to the initial condition was linear over 5 min and the system was balanced for 6 min. 2-OH-E⁺ was detected through the fluorescence detector with λ_{ex} = 480 nm, λ_{em} = 580 nm. The analyte peak was integrated and plotted against a 2-OH-E⁺ standard

curve prepared as previously described [35]. Briefly, DHE (50 μM) was oxidized by a xanthine/xanthine oxidase system (1 mM xanthine and 100 $\mu\text{g}/\text{mL}$ xanthine oxidase) in 10 mM phosphate buffer, pH 7.4, containing DTPA (100 μM) at 37°C for 30 min in the dark. Aliquots of this reaction were injected into the HPLC under the conditions described above and the 2-OH-E⁺ was collected and concentrated in a vacuum centrifuge (speed-vacuum). The obtained residue was suspended in DMSO and absorbance was measured at pH 7.4 for adequate deprotonation [36]. The concentration of 2-OH-E⁺ was calculated using its molar absorption coefficient $\epsilon_{475\text{nm}} = 1.2 \times 10^4 \text{ M}^{-1} \cdot \text{cm}^{-1}$ [37]. All of the above procedures were performed under minimal exposure to light.

2.8. Quantification of glutathione reduced (GSH) and oxidized (GSSG)

Purified neutrophils (5×10^6) were activated with *Pseudomonas aeruginosa* and incubated with different concentrations of uric acid in 180 μL PBS/glucose for 1h at 37°C as described by Carvalho et al, 2018 [22].

Briefly, 18 μL extraction buffer (2% TCA; 1 mM DTPA) and 2 μL internal standard (N-acetyl-cysteine, NAC, 2 $\mu\text{g}/\text{mL}$) were added to the samples, followed by 45 s vortexing and incubation on ice for 30 minutes. The lysed samples were diluted in 200 μL mobile phase A (0.75 mM ammonium formate; 0.01% formic acid and 1% methanol) and cell debris were removed by centrifugation at $5000 \times g$, 4°C for 10 minutes. Supernatants were collected, filtered (0.22 μm filters) and injected into the LC/MS/MS system.

The chromatographic method was developed in a Nexera UPLC system (Shimadzu), with C18 Kinetex analytical column (100 mm \times 2.10 mm, 2.6 μm) (Phenomenex) and mobile phase A (0.75 mM ammonium formate; acid formic 0.01%) and B (methanol), in a flow of 0.2 mL/min. The compounds were eluted according to a gradient: 1% B 0-5 minutes; 80% B 6-10 minutes; 1% B 10-11 minutes. Then, the column was equilibrated with 1% B, until 20 minutes. The column temperature was adjusted to 25°C and the injection volume to 10 μL . The analysis

was performed on 6600 Triple-TOF (AB Sciex) coupled to the electrospray ionization source (ESI), operating in positive mode, with the source temperature at 450°C and spray voltage 5500 V. For identification and quantification the mass transitions were used: GSH $[M+H]^+$ (m/z 308.0911 \rightarrow 179.0462), GSSG $[M+H]^+$ (m/z 613.1592 \rightarrow 355.0741), GSSG $[M+H]^{++}$ (m/z 307.0863 \rightarrow 177.0328) and internal standard, NAC (m/z 164.0 \rightarrow 76.0215). The collision energy used to generate the fragments was specific for each analyte (22 V, GSH; 32 V, GSSG; 25 V, NAC), with the tune voltage (DP) equal to 80 V. The concentrations of GSH and GSSG were obtained by the GSH/NAC or GSSG/NAC area ratios plotted against a standard curve.

2.9. Oxidation of Peroxiredoxin 1

dHL-60 cells (3×10^6) were activated with *Pseudomonas aeruginosa* (3×10^7) and incubated in the presence or absence of uric acid (200 μ M) for 1 hour at 37°C. dHL-60 cells were also activated by the aseptic stimulus PMA (100 ng/mL). After incubation, the cells were centrifuged at $1000 \times g$ and the pellets were suspended in 500 μ l PBS solution containing 50 mM NEM (previously treated with catalase, 10 μ g/mL) and incubated for 20 min at room temperature. Subsequently, cells were centrifuged, the pellet was lysed with lysis buffer (50 mM Tris base pH 7.5; 150 mM NaCl; 1% Igepal) containing protease inhibitors in the concentration suggested by the supplier (Roche) and incubated on ice for 15 min with shaking in vortex for every 5 min. After that, the samples were centrifuged at $20,000 \times g$ for 15 min at 4°C and the supernatant was collected.

The proteins were quantified by Bradford [38] and separated in a SDS-PAGE. A total of 20 μ g cell extract proteins was applied to the 12% polyacrylamide gel and separated at 200 V for 45 min. Subsequently, the proteins were transferred to a PVDF membrane and incubated with blocking solution (5% skimmed milk) for 1 hour under agitation. The membrane was washed with TBS-T (containing 0.1% tween-20) and incubated overnight with the primary antibody

(anti-Prx1, 1: 10000; AbFrontier). In the next day, the membrane was washed again and incubated for 1 h with the secondary antibody (anti-rabbit, 1:10000, Sigma Aldrich). Subsequently, the membrane was washed and the bands were developed by ECL through a photo-documenter (Uvitec Cambridge). The quantification of the bands was performed by the ImageJ software. The percentage of Prx1 dimer was obtained dividing the intensity of dimer by the total Prx1 (dimer + monomer) $\times 100$ as described elsewhere [39].

2.10. Proteomics analysis

Neutrophils (2×10^6) were incubated with biotinylated ethyl-ester glutathione (200 μM , BIOGEE, Thermofisher) for 30 min at 37°C. Then, cells were washed with PBS/glucose and centrifuged at $400 \times g$ for 10 min at 4°C, resuspended in PBS/glucose and activated with opsonized *Pseudomonas aeruginosa* (2×10^7 , 1h) or PMA (100 ng/mL, 30 min), 37°C, in the presence or absence of uric acid (200 μM). A positive control was performed by incubating neutrophils with diamide (1 mM).

Samples were then lysed with a non-denaturing buffer (50 mM Tris-base pH 7.4; 0.1 mM EDTA; 0.1 mM EGTA; 150 mM NaCl; 1 mM sodium orthovanadate; 1 mM sodium fluoride; 1% deoxycholate; 100 mM NEM; 1 mM sodium orthovanadate and protease inhibitor cocktail (Roche) for 15 min at 4°C. After that, they were centrifuged $20,000 \times g$ for 15 min at 4°C and the supernatant was incubated for 18 hours with streptavidin magnetic beads (Promega) to capture proteins conjugated to glutathione-biotin. Samples were placed on a magnetic rack to capture the beads (containing glutathionylated proteins) and the supernatant (containing non-glutathionylated proteins) was removed. Bead precipitated was washed with three different buffers to remove proteins that were not biotinylated: buffer I (50 mM HEPES, pH 7.5, 500 mM NaCl, 1 mM EDTA), buffer II (10 mM Tris-HCl, pH 7.4, + 250 mM LiCl + 1 mM EDTA + 1% deoxycholate) and buffer III (50 mM Tris-HCl, pH 7.4). After wash, the bead fixed proteins were incubated with reducing buffer (100 mM ammonium bicarbonate, 10 mM DTT

and 0.4% deoxycolate) for 1 hour at 37°C. Subsequently, the samples were alkylated with iodoacetamide (15 mM) and digested with trypsin (1:40, w/w Protein; gold standard, mass spectrometry grade, Madison, WI) for 4 h at 37°C. A second aliquot of enzyme (1:50, w/w protein) was added, and samples were incubated overnight at 37 °C. After acidic hydrolysis with 2% trifluoroacetic acid, samples were desalted using the StageTip protocol [40]. The peptides were dried and resuspended in 0.1% formic acid (final protein concentration of 25 ng/μL). The protocol summary is shown in the **Figure 1**.

Tryptic peptides (50 ng) were injected into a reversed-phase nano-column BEH C18 1.7 μm (100 μm x 100 mm; Waters, Milford, MA, USA) coupled to a nanoACQUITY UPLC System (Waters, Milford, MA, USA) and eluted at a flow rate of 400 nL/min. The peptides were separated using a linear gradient solvent A (0.1% formic acid in water, v/v) and solvent B (acetonitrile containing 0.1% formic acid, v/v). The gradient linear with 2–25% B for 110 min was followed by 25–45% B for 20 min. After that, the percentage of solvent B was increased to 85% within 1 min and maintained for 5 min for washing the column. Re-equilibration of the system with 98% A for 10 min was performed before each run. The peptides identification was performed using a Triple TOF 6600 instrument (Sciex, Concord, ON) equipped with a nanoSpray ion source (nESI/MS/MS) in positive mode and ion source at 2.4 kV. Information-dependent acquisition (IDA) was used for analysis of MS/MS. The nebulizer gas (GS1) was set to 20 psi and declustering potential of 80 V. Each MS/MS was obtained by dynamic collision energy.

Tandem mass spectrometry (MS/MS) spectra were searched against the reviewed UniProt-Human database (version 109, 20 404 entries), using the MaxQuant search engine (version 1.6.3.3) [41] with fixed Cys-N-ethylmaleimide alkylation and Cys-carbamidomethylation, Met oxidation and N-terminal acetylation as variable modification. MaxQuant default mass tolerance was used for precursor and product ions. The precursor mass tolerance was set to 20

ppm for search. Trypsin was selected as the protease and two missed cleavages were allowed. The results were processed only for proteins identified with ≥ 2 peptides (at least one of them unique) and with score minimum for modified peptides ≥ 40 in the entire dataset identified by Maxquant. The label-free was also used for quantification.

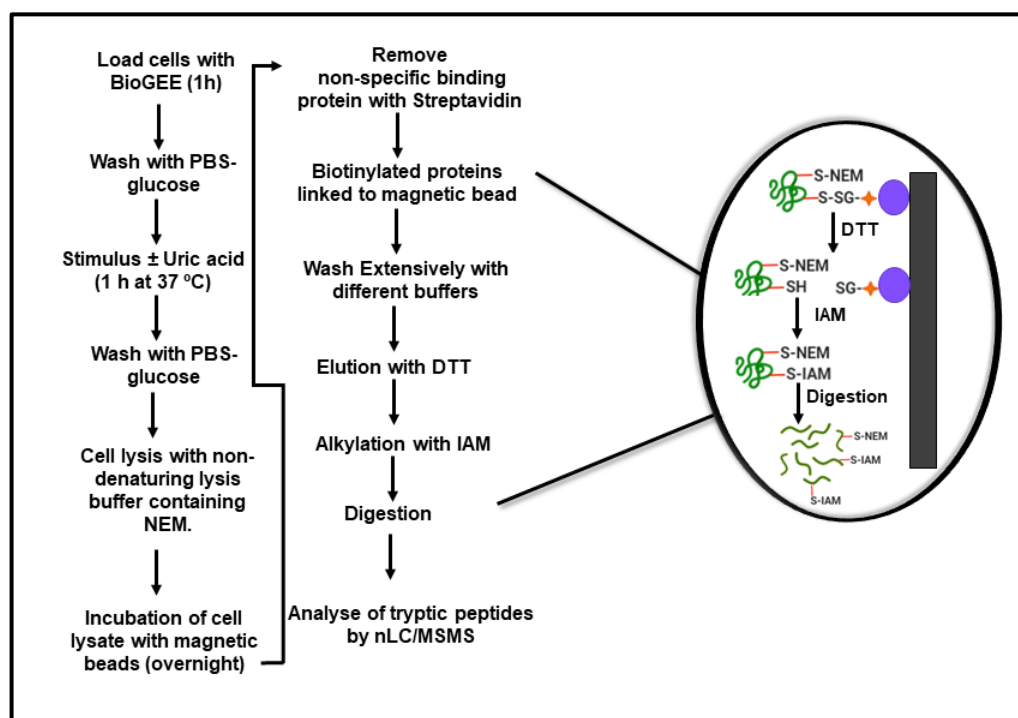


Figure 1. Workflow for glutathionylated protein analysis in neutrophils. Diagram show all the steps performed in the experiment using biotinylated ethyl-ester glutathione (BioGEE) and magnetic beads.

2.11. Lipidomic of neutrophils

Peripheral blood purified neutrophils (1.5×10^6) were activated with opsonized *Pseudomonas aeruginosa* (1.5×10^7) and incubated in the absence or presence of uric acid (0.2 mM) in PBS/glucose for 60 min at 37°C. After incubation, cells were centrifuged at $400 \times g$ for 10 min at 4°C and the precipitate was submitted to lipid extraction according to Yoshida et al, 2008 [42].

Briefly, the pellet was suspended in a mixture of 400 μ L 10 mM PBS (pH 7.4) containing DTPA (100 μ M), 400 μ L methanol containing butylated hydroxytoluene (BHT, 0.1 mM) and

100 μ L methanol containing 1000 ng of each internal standard (ceramide (Cer, d18:1/17:0 and d18:1/10:0), sphingomyelin (SM, d18:1/17:0), cardiolipin (CL, tetra 14:0), phosphatidylcholine (PC, 17:0/17:0 and 14:0/14:0), ethanolamine (PE, 17:0/17:0 and 14:0/14:0), serine and glycerol (PS, PG 17:0/17:0), smooth PC (17:0), smooth PE (17:1), phosphatidic acid (PA, 17:0/17:0) and triacylglycerol (TAG, triple 17:0; 14:0x3), cholesterol ester (Chol ester 10:0). The samples were homogenized for 30s in a vortex and after the addition of 2 mL of chloroform: ethyl acetate (4: 1) they were again homogenized for 30s in the vortex. The mixture was centrifuged at $1500 \times g$ for 3 min at 4°C, the lower organic phase was collected and then dried under a flow of N₂. The dry lipid extract was reconstituted with 100 μ L isopropanol [42].

The extracted lipids were analysed by UPLC (Nexera, Shimadzu, Kyoto, Japan) coupled to the TripleTOF 6600 mass spectrometer (Sciex, Framingham, MA). The lipids were separated on a UPLC Cortecs® C18 column (2.1 x 100 mm; 1.6 μ m particle size; Waters) maintained at 35°C with a flow of 0.2 mL/min. The mobile phase used was (A) water:acetonitrile (60:40) and (B) isopropanol:acetonitrile:water (88:10:2) containing 10 mM ammonium acetate (in negative ESI⁻) or ammonium formate (in positive mode, ESI⁺). The gradient was 40-100% B in 10 min, 100% B in 10-12 min, 100-40% B in 12-13 min, and 40% B 13-20 min. The spray voltage applied was 4500 (ESI⁻) and 5500 (ESI⁺). The cone voltage applied was (+/-) 80 V. The mass spectrometer was operated in positive and negative ionization modes, and the scan range mass-to-charge ratio used was 200-2000 Da. Data for lipid molecular species identification and quantification was obtained by information-dependent acquisition (IDA®) using a period cycle time of 1.05s with 100 ms acquisition time for MS1 scan and 25 ms acquisition time to obtain the top 36 precursor ions. Data acquisition was performed using Analyst® 1.7.1 with an ion spray voltage of -4.5 kV and 5.5 kV (for negative and positive modes, respectively) and the cone voltage at +/- 80 V. The curtain gas was set at 25 psi, nebulizer and heater gases at 45 psi and interface heater of 450°C.

The detected lipids were identified manually by the MS/MS spectrum using PeakView and by an in-house manufactured Excel-based macro. Peak area of each lipid specie was obtained by MS data from MultiQuant® and divided by the peak area of the corresponding internal standard. The concentration of each lipid species was calculated by the area ratio multiplied by the internal standard amount. The total amount of lipids was expressed in $\mu\text{g}/1.5 \times 10^6$ cells. Data are presented as mean \pm SEM, calculated by summing the individual lipid species within each class.

2.12. Statistical analysis

The data were expressed as the mean \pm error of the mean of at least three independent experiments. Those experiments that obeyed a normal distribution were analysed by one-way analysis of variance (ANOVA) with Newman-Keuls post-hoc test. For those that did not fit in a normal distribution a non-parametric analysis followed by Mann Whitney test was employed. Statistical analyses were performed in the GraphPad Prism software version 5.0. Differences were considered significant when $p < 0.05$.

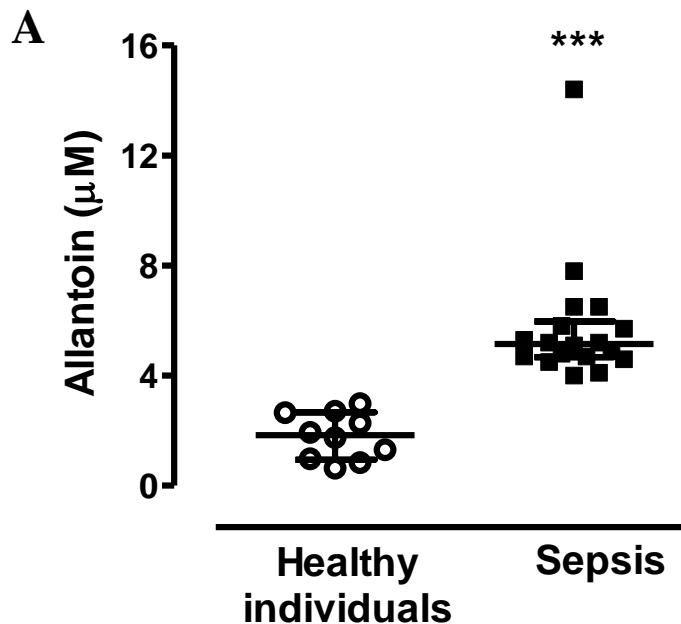
For lipidomic analysis, the data were transformed into log and the statistical significance ($p < 0.05$) evaluated by one-way ANOVA followed by Tukey's post-hoc test, using the Metaboanalyst Software [43]. Next, we performed a heatmap analysis using only lipids that were statistically altered in the different groups. The distances of the "nodes" between the analytes and the samples were measured using Pearson and Ward's correlation algorithm.

3. RESULTS

3.1 Allantoin is elevated in plasma of septic patients and in neutrophils infected with *Pseudomonas aeruginosa*

Oxidation of uric acid is a relevant event in inflammatory processes and vascular disease. Clinical studies revealed an enhancement of allantoin, the main product of uric acid oxidation, in plasma, synovial liquid, bronchoalveolar fluid and atherosclerotic plaque of patients suffering from gout, rheumatoid arthritis, diabetes, atherosclerosis and cystic fibrosis [44-47]. In this study, we showed that allantoin was significantly elevated in plasma of septic patients compared to healthy individuals (**Figure 2A**). These results confirm that urate is significantly oxidized in plasma of septic patients.

Allantoin was also significantly augmented after stimulation of peripheral blood neutrophils from healthy volunteers with *Pseudomonas aeruginosa*. The oxidation of uric acid to allantoin was directly dependent on the concentration of uric acid, on the activity of myeloperoxidase and on the presence of superoxide (**Figure 2B**). The diminution of allantoin in presence of SOD suggested that at least half of the total allantoin is coming from urate hydroperoxide, which is the product of the combination of urate free radical with superoxide radical [6].



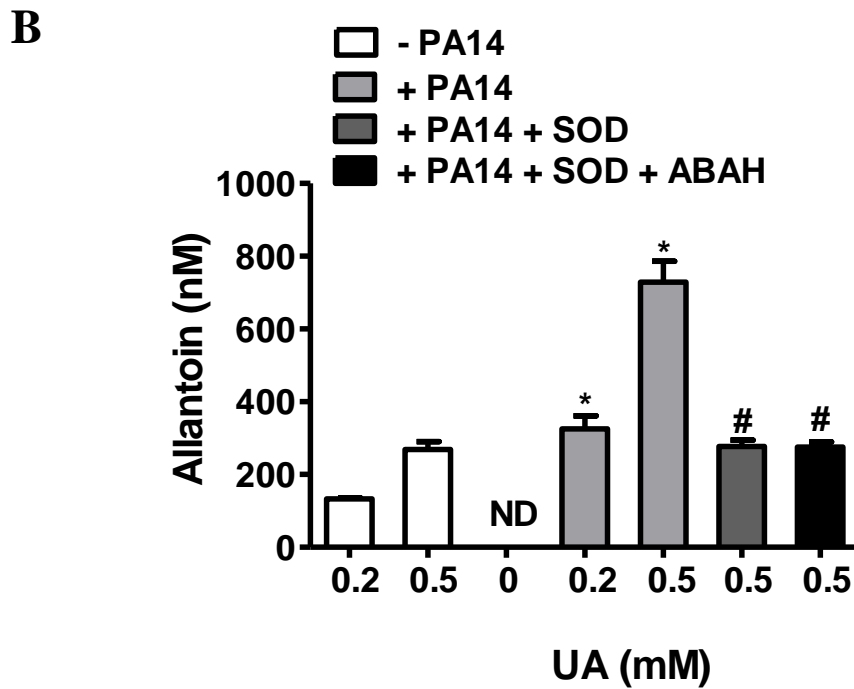


Figure 2: Allantoin is elevated in plasma of patients with sepsis and in neutrophils infected with *Pseudomonas aeruginosa*. (A) Dot plot of allantoin concentration and median with interquartile delimitation. Non-parametric analyses using Mann Whitney (***) $p < 0.0001$). (B) Purified peripheral blood neutrophils (5×10^6) were activated with *Pseudomonas aeruginosa* and incubated with uric acid (0.2 or 0.5 mM), SOD (100 $\mu\text{g}/\text{mL}$) alone or SOD + ABAH (300 μM) for 30 min at 37°C. The bars represent the mean \pm standard error of the mean of three independent experiments. Statistical analyses were performed by one-way ANOVA followed by the Newman-Keuls test. The symbol (*) indicates a significant difference with their respective control group 0.2 or 0.5 mM in the absence of PA14 ($p < 0.05$) and (#) indicates a significant difference with the group in the presence of PA14 and 0.5 mM urate ($p < 0.05$).

3.2 Urate-derived adducts are elevated in plasma albumin from septic patients.

Oxidation of uric acid produces unstable intermediates that react with lysine residues in albumin to yield adducts with a mass addition of 140 Da [28]. These adducts were significantly enhanced by activation of neutrophils [28] and were positively correlated with heart failure and death events in patients (Silva et al., in preparation). Here, we compared the presence of these same urate-derived adducts in plasma albumin from septic and healthy individuals.

Two modified peptides (LAK³⁷⁵TYETTLEK and NLGK⁴⁵⁶VGSK) were monitored and normalized by the unmodified peptide (TYETTLEK). The uratylated peptide LAK³⁷⁵TYETTLEK was significantly augmented in septic patients ($p < 0.0001$) when compared to healthy individuals (**Figure 3A**). However, the NLGK⁴⁵⁶VGSK peptide was not different among the two groups (**Figure 3B**). The positive Spearman correlation ($R = 0.7146$) between the uratylated peptide LAK³⁷⁵TYETTLEK and allantoin in septic patients and healthy individuals was highly significant ($p < 0.0001$) (**Figure 4**). This strength the evidence that the oxidation of uric acid is an important event in sepsis and, whilst a part of these intermediate breakdown to allantoin, another part can form irreversible covalent adducts to albumin. Together, allantoin and the uratylated peptide from albumin can be a useful tool in the prognosis of infectious disease.

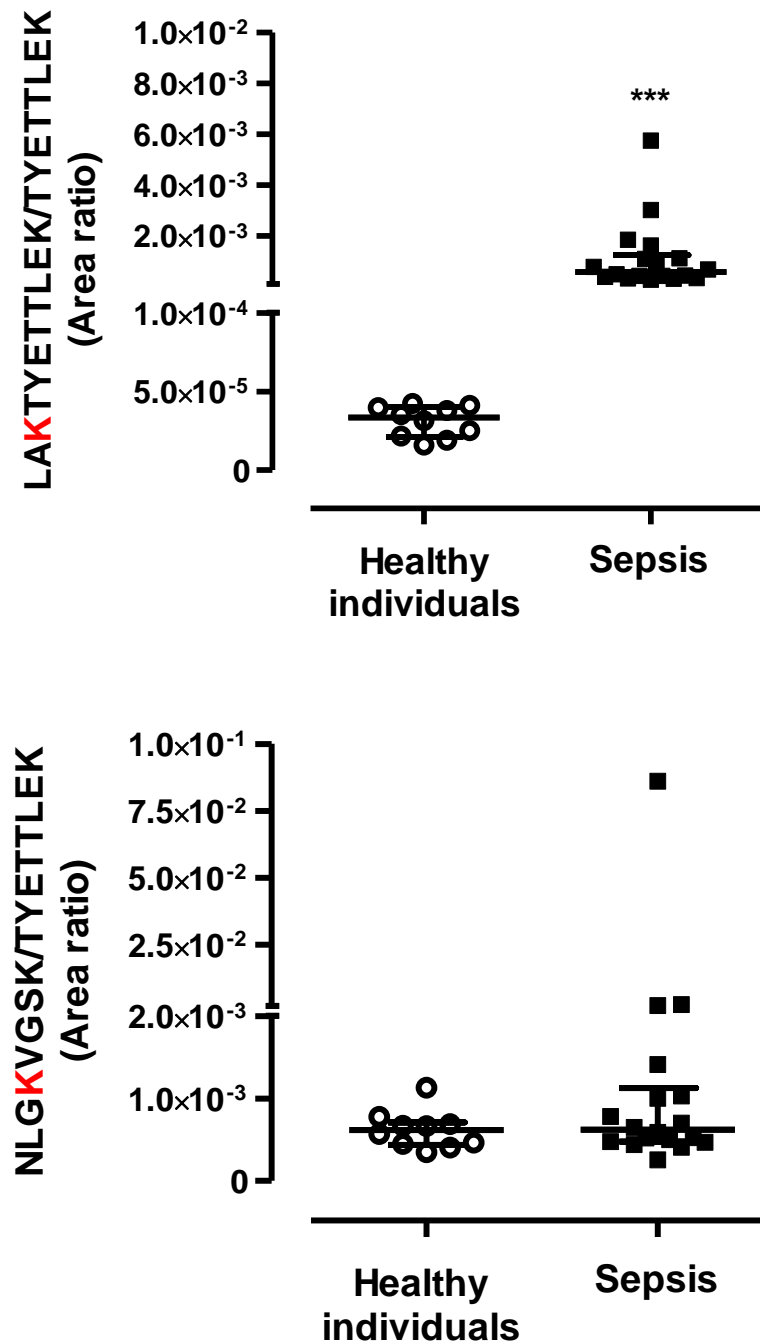


Figure 3. Uratylation of albumin is elevated in plasma of patients with sepsis. Protein from plasma (10 μ L) of healthy donors (n=10) and patients with sepsis (n=18) were denatured, reduced (5 mM, DTT), alkylated (15 mM, IAM) and digested with trypsin. Using SRM method, we monitored the mass transition of two tryptic peptides with a mass addition of 140 Da on lysine residues (**K**) and the unmodified peptides (TYETTLEK) of albumin. All SRM data were processed using MultiQuant. Plots show individual points and median with interquartile range of the area ratio. The area ratio was obtained by normalization of modified peptides divided unmodified peptide (TYETTLEK). Non-parametric two-tailed analyses, (***) $p < 0.0001$) by Mann Whitney test.

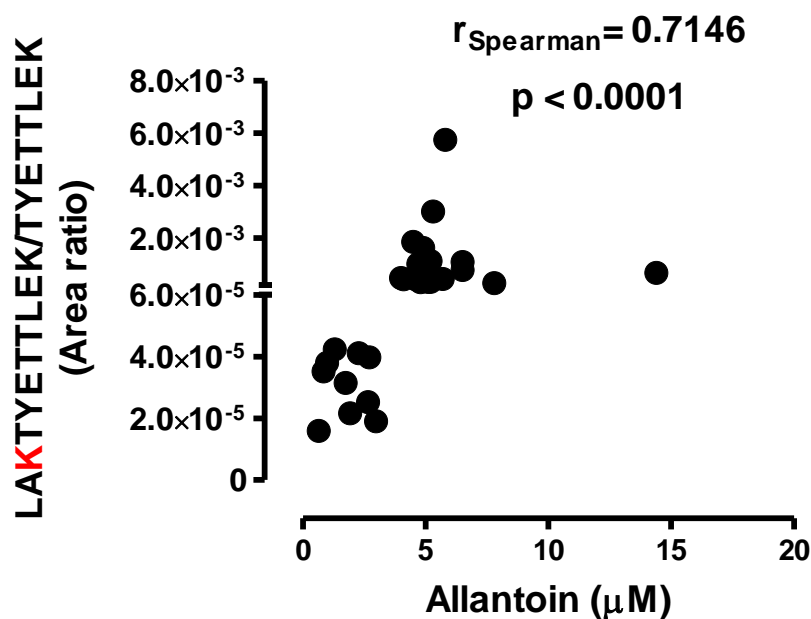


Figure 4. Uratylation of albumin correlates with allantoin. Plasma allantoin and uratylated peptide (LAKTYETTLEK) from healthy donors and septic patients. The area ratio was obtained dividing the uratylated peptide (LAKTYETTLEK) area by the unmodified peptide (TYETTLEK) area. Data were analysed using Spearman correlation two-tailed test (n=28).

3.3 Effect of uric acid on superoxide production

In previous studies we demonstrated that oxidation of uric acid further increased the production of superoxide after activation of NADPH oxidase in dHL-60 cells by the aseptic stimulus PMA [21]. The effect of uric acid on superoxide production was less efficient, but still significant, in dHL-60 challenged with *Pseudomonas aeruginosa* [22].

Despite their similar ability to produce superoxide, dHL-60 and neutrophils express different amounts of NADPH oxidase subunits [48, 49] and we wondered whether uric acid would increase superoxide production in neutrophils as it does in dHL-60. Concentration of superoxide was much higher in the extra (**Figure 5A**) than in the intracellular (**Figure 5B**) milieu, being the main contributor to the overall superoxide of the system (**Figure 5C**). Uric acid did not further increase the levels of superoxide, differently to the observed in dHL-60

cells [21, 22]. Inhibition of myeloperoxidase and, consequently, diminution of urate free radical, also did not affect total superoxide concentration.

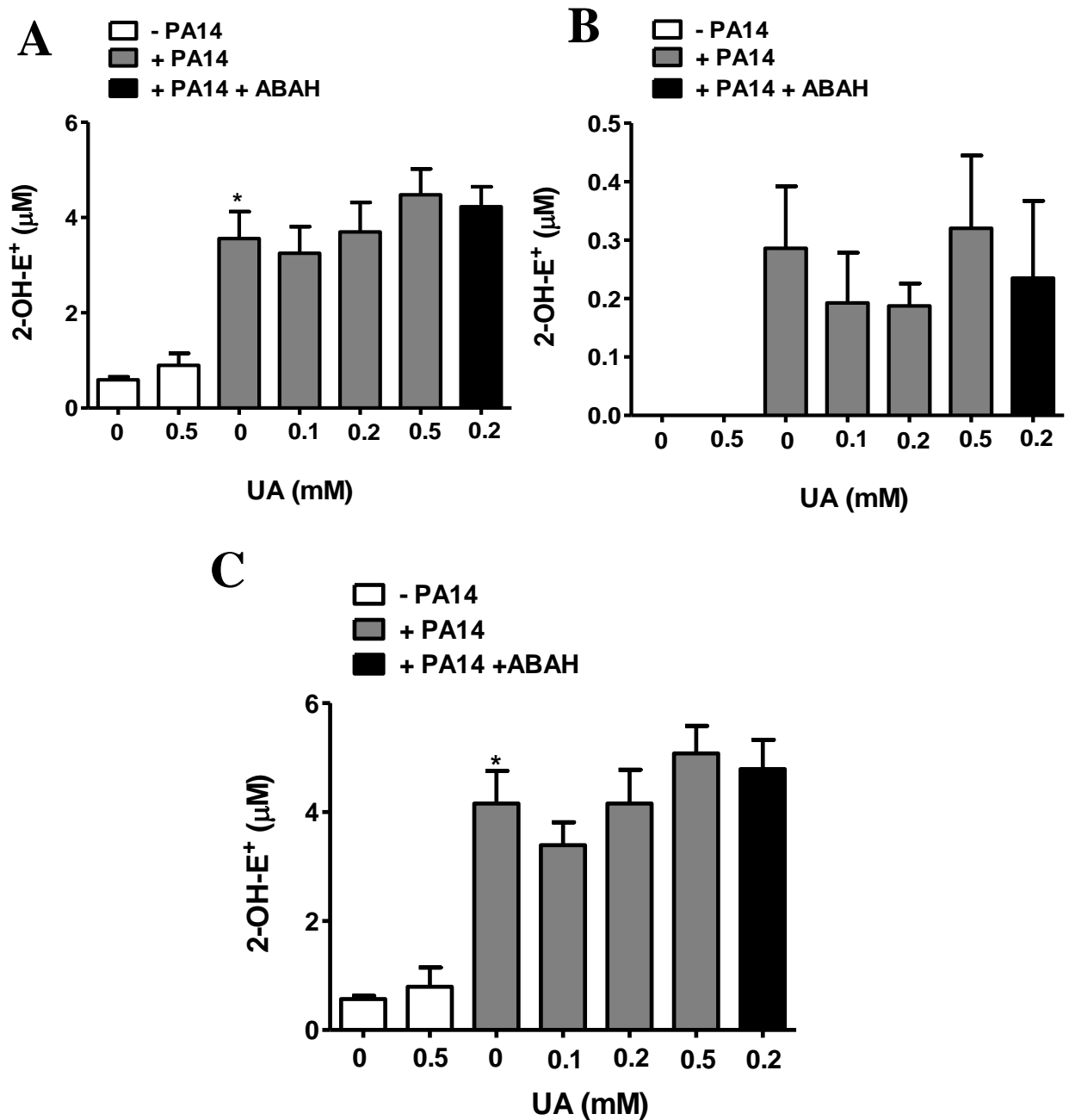


Figure 5. Effect of uric acid on superoxide production in neutrophils activated with *Pseudomonas aeruginosa* (PA14). Neutrophils (2×10^6) were incubated with DHE (50 μ M), uric acid (UA, 0-0.5 mM), ABAH (50 μ M) 5 min before uric acid (0.2 mM) and activated with opsonized *Pseudomonas aeruginosa* (2×10^7) for 60 min. Extra (A) and intracellular (B) samples were separated in an HPLC

system and the peak area referring to 2-OH-E⁺ ($\lambda_{\text{ex}} = 480 \text{ nm}$, $\lambda_{\text{em}} = 580 \text{ nm}$) was integrated and plotted against a standard curve. Total superoxide was also calculated by the sum of the extra + intracellular (C). The bars are the mean \pm S.E.M of three independent experiments. Statistical analyses were performed by one-way ANOVA followed by the Newman-Keuls post-test, * $p < 0.05$ from the group without PA14 (white bars)

3.4 Effect of uric acid on glutathione oxidation

The production of urate free radical and urate hydroperoxide in activated neutrophils could induce a redox imbalance toward an oxidative environment. In dHL-60, uric acid further decreased the rate GSH/GSSG (reduced/oxidized glutathione) induced by PMA, but did not change that induced by *Pseudomonas aeruginosa* [21, 22]. In neutrophils, the infection with *Pseudomonas aeruginosa* did not alter the GSH (**Figure 6A**), but increased GSSG (**Figure 6B**) and uric acid (0.5 mM) further increased GSSG levels. GSSG was not detected in non-infected cells, therefore, the GSH/GSSG ratio could not be calculated in this group (**Figure 6C**). These results demonstrated that the oxidative status of neutrophils infected with *Pseudomonas aeruginosa* is slightly affected by uric acid toward a pro-oxidant environment.

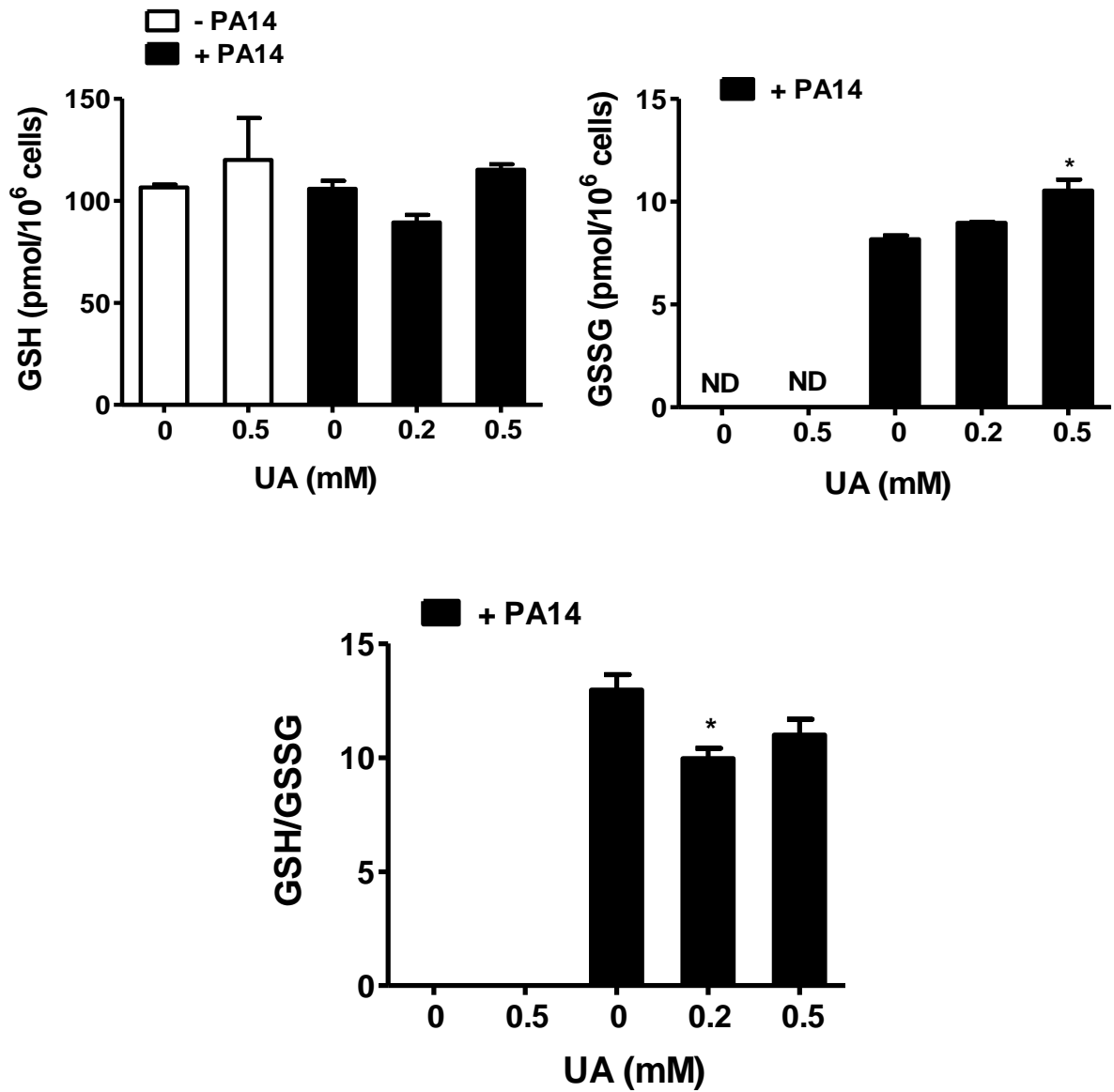
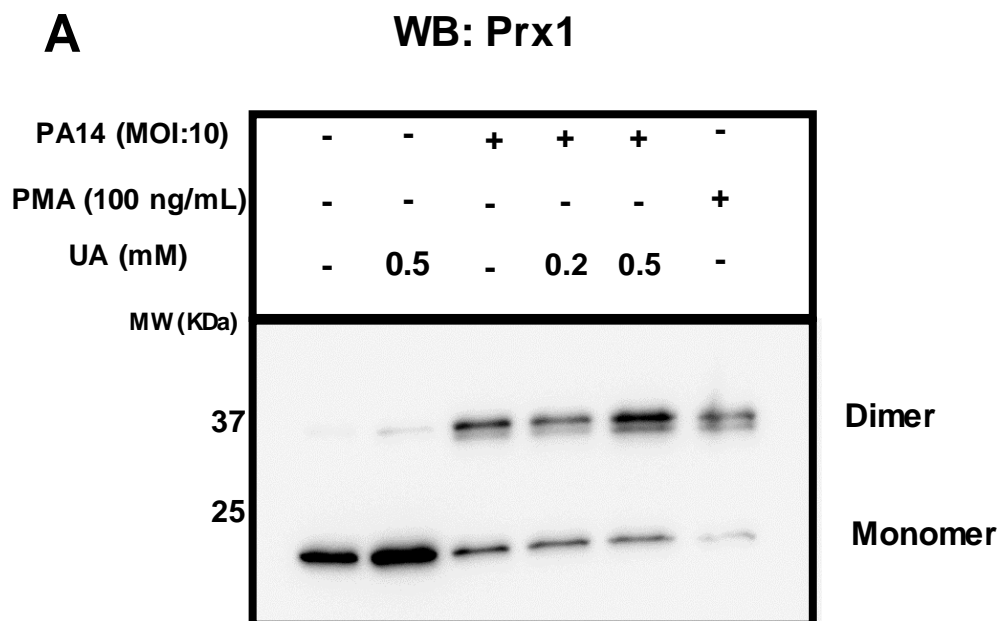


Figure 6. Uric acid increases GSSG in neutrophils infected with *Pseudomonas aeruginosa* (PA14). Neutrophils (5×10^6) were challenged with *Pseudomonas aeruginosa* (MOI 10) for 1 h in the presence or absence of uric acid (UA, 0.2 or 0.5 mM). The intracellular and extracellular contents were injected into the LC/MS/MS and the mass for GSH $[M+H]^+$ (m/z 308.0911 \rightarrow 179.0462), GSSG $[M+H]^+$ (m/z 613.1592 \rightarrow 355.0741) + GSSG $[M+2H]^{2+}$ (m/z 307.0863 \rightarrow 177.0328) were normalized by the internal standard and plotted against a standard curve. The bars represent the mean \pm standard error of the mean of three independent experiments. Statistical analyses were performed by one-way ANOVA, followed by Newman-Keuls test, * $p < 0.05$ from the group infected with PA14 without uric acid.

3.5 Effect of uric acid on the oxidation of Peroxiredoxin 1

Thiols from peroxiredoxins are prone to oxidation by urate hydroperoxide [29] and it might alter redox signalling. Because peroxiredoxins are the first sensors for peroxides in the cell [50, 51], we monitored peroxiredoxin 1 oxidation in neutrophil-like cells (dHL-60) infected with *Pseudomonas aeruginosa*.

The neutrophil-like cells (dHL-60) were chosen because peroxiredoxin 1 is mostly oxidized in non-activated peripheral blood neutrophils, making the analysis of the redox state of the enzyme difficult [39]. As demonstrated in **figure 7**, activation of NADPH oxidase by PMA or *Pseudomonas aeruginosa* induced formation of peroxiredoxin 1 disulphide-dimer. The presence of uric acid did not further significantly increase the oxidation of Peroxiredoxin 1 in cells activated with bacteria (**Figure 7B**). Because the oxidation of Peroxiredoxin is too pronounced in dHL-60 activated with *Pseudomonas aeruginosa*, the detection of any additional effect of uric acid could not be properly evaluate in this model and uric acid probably do not further contribute to Peroxiredoxin 1 oxidation in neutrophils during the oxidative burst.



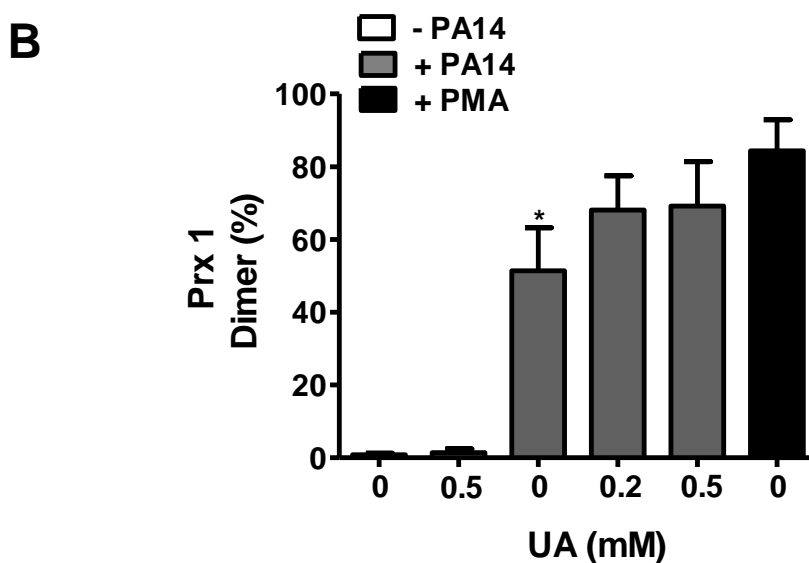


Figure 7. Effect of uric acid on the oxidation of Peroxiredoxin 1. dHL-60 cells (3×10^6) were activated with *Pseudomonas aeruginosa* PA14 (3×10^7) and incubated in presence or in absence of uric acid for 60 minutes. The cell extract (20 μ g of protein) was applied on a non-reducing SDS polyacrylamide gel and Western Blotting was performed with antibody against Prx1 (A). The intensity of the dimer band was divided by the intensity of the total Prx1 (dimer + monomer) (B). The bars represent the mean \pm standard error of the mean of three independent experiments. Statistical analysis was performed by one-way ANOVA followed by the Newman-Keuls test. The symbol (*) indicates a significant difference from control groups in the absence of PA14 and uric acid ($p < 0.05$).

3.6 Effect of uric acid on protein glutathionylation

Protein glutathionylation is an important mechanism for redox regulation and redox signalling [52]. Here, we evaluated whether uric acid would affect protein glutathionylation in neutrophils activated with PMA or *Pseudomonas aeruginosa*.

The neutrophil protein defensin 3 was glutathionylated in all groups tested (non-activate, PMA and *Pseudomonas aeruginosa* activated neutrophils and upon treatment with uric acid (**Figure 8**). None exclusive protein was found in non-activated cells (**Figure 8A-C**).

Neutrophils activated with *Pseudomonas aeruginosa* and *Pseudomonas aeruginosa* plus uric acid presented the exclusive glutathionylated proteins cornifina A and eosinophil peroxidase,

respectively. Whereas azurocidin and the antimicrobial protein cathelicidina were glutathionylated in both *Pseudomonas aeruginosa* and *Pseudomonas aeruginosa* plus uric acid groups (**Figure 8A**).

None exclusive glutathionylated proteins were found in neutrophils incubated with PMA (**Figure 8B**) or with the oxidizing agent diamide (**Figure 8C**). However, five exclusive glutathionylated proteins were found in neutrophils incubated with PMA plus uric acid (**Figure 8B**). Among these, the S100A8 protein (Calprotectin), an important manganese and zinc chelating protein with antimicrobial activity was identified (**Figure 8B**). Treatment with diamide induced glutathionylation of the same proteins as PMA plus uric acid treatment (**Figure 8C**). Altogether, these results show that a different conjunct of proteins is glutathionylated in presence of uric acid in the oxidative burst. These proteins were also glutathionylated when neutrophils were incubated with the thiol oxidant diamide, showing that uric acid can further induce thiol oxidation in inflammation.

It is noteworthy to mention that the recovery of glutathionylated proteins was much lower than the expected and this may be due to the use of magnetic beads in sample preparation. Therefore, we will repeat this experiment using different beads to improve detection. Negative controls in the absence of BIOGEE were performed and no modified proteins were identified (data not shown). The intracellular proteins that were not captured by streptavidin are shown in the **Table S1**.

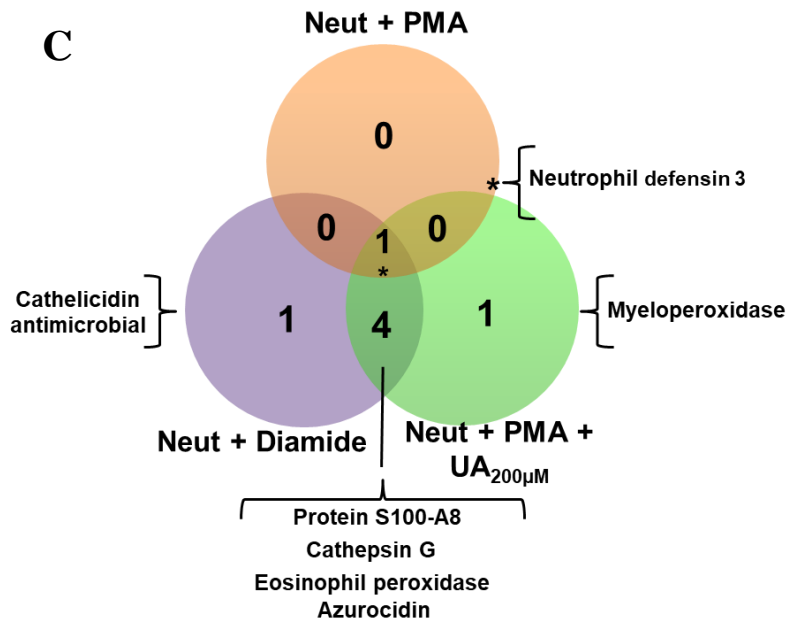
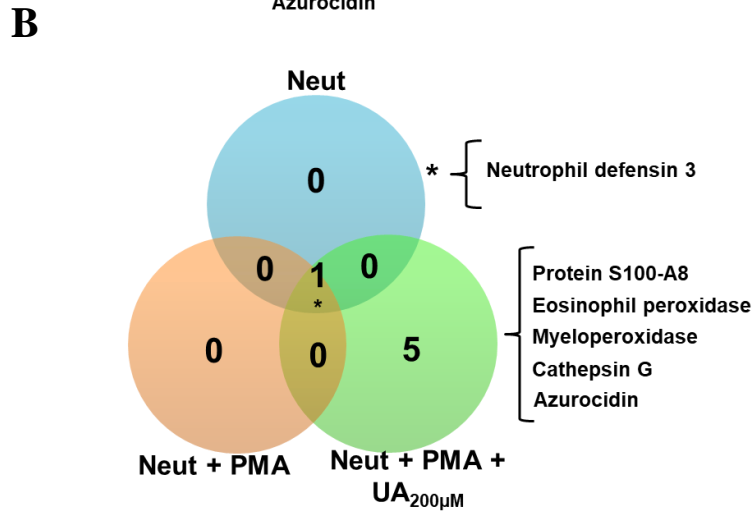
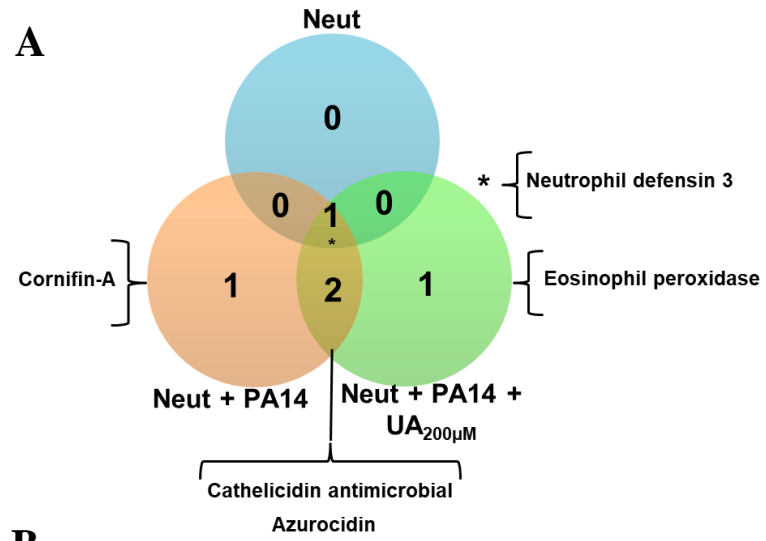


Figure 8. Glutathionylated proteins identified in neutrophils. Venn diagram showing the overlap and the exclusive of proteins that were glutathionylated in naïve, PMA-activated or PMA-activated plus uric acid (200 μ M) neutrophils (**A**); naïve, *Pseudomonas aeruginosa* (PA14)-activated or *Pseudomonas aeruginosa* (PA14)-activated plus uric acid (200 μ M) neutrophils (**B**); naïve, diamide (1 mM) or PMA-activated plus uric acid (200 μ M) neutrophils (**C**). The data represent proteins that were captured by streptavidin beads and obtained at least one carbamidomethylation (IAM) modification on cysteine.

3.7 Effect of uric acid on the lipid profile

Besides modulation of proteins redox sensitive, an oxidizing environment can cause lipid remodelling and this can trigger different cellular responses [53]. Knowing this, our next step was to evaluate the lipid profile in activated neutrophils with *Pseudomonas aeruginosa* in the presence or in the absence of uric acid.

For this assay, we used an indirect lipidomic approach and thus identified 175 lipid species in the total neutrophil samples (untreated and treated), which were classified into 15 subclasses. A total of 103 phospholipids, 22 sphingolipids and 50 neutral lipids were found. This data shows the diversity of lipid molecules among the subclasses and the most abundant lipids in these cells were triacylglycerols (TAG) and phosphatidylethanolamine plasmalogen (pPE) (**Figure 9**).

To assess the effect of uric acid on the modulation of lipid profile, we used a clustering analysis (**Figure 10**). Twenty eight lipids were significantly altered when all experimental groups were compared against each other. There was an increase in the levels of 19 different types of TAG in activated-neutrophils and it was further increased by the incubation with uric acid. In addition, uric acid increased 2 different types of diacylglycerol (DAG) and membrane cholesterol in activated neutrophils. Together these results provide important insights into the modulation of lipid profile by uric acid in activated neutrophils.

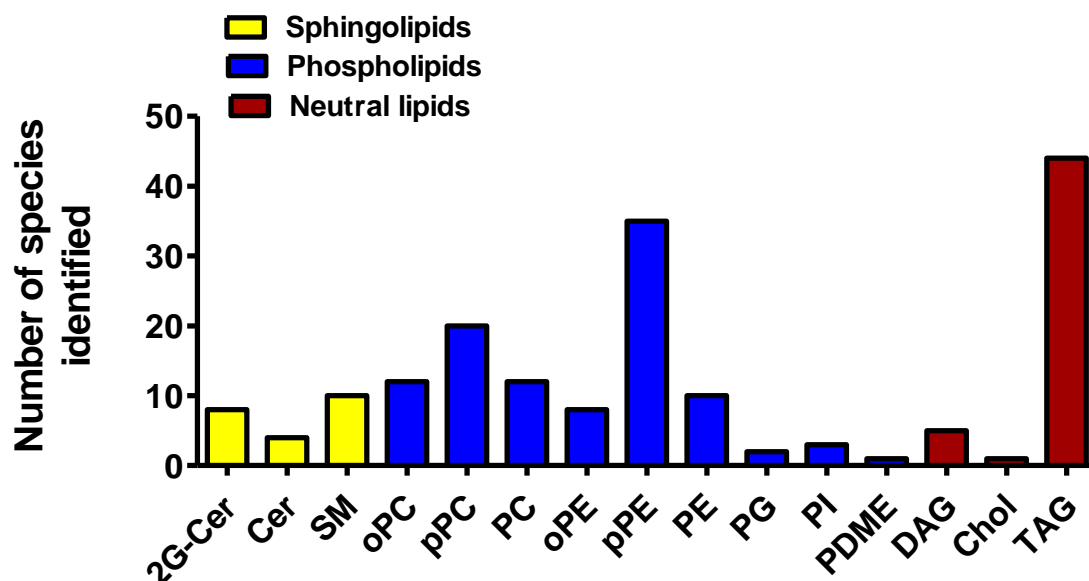


Figure 9. Identified lipids in neutrophils. The lipids found in different neutrophil treatments were combined in columns for different classes: 2-glycerol-ceramide (2G-Cer), ceramide (Cer), sphingomyelin (SM), o-phosphatidylcholine (oPC), phosphatidylcholine plasmalogen (pPC), phosphatidylcholine (PC), o-phosphatidylethanolamine (oPE), plasmalogen phosphatidylethanolamine (pPE), phosphatidylglycerol (PG), phosphatidylinositol (PI), phosphatidylmethylethanolamine (PDME), diacylglycerol (DAG), triacylglycerol (TAG) and cholesterol (Chol).

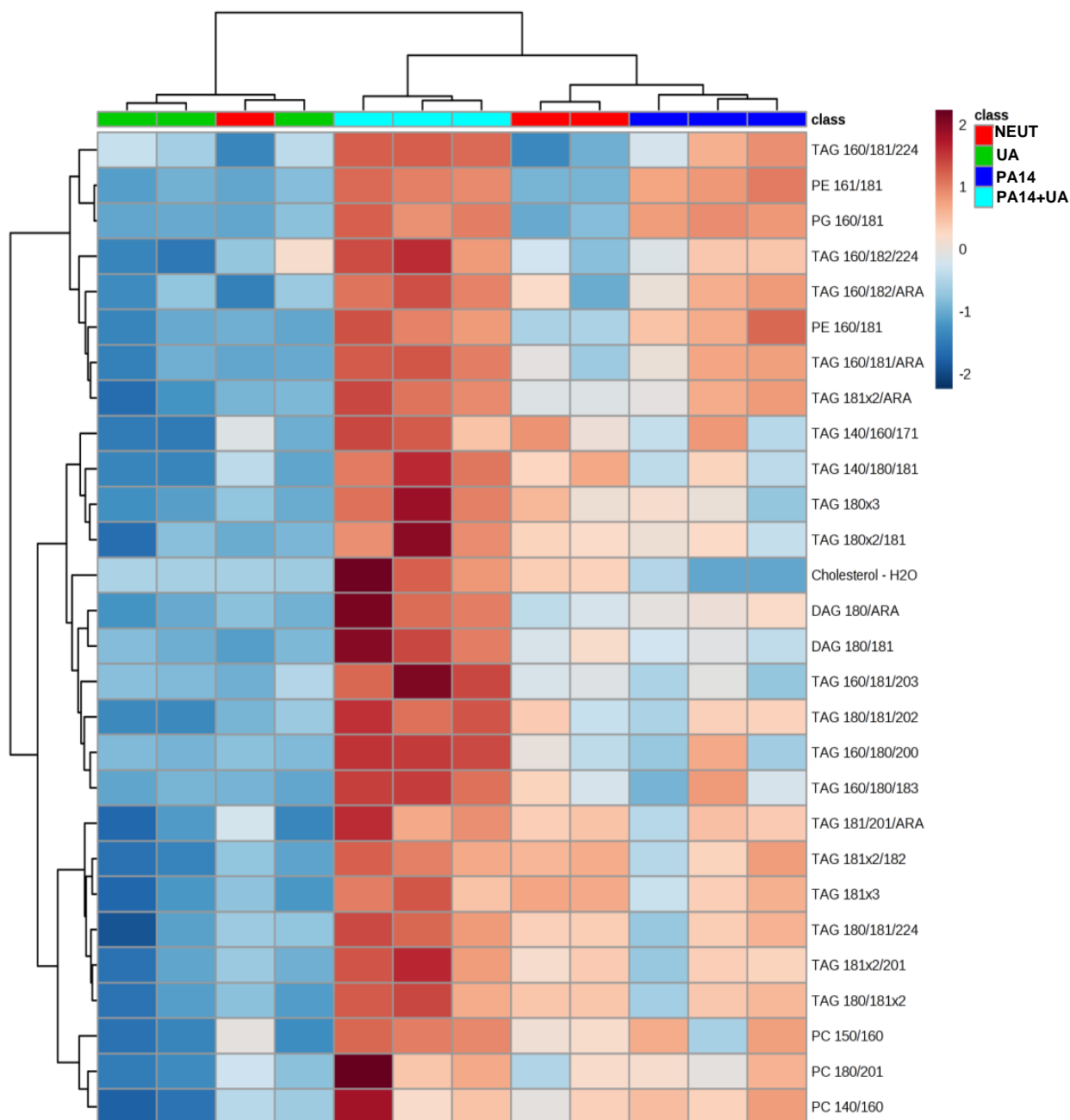


Figure 10. Heatmap of the most significant distinct lipids in neutrophils. Neutrophils (1.5×10^6) were infected with *Pseudomonas aeruginosa* (1.5×10^7) in the presence or absence of uric acid (0.2 mM) in PBS/glucose at 37°C for 60 min. Twenty-eight lipids are shown in the rows and the different samples are in the columns. Statistical significance was assessed by one-way ANOVA followed by Tukey's post-test ($p < 0.05$) using Metaboanalyst. The distance was measured using Pearson and Ward's clustering algorithm. Each colored cell on the heatmap corresponds to the concentration that was normalized by each respective internal standard. Log transformation was used for data normalization value.

4. DISCUSSION

Our findings demonstrated higher levels of allantoin in plasma of patients with sepsis when compared to healthy individuals and in isolated neutrophils infected with *Pseudomonas aeruginosa* in presence of uric acid. Allantoin is thought to be an inert end product of uric acid oxidation and, therefore, the antioxidant effect of uric acid has usually been considered prevalent. However, previous studies from our and other groups revealed that intermediates generated during the oxidation of uric acid can trigger a free radical chain reaction [4, 6], oxidize and inactivate enzymes [21, 28, 29, 54, 55] and form adducts with lysine residues in albumin [28][Silva et al., under preparation]. The present study corroborates these findings by demonstrating an increase in urate derivative-adducts in plasma albumin of patients with sepsis.

We had previously demonstrated that the activation of isolated neutrophils by PMA generates the oxidant urate hydroperoxide [21]. Here, we could not detect urate hydroperoxide (data not shown) probably because the oxidative burst induced by *Pseudomonas aeruginosa* is confined into the phagosome. Differently from the stimulation with bacteria, incubation of neutrophils with PMA induces the assemblage of the multimeric enzyme NADPH oxidase on the neutrophil plasma membrane and the electron transfer to oxygen occurs at the extracellular environment [56, 57]. In addition, the neutrophil granules discharge their content to the extracellular milieu promoting the external production of hypochlorous acid and urate hydroperoxide by myeloperoxidase. Oppositely, the engulfment of bacteria by neutrophils and formation of phagosome promotes the NADPH oxidase assemblage on the phagosomal membrane and the granule are discharged within this compartment [58]. The phagosomal confinement of urate hydroperoxide likely promotes its rapid reaction with proteins compromising its direct detection. Because of this, we were only able to detect the increase of its breakdown product, allantoin.

Likewise, we had detected that uric acid increased superoxide in neutrophils activated with PMA [21], but no effect of uric acid was seen when the stimulus was *Pseudomonas aeruginosa*, probably due to the different compartmentalization of the oxidative burst in PMA *versus* bacterial stimulus.

The oxidation of uric acid by inflammatory enzymes prevented the formation of hypochlorous acid, an important microbicide and thus, decreased the ability of inflammatory cells to kill *Pseudomonas aeruginosa* [22]. In addition, oxidation of uric acid was correlated with a worse outcome in patients with cystic fibrosis infected with *Pseudomonas aeruginosa* and the levels of plasma uric acid were also correlated with a worse prognosis in sepsis [23, 24]. In the present study we demonstrated, for the first time, that the oxidation of uric acid is relevant in sepsis, suggesting the monitoring of allantoin and uratylated peptides in plasma albumin as an useful biomarker in sepsis progression. The modification of albumin by urate-derivative adducts could affect protein function and have a role in endothelial injury and sepsis progression. However, further studies are necessary to clarify this hypothesis.

An additional role for uric acid oxidation in inflammation and sepsis is due to a possible depletion of ascorbate. It has been well known that plasma ascorbate undergoes an abrupt decrease in sepsis and low levels of ascorbate are associated with a worse prognosis and death event in sepsis [59-61]. The urate free radical formed in inflammatory conditions can quickly abstract one-electron from ascorbate, regenerating uric acid in detriment of ascorbate. [62].

Recently, we showed that urate hydroperoxide oxidized sulfur-containing amino acids and glutathione [20], reacted faster with peroxiredoxins 1 and 2 [29] and the protein disulfide isomerase [6]. Therefore, if in one hand uric acid decreased the abundance of the oxidant hypochlorous acid, on the other hand it promoted a more oxidative environment due the production of urate free radical and urate hydroperoxide [21]. These previous data are in

agreement with the present study since uric acid increased GSSG levels in neutrophils infected with *Pseudomonas aeruginosa*.

As mentioned above, peroxiredoxin 1 and 2 are among the main targets to urate hydroperoxide and they can selectively affect cell signalling through redox relay [30, 63]. In the current work, however, no additional oxidation of peroxiredoxin 1 was evidenced by the presence of uric acid when dHL-60 cells were infected with *Pseudomonas aeruginosa*. The absence of any further oxidation could be due to a confinement of urate hydroperoxide into the phagosome and also because the oxidation of peroxiredoxin 1 was already too pronounced in this model, limiting the detection of any extra effect. The oxidation of peroxiredoxin by hydrogen peroxide would be prevalent in this situation since this oxidant can easily diffuse from the phagosome. Therefore, the oxidation of uric acid probably does not contribute to the oxidation of peroxiredoxin 1 in neutrophils-like infected with *Pseudomonas aeruginosa*.

Under an oxidative condition urate hydroperoxide can induce reversible or irreversible oxidative modifications to susceptible proteins [64]. Reversible modifications such as S-glutathionylation may protect proteins against permanent oxidative damage and/or modulate their functions [65]. In support to this, we proposed that the oxidation of uric acid promotes glutathionylation of proteins in neutrophils activated with bacteria or PMA. Our preliminary results showed that uric acid induced glutathionylation of calprotectin (S100-A8), an important microbicide protein in neutrophils. Calprotectin is composed of two monomers S100A8 and S100A9 [66], both sensitive to oxidative modifications [67-69]. The oxidation of N-terminal cysteine of S100A9 and N-terminal methionine of S100A8 by hypochlorous acid promotes cross-linking of both monomers and formation of methionine sulfoxide, respectively. These oxidative modifications on calprotectin prevent its ability to chelate metals allowing bacterial growth [70]. Besides, S-glutathionylation of S100A9 induced conformational changes decreasing the neutrophil adhesion to fibronectin, suggesting a decreased inflammatory

response [70, 71]. Taken together with our results, the post-translational modifications in presence of uric acid might affect the ability of the protein to chelate metals disrupting the microbicide activity of neutrophils. Therefore, besides affecting hypochlorous acid formation, the glutathionylation of the S100A8 protein may be a possible additional mechanism by which uric acid decreases the microbicidal capacity of inflammatory cells. However, further studies are required to elucidate whether S-glutathionylation of calprotectin in the presence of uric acid has consequences upon protein function and infection.

Here, we also demonstrated that uric acid induced an increase of triacylglycerols (TAG) levels in neutrophils infected with *Pseudomonas aeruginosa*. There is some evidence that oxidized products of uric acid can react with lipids and contribute to oxidative stress [4]. A recent study showed that oxidative stress induces the formation of lipids droplets, cytoplasmic organelles that contain significant quantities of TAGs and cholesteryl esters [72]. The formation of lipid droplets depends on the enzymatic shuffling of PUFAs (polyunsaturated fatty acids) from membranes to TAGs that are then directed to the core of droplets [53]. It consists of an antioxidant mechanism because, within the droplet, the lipids are less vulnerable to peroxidation. The formation of lipid droplets in cells culminates in the production of inflammatory mediators that amplify the response to the infection [73]. Therefore, our results indicate that uric acid induces an increase of lipid droplets during infection and this may have implications to host defence. Interestingly, these data corroborate the study that showed the increase of lipids droplets in a neural stem cell niche exposed to an oxidative environment [53].

Uric acid also increased the content TAG esterified to arachidonic acid together with other two different unsaturated fatty acids in neutrophils activated with *Pseudomonas aeruginosa*. These unsaturated fatty acids contribute to membrane fluidity [57]. Moreover, arachidonic acid is a precursor of eicosanoids that are directly related to inflammatory and allergic processes, platelet aggregation, and recruitment of immune cells [58]. Taken together, the lipid

remodelling points out to an indirect pro-inflammatory mechanism triggered by uric acid, not yet described.

5. CONCLUSION

In summary, this study reveals the oxidant effect of uric acid in infection. We demonstrated, for the first time, a marked increase of urate-derived adducts in plasma albumin of patients with sepsis. During the oxidative burst triggered by neutrophil infection, the oxidation of uric acid by myeloperoxidase induced an increase in glutathione oxidation and glutathionylation of exclusive proteins. Interestingly, the oxidizing effects of uric acid culminated in the modulation of lipid profile and thus, the monitoring of certain lipids may be used to assess inflammation and oxidative stress caused by uric acid. In conclusion, our data opens up a new insight into the mechanisms by which uric acid can propagate the inflammatory response in infection.

6. REFERENCES

1. Becker, B.F., *Towards the physiological function of uric acid*. Free Radic Biol Med, 1993. **14**(6): p. 615-31.
2. Ames, B.N., et al., *Uric acid provides an antioxidant defense in humans against oxidant- and radical-caused aging and cancer: a hypothesis*. Proc Natl Acad Sci U S A, 1981. **78**(11): p. 6858-62.
3. Johnson, R.J., et al., *The planetary biology of ascorbate and uric acid and their relationship with the epidemic of obesity and cardiovascular disease*. Med Hypotheses, 2008. **71**(1): p. 22-31.
4. Santos, C.X., E.I. Anjos, and O. Augusto, *Uric acid oxidation by peroxynitrite: multiple reactions, free radical formation, and amplification of lipid oxidation*. Arch Biochem Biophys, 1999. **372**(2): p. 285-94.
5. Maples, K.R. and R.P. Mason, *Free radical metabolite of uric acid*. J Biol Chem, 1988. **263**(4): p. 1709-12.
6. Meotti, F.C., et al., *Urate as a physiological substrate for myeloperoxidase: implications for hyperuricemia and inflammation*. J Biol Chem, 2011. **286**(15): p. 12901-11.
7. Feig, D.I., D.H. Kang, and R.J. Johnson, *Uric acid and cardiovascular risk*. N Engl J Med, 2008. **359**(17): p. 1811-21.
8. Lotufo, P.A., et al., *Serum Uric Acid and Prehypertension Among Adults Free of Cardiovascular Diseases and Diabetes: Baseline of the Brazilian Longitudinal Study of Adult Health (ELSA-Brasil)*. Angiology, 2015. **67**(2): p. 180-6.
9. Ehsan Qureshi, A., S. Hameed, and A. Noeman, *Relationship of serum uric Acid level and angiographic severity of coronary artery disease in male patients with acute coronary syndrome*. Pak J Med Sci, 2013. **29**(5): p. 1137-41.
10. Gur, M., et al., *Relation of serum uric acid levels with the presence and severity of angiographic coronary artery disease*. Angiology, 2008. **59**(2): p. 166-71.
11. Gur, M., et al., *Uric acid and high sensitive C-reactive protein are associated with subclinical thoracic aortic atherosclerosis*. J Cardiol, 2013. **61**(2): p. 144-8.
12. Choi, H.K., et al., *Pathogenesis of gout*. Ann Intern Med, 2005. **143**(7): p. 499-516.
13. Sautin, Y.Y., et al., *Adverse effects of the classic antioxidant uric acid in adipocytes: NADPH oxidase-mediated oxidative/nitrosative stress*. Am J Physiol Cell Physiol, 2007. **293**(2): p. C584-96.
14. Thomas, M.J., *Urate causes the human polymorphonuclear leukocyte to secrete superoxide*. Free Radic Biol Med, 1992. **12**(1): p. 89-91.
15. Shi, Y., J.E. Evans, and K.L. Rock, *Molecular identification of a danger signal that alerts the immune system to dying cells*. Nature, 2003. **425**(6957): p. 516-21.
16. Shi, Y., *Caught red-handed: uric acid is an agent of inflammation*. J Clin Invest, 2010. **120**(6): p. 1809-11.
17. Martinon, F., et al., *Gout-associated uric acid crystals activate the NALP3 inflammasome*. Nature, 2006. **440**(7081): p. 237-41.
18. Kettle, A.J. and C.C. Winterbourn, *Myeloperoxidase: a key regulator of neutrophil oxidant production*. Redox Rep, 1997. **3**(1): p. 3-15.
19. Klebanoff, S.J., *Myeloperoxidase-halide-hydrogen peroxide antibacterial system*. J Bacteriol, 1968. **95**(6): p. 2131-8.
20. Patricio, E.S., et al., *Chemical Characterization of Urate Hydroperoxide, A Pro-oxidant Intermediate Generated by Urate Oxidation in Inflammatory and Photoinduced Processes*. Chem Res Toxicol, 2015. **28**(8): p. 1556-66.
21. Silva, R.P., et al., *Identification of urate hydroperoxide in neutrophils: A novel pro-oxidant generated in inflammatory conditions*. Free Radic Biol Med, 2018. **126**: p. 177-186.

22. Carvalho, L.A.C., et al., *Uric acid disrupts hypochlorous acid production and the bactericidal activity of HL-60 cells*. Redox Biol, 2018. **16**: p. 179-188.
23. Dickerhof, N., et al., *Oxidized glutathione and uric acid as biomarkers of early cystic fibrosis lung disease*. J Cyst Fibros, 2017. **16**(2): p. 214-221.
24. Chuang, C.C., et al., *Serum total antioxidant capacity reflects severity of illness in patients with severe sepsis*. Critical Care, 2006. **10**(1).
25. Tsai, K., et al., *Is the endogenous peroxy-radical scavenging capacity of plasma protective in systemic inflammatory disorders in humans?* Free Radic Biol Med, 2000. **28**(6): p. 926-33.
26. MacKinnon, K.L., et al., *Measures of total free radical activity in critically ill patients*. Clinical Biochemistry, 1999. **32**(4): p. 263-268.
27. Akbar, S.R., et al., *Hyperuricemia: An Early Marker for Severity of Illness in Sepsis*. Int J Nephrol, 2015. **2015**: p. 301021.
28. Turner, R., et al., *Conjugation of urate-derived electrophiles to proteins during normal metabolism and inflammation*. J Biol Chem, 2018. **293**(51): p. 19886-19898.
29. Carvalho, L.A., et al., *Urate hydroperoxide oxidizes human peroxiredoxin 1 and peroxiredoxin 2*. J Biol Chem, 2017.
30. Mineiro, M.F., et al., *Urate hydroperoxide oxidizes endothelial cell surface protein disulfide isomerase-A1 and impairs adherence*. Biochimica Et Biophysica Acta-General Subjects, 2020. **1864**(3).
31. Carr, A.C., et al., *Circulating myeloperoxidase is elevated in septic shock and is associated with systemic organ failure and mortality in critically ill patients*. Free Radic Biol Med, 2019.
32. Vincent, J.L., et al., *Use of the SOFA score to assess the incidence of organ dysfunction/failure in intensive care units: results of a multicenter, prospective study. Working group on "sepsis-related problems" of the European Society of Intensive Care Medicine*. Crit Care Med, 1998. **26**(11): p. 1793-800.
33. Turner, R., L.K. Stamp, and A.J. Kettle, *Detection of allantoin in clinical samples using hydrophilic liquid chromatography with stable isotope dilution negative ion tandem mass spectrometry*. J Chromatogr B Analyt Technol Biomed Life Sci, 2012. **891-892**: p. 85-9.
34. Zielonka, J., J. Vasquez-Vivar, and B. Kalyanaraman, *Detection of 2-hydroxyethidium in cellular systems: a unique marker product of superoxide and hydroethidine*. Nat Protoc, 2008. **3**(1): p. 8-21.
35. Zhao, H., et al., *Detection and characterization of the product of hydroethidine and intracellular superoxide by HPLC and limitations of fluorescence*. Proc Natl Acad Sci U S A, 2005. **102**(16): p. 5727-32.
36. Zielonka, J., et al., *Mechanistic similarities between oxidation of hydroethidine by Fremy's salt and superoxide: stopped-flow optical and EPR studies*. Free Radic Biol Med, 2005. **39**(7): p. 853-63.
37. Zielonka, J., J. Vasquez-Vivar, and B. Kalyanaraman, *The confounding effects of light, sonication, and Mn(III)TBAP on quantitation of superoxide using hydroethidine*. Free Radic Biol Med, 2006. **41**(7): p. 1050-7.
38. Kruger, N.J., *The Bradford method for protein quantitation*. Methods Mol Biol, 1994. **32**: p. 9-15.
39. de Souza, L.F., et al., *Peroxiredoxin expression and redox status in neutrophils and HL-60 cells*. Free Radic Biol Med, 2019. **135**: p. 227-234.
40. Rappsilber, J., M. Mann, and Y. Ishihama, *Protocol for micro-purification, enrichment, pre-fractionation and storage of peptides for proteomics using StageTips*. Nat Protoc, 2007. **2**(8): p. 1896-906.
41. Cox, J. and M. Mann, *MaxQuant enables high peptide identification rates, individualized p.p.b.-range mass accuracies and proteome-wide protein quantification*. Nat Biotechnol, 2008. **26**(12): p. 1367-72.

42. Yoshida, Y., et al., *Simultaneous measurement of F2-isoprostane, hydroxyoctadecadienoic acid, hydroxyeicosatetraenoic acid, and hydroxycholesterols from physiological samples*. Anal Biochem, 2008. **379**(1): p. 105-15.
43. Xia, J. and D.S. Wishart, *Using MetaboAnalyst 3.0 for Comprehensive Metabolomics Data Analysis*. Curr Protoc Bioinformatics, 2016. **55**: p. 14.10.1-14.10.91.
44. Stamp, L.K., et al., *Myeloperoxidase and oxidation of uric acid in gout: implications for the clinical consequences of hyperuricaemia*. Rheumatology (Oxford), 2014. **53**(11): p. 1958-65.
45. Chung, W.Y. and I.F. Benzie, *Plasma allantoin measurement by isocratic liquid chromatography with tandem mass spectrometry: method evaluation and application in oxidative stress biomonitoring*. Clin Chim Acta, 2013. **424**: p. 237-44.
46. Stamp, L.K., et al., *Myeloperoxidase and oxidative stress in rheumatoid arthritis*. Rheumatology (Oxford), 2012. **51**(10): p. 1796-803.
47. Ciari, I., et al., *Antioxidant status and purine bases in carotid artery plaque*. Nucleosides Nucleotides Nucleic Acids, 2008. **27**(6): p. 624-7.
48. Inoue, Y., et al., *Induction of phagocyte oxidase components during human myeloid differentiation: independent protein expression and discrepancy with the function*. Biosci Biotechnol Biochem, 2001. **65**(11): p. 2581-4.
49. Muranaka, S., et al., *Mechanism and characteristics of stimuli-dependent ROS generation in undifferentiated HL-60 cells*. Antioxid Redox Signal, 2005. **7**(9-10): p. 1367-76.
50. Winterbourn, C.C. and M.B. Hampton, *Redox biology: signaling via a peroxiredoxin sensor*. Nat Chem Biol, 2015. **11**(1): p. 5-6.
51. Rhee, S.G., H.Z. Chae, and K. Kim, *Peroxiredoxins: a historical overview and speculative preview of novel mechanisms and emerging concepts in cell signaling*. Free Radic Biol Med, 2005. **38**(12): p. 1543-52.
52. Salzano, S., et al., *Linkage of inflammation and oxidative stress via release of glutathionylated peroxiredoxin-2, which acts as a danger signal*. Proc Natl Acad Sci U S A, 2014. **111**(33): p. 12157-62.
53. Bailey, A.P., et al., *Antioxidant Role for Lipid Droplets in a Stem Cell Niche of Drosophila*. Cell, 2015. **163**(2): p. 340-53.
54. Mineiro, M.F., et al., *Urate hydroperoxide oxidizes endothelial cell surface protein disulfide isomerase-A1 and impairs adherence*. Biochim Biophys Acta Gen Subj, 2020. **1864**(3): p. 129481.
55. Aruoma, O.I. and B. Halliwell, *Inactivation of alpha 1-antiproteinase by hydroxyl radicals. The effect of uric acid*. FEBS Lett, 1989. **244**(1): p. 76-80.
56. Kono, H. and K.L. Rock, *How dying cells alert the immune system to danger*. Nat Rev Immunol, 2008. **8**(4): p. 279-89.
57. Winterbourn, C.C., A.J. Kettle, and M.B. Hampton, *Reactive Oxygen Species and Neutrophil Function*. Annu Rev Biochem, 2016. **85**: p. 765-92.
58. Winterbourn, C.C. and A.J. Kettle, *Redox reactions and microbial killing in the neutrophil phagosome*. Antioxid Redox Signal, 2013. **18**(6): p. 642-60.
59. Marik, P.E., *Vitamin C for the treatment of sepsis: The scientific rationale*. Pharmacol Ther, 2018. **189**: p. 63-70.
60. Yamaguchi, J., et al., *Increased oxidative stress and renal injury in patients with sepsis*. J Clin Biochem Nutr, 2018. **63**(2): p. 137-143.
61. Moskowitz, A., et al., *Ascorbic acid, corticosteroids, and thiamine in sepsis: a review of the biologic rationale and the present state of clinical evaluation*. Crit Care, 2018. **22**(1): p. 283.
62. Frei, B., R. Stocker, and B.N. Ames, *Antioxidant defenses and lipid peroxidation in human blood plasma*. Proc Natl Acad Sci U S A, 1988. **85**(24): p. 9748-52.
63. Carvalho, L.A.C., et al., *Urate hydroperoxide oxidizes human peroxiredoxin 1 and peroxiredoxin 2*. J Biol Chem, 2017. **292**(21): p. 8705-8715.
64. England, K. and T.G. Cotter, *Direct oxidative modifications of signalling proteins in mammalian cells and their effects on apoptosis*. Redox Rep, 2005. **10**(5): p. 237-45.

65. Dalle-Donne, I., et al., *S-glutathionylation in protein redox regulation*. Free Radic Biol Med, 2007. **43**(6): p. 883-98.
66. Nacken, W., et al., *S100A9/S100A8: Myeloid representatives of the S100 protein family as prominent players in innate immunity*. Microsc Res Tech, 2003. **60**(6): p. 569-80.
67. McCormick, M.M., et al., *S100A8 and S100A9 in human arterial wall. Implications for atherogenesis*. J Biol Chem, 2005. **280**(50): p. 41521-9.
68. Raftery, M.J., et al., *Novel intra- and inter-molecular sulfinamide bonds in S100A8 produced by hypochlorite oxidation*. J Biol Chem, 2001. **276**(36): p. 33393-401.
69. Lim, S.Y., et al., *S-glutathionylation regulates inflammatory activities of S100A9*. J Biol Chem, 2010. **285**(19): p. 14377-88.
70. Magon, N.J., et al., *Oxidation of calprotectin by hypochlorous acid prevents chelation of essential metal ions and allows bacterial growth: Relevance to infections in cystic fibrosis*. Free Radic Biol Med, 2015. **86**: p. 133-44.
71. Lim, S.Y.M.S.F.o.M.U., *Functional roles of oxidative modifications of S100A8 and S100A9*, C.M.S.F.o.M.U. Geczy, I.B. Dawes, and F.o.S.U. Biomolecular Sciences, Editors. 2010.
72. Young, S.G. and R. Zechner, *Biochemistry and pathophysiology of intravascular and intracellular lipolysis*. Genes Dev, 2013. **27**(5): p. 459-84.
73. Walpole, G.F.W., S. Grinstein, and J. Westman, *The role of lipids in host-pathogen interactions*. IUBMB Life, 2018. **70**(5): p. 384-392.

7. SUPPLEMENTARY MATERIAL

Table S1. Proteins identified in infected and non-infected neutrophils with *Pseudomonas aeruginosa* using redox array.

PROTEIN NAME	PROTEIN IDs
6-phosphogluconate dehydrogenase, decarboxylating	P52209
78 kDa glucose-regulated protein	P11021
Actin, cytoplasmic 1	P60709
Actin, gamma-enteric smooth muscle;	P63267
Actin, alpha skeletal muscle;	P68133
Actin, alpha cardiac muscle 1;	P68032
Actin, aortic smooth muscle	P62736
Actin-related protein 2	P61160
Actin-related protein 2/3 complex subunit 1B	O15143
Actin-related protein 2/3 complex subunit 2	O15144
Actin-related protein 2/3 complex subunit 3	O15145
Actin-related protein 2/3 complex subunit 5	O15511
Actin-related protein 3	P61158
Activated RNA polymerase II transcriptional coactivator p15	P53999
Adenylyl cyclase-associated protein 1	Q01518
Adipocyte plasma membrane-associated protein	Q9HDC9
ADP-ribosyl cyclase/cyclic ADP-ribose hydrolase 2	Q10588
ADP-ribosylation factor 1;	P84077
ADP-ribosylation factor 3;	P61204
ADP-ribosylation factor 5	P84085
Alpha-1-antitrypsin; Short peptide from AAT	P01009
Alpha-2-macroglobulin	P01023
Alpha-actinin-1	P12814
Alpha-actinin-4	O43707

Alpha-enolase	P06733
Annexin A1	P04083
Annexin A11	P50995
Annexin A3	P12429
Annexin A5	P08758
Annexin A6	P08133
Apolipoprotein A-I; Proapolipoprotein A-I	P02647
Apolipoprotein C-I;Truncated apolipoprotein C-I	P02654
Apoptosis-associated speck-like protein containing a CARD	Q9ULZ3
Arachidonate 5-lipoxygenase-activating protein	P20292
Arginase-1	P05089
ATP synthase subunit alpha, mitochondrial	P25705
Azurocidin	P20160
Bactericidal permeability-increasing protein	P17213
Beta-actin-like protein 2	Q562R1
BH3-interacting domain death agonist	P55957
Bone marrow proteoglycan;Eosinophil granule major basic protein	P13727
Brain acid soluble protein 1	P80723
Calnexin	P27824
Calponin-2	Q99439
Catalase	P04040
Cathelicidin antimicrobial peptide;Antibacterial protein FALL-39;Antibacterial protein LL-37	P49913
Cathepsin G	P08311
Chitotriosidase-1	Q13231
Chloride intracellular channel protein 1	O00299
Coactosin-like protein	Q14019
Cofilin-1	P23528
Complement C3	P01024

Cornifin-A	P35321
Cornifin-B	P22528
Coronin-1 ^a	P31146
Costars family protein ABRACL	Q9P1F3
Cysteine-rich secretory protein 3	P54108
Cytochrome b-245 light chain	P13498
Dermcidin;Survival-promoting peptide;DCD-1	P81605
Desmoplakin	P15924
EF-hand domain-containing protein D2	Q96C19
Eosinophil cationic protein	P12724
Eosinophil peroxidase	P11678
Erythrocyte band 7 integral membrane protein	P27105
Exportin-5	Q9HAV4
F-actin-capping protein subunit beta	P47756
Fatty acid-binding protein, epidermal	Q01469
Ficolin-1	O00602
Filamin-A	P21333
Folate receptor gamma;	P41439
Folate receptor beta	P14207
Fructose-bisphosphate aldolase A	P04075
Gelsolin	P06396
Glucose-6-phosphate 1-dehydrogenase	P11413
Glucose-6-phosphate isomerase	P06744
Glutathione S-transferase P	P09211
Glyceraldehyde-3-phosphate dehydrogenase	P04406
Glycogen phosphorylase, liver form	P06737
Glycogenin-1	P46976
Grancalcin	P28676
Granulins;	P28799

Guanine nucleotide-binding protein G(i) subunit alpha-2	P04899
Guanine nucleotide-binding protein subunit beta-4	Q9HAV0
Guanine nucleotide-binding protein G(I)/G(S)/G(T) subunit beta-2	P62879
Haptoglobin;Haptoglobin alpha chain Haptoglobin beta chain	P00738 P00739
Heat shock 70 kDa protein 1B	P0DMV9
Heat shock 70 kDa protein 1A	P0DMV8
Heat shock cognate 71 kDa protein	P11142
Heat shock-related 70 kDa protein 2	P54652
Heat shock protein HSP 90-alpha	P07900
Heat shock protein HSP 90-beta	P08238
Hematopoietic lineage cell-specific protein	P14317
Hemoglobin subunit alpha	P69905
Hemoglobin subunit beta;LVV-hemorphin-7;Spinorphin	P68871
Hemoglobin subunit delta	P02042
Hemopexin	P02790
Heterogeneous nuclear ribonucleoprotein K	P61978
Heterogeneous nuclear ribonucleoproteins A2/B1	P22626
Hexokinase-3	P52790
High mobility group protein B1	P09429
High mobility group protein B2	P26583
Histone H1.2	P16403
Histone H1.3	P16402
Histone H1.4	P10412
Histone H1	P22492
Histone H1.1	Q02539
Histone H1.5	P16401
Histone H2A	Q71UI9
Histone H2B	Q99880

Histone H2B type 3-B	Q8N257
Histone H3.2	Q71DI3
Histone H3.1t	Q16695
Histone H3.3	P84243
Histone H3.1	P68431
Histone H3.3C	Q6NXT2
Histone H4	P62805
Ig alpha-1 chain C region	P01876
Ig gamma-1 chain C region	P01857
Ig gamma-2 chain C region	P01859
Ig kappa chain C region	P01834
Ig lambda-6 chain C region	P0DOY3
Ig lambda-7 chain C region	P0DOY2
Ig lambda-1 chain C regions	P0CF74
Immunoglobulin lambda-like polypeptide 5	A0M8Q6
Ig mu chain C region	P01871
Integrin alpha-M	P11215
Integrin beta-2	P05107
Keratinocyte proline-rich protein	Q5T749
Lactotransferrin;Lactoferricin-H;Kaliocin-1;Lactoferroxin-A;Lactoferroxin-B;Lactoferroxin-C	P02788
Lamin-B1	P20700
Leukocyte elastase inhibitor	P30740
Leukotriene A-4 hydrolase	P09960
LIM and SH3 domain protein 1	Q14847
L-lactate dehydrogenase A chain	P00338
Lymphocyte-specific protein 1	P33241
Lysozyme C	P61626
Macrophage-capping protein	P40121

Matrix metalloproteinase-9	P14780
Moesin	P26038
Myeloblastin	P24158
Myeloid cell nuclear differentiation antigen	P41218
Myeloperoxidase;	P05164
Myosin light polypeptide 6	P60660
Myosin regulatory light chain 12A	P19105
Myosin-14	Q7Z406
Myosin-9	P35579
Na(+)/H(+) exchange regulatory cofactor NHE-RF1	O14745
Neutrophil collagenase	P22894
Neutrophil cytosol factor 2	P19878
Neutrophil defensin 3	P59666
Neutrophil defensin 1	P59665
Neutrophil elastase	P08246
Neutrophil gelatinase-associated lipocalin	P80188
Nicotinamide phosphoribosyltransferase	P43490
Non-secretory ribonuclease	P10153
Olfactomedin-4	Q6UX06
Peptidoglycan recognition protein 1	O75594
Peptidyl-prolyl cis-trans isomerase A	P62937
Peroxiredoxin-5, mitochondrial	P30044
Peroxiredoxin-6	P30041
Phosphoglycerate kinase 1	P00558
Phosphoglycerate mutase 1	P18669
Phospholipase B-like 1	Q6P4A8
Plastin-2	P13796
Profilin-1	P07737
Prosaposin	P07602

Protein disulfide-isomerase	P07237
Protein S100-A11	P31949
Protein S100-A12	P80511
Protein S100-A4	P26447
Protein S100-A6	P06703
Protein S100-A8	P05109
Protein S100-A9	P06702
Protein S100-P	P25815
Protein-arginine deiminase type-4	Q9UM07
Purine nucleoside phosphorylase	P00491
Putative elongation factor 1-alpha-like 3	Q5VTE0
Elongation factor 1-alpha 1	P68104
Elongation factor 1-alpha 2	Q05639
Putative neutrophil cytosol factor 1C	A8MVU1
Neutrophil cytosol factor 1	P14598
Putative neutrophil cytosol factor 1B	A6NI72
Pyruvate kinase PKM	P14618
Rab GDP dissociation inhibitor beta	P50395
Ras GTPase-activating-like protein IQGAP1	P46940
Ras-related C3 botulinum toxin substrate (1, 2 and 3)	P63000; P60763; P15153
Ras-related protein Rab-11A	P62491
Ras-related protein Rab-11B	Q15907
Ras-related protein Rab-13	P51153
Ras-related protein Rab-8B	Q92930
Ras-related protein Rab-8	P61006
Ras-related protein Rab-10	P61026
Ras-related protein Rab-1B	Q9H0U4
Putative Ras-related protein Rab-1C	Q92928
Ras-related protein Rab-1A	P62820

Ras-related protein Rab-15	P59190
Ras-related protein Rab-27A	P51159
Ras-related protein Rab-3D	O95716
Ras-related protein Rab-3B	P20337
Ras-related protein Rab-3A	P20336
Ras-related protein Rab-3C	Q96E17
Ras-related protein Rab-7a	P51149
Ras-related protein Rap-1A	P62834
Ras-related protein Rap-1b	P61224
Receptor-type tyrosine-protein phosphatase C	P08575
Resistin	Q9HD89
Rho GDP-dissociation inhibitor 1	P52565
Rho GDP-dissociation inhibitor 2	P52566
Serotransferrin	P02787
Serum albumin	P02768
SH3 domain-binding glutamic acid-rich-like protein	O75368
SH3 domain-binding glutamic acid-rich-like protein 3	Q9H299
Spectrin alpha chain, non-erythrocytic 1	Q13813
Synaptic vesicle membrane protein VAT-1 homolog	Q99536
Talin-1	Q9Y490
Talin-2	Q9Y4G6
Thioredoxin	P10599
Thymosin beta-4; Hematopoietic system regulatory peptide	P62328
Transaldolase	P37837
Transforming protein RhoA	P61586
Rho-related GTP-binding protein RhoC	P08134
Transketolase	P29401
Triosephosphate isomerase	P60174
Tropomyosin alpha-3 chain	P06753

Tubulin alpha	Q9BQE3
Ubiquitin-60S ribosomal protein L40	P62987
Ubiquitin;60S ribosomal protein L40	P62979
Ubiquitin;40S ribosomal protein S27a;Polyubiquitin-	P0CG47
Ubiquitin Polyubiquitin-C;Ubiquitin	P0CG48
Unconventional myosin-If	O00160
Vimentin	P08670
Vinculin	P18206

The data indicates proteins identified only in cell lysates after different treatments. The neutrophils were activated with PA14 or PMA in the presence or in the absence of uric acid. Some controls were also performed using Diamide or ABAH (MPO inhibitor).

2. FINAL REMARKS

In summary, this thesis shows the oxidative metabolism of uric acid and its pro-oxidant role in inflammatory diseases, such as cardiovascular disease and sepsis. Our results reveal a novel and relevant oxidant, urate hydroperoxide, produced by uric acid oxidation during the inflammatory oxidative burst. This uric acid-derivative oxidizing agent oxidizes glutathione contributing to a more oxidative cellular environment, as described in the first Chapter.

Moreover, when uric acid is oxidized it forms several reactive intermediates that modify serum albumin by forming adducts on lysine residues, a process denominated oxidative uratylation. Here, our results demonstrated that urate is oxidized in patients with heart failure and diabetes, most likely via an inflammatory process involving neutrophils. The resulting urate-derived products modified serum albumin and the uratylated peptides are potential biomarkers of inflammatory and cardiovascular disease, as described in the second chapter.

We also demonstrate, for the first time, the high production of urate-derived adducts and allantoin in plasma of patients with sepsis when compared to healthy donors. Besides, oxidation of uric acid in neutrophils that were infected with *Pseudomonas aeruginosa* induced and increase in glutathione oxidation, protein S-glutathionylation and alterations in neutrophil lipid profile, as shown in the third chapter.

In conclusion, this thesis reveals that the oxidation of uric acid in inflammation imbalance the cellular redox state towards a more oxidative condition and opens up a new insight into how uric acid can propagate inflammatory response. The latter may contribute to the development of cardiovascular diseases and to the worse prognosis in infectious diseases.

3. REFERENCES

- Abu-Soud, H. M., and S. L. Hazen. 2000. 'Nitric oxide is a physiological substrate for mammalian peroxidases', *J Biol Chem*, 275: 37524-32.
- Ahmed, M., W. Taylor, P. R. Smith, and M. A. Becker. 1999. 'Accelerated transcription of PRPS1 in X-linked overactivity of normal human phosphoribosylpyrophosphate synthetase', *J Biol Chem*, 274: 7482-8.
- Akbar, S. R., D. M. Long, K. Hussain, A. Alhajhusain, U. S. Ahmed, H. I. Iqbal, A. W. Ali, R. Leonard, and C. Dalton. 2015. 'Hyperuricemia: An Early Marker for Severity of Illness in Sepsis', *Int J Nephrol*, 2015: 301021.
- Ali Khan, Hyder, and Bulent Mutus. 2014. 'Protein disulfide isomerase a multifunctional protein with multiple physiological roles', *Frontiers in Chemistry*, 2.
- Allegra, M., P. G. Furtmüller, G. Regelsberger, M. L. Turco-Liveri, L. Tesoriere, M. Perretti, M. A. Livrea, and C. Obinger. 2001. 'Mechanism of reaction of melatonin with human myeloperoxidase', *Biochem Biophys Res Commun*, 282: 380-6.
- Álvarez-Lario, B., and J. Macarrón-Vicente. 2010. 'Uric acid and evolution', *Rheumatology (Oxford)*, 49: 2010-5.
- Ames, B. N., R. Cathcart, E. Schwiers, and P. Hochstein. 1981. 'Uric acid provides an antioxidant defense in humans against oxidant- and radical-caused aging and cancer: a hypothesis', *Proc Natl Acad Sci U S A*, 78: 6858-62.
- Anatoliotakis, N., S. Deftereos, G. Bouras, G. Giannopoulos, D. Tsounis, C. Angelidis, A. Kaoukis, and C. Stefanadis. 2013. 'Myeloperoxidase: expressing inflammation and oxidative stress in cardiovascular disease', *Curr Top Med Chem*, 13: 115-38.
- Arai, Y., Y. Nishinaka, T. Arai, M. Morita, K. Mizugishi, S. Adachi, A. Takaori-Kondo, T. Watanabe, and K. Yamashita. 2014. 'Uric acid induces NADPH oxidase-independent neutrophil extracellular trap formation', *Biochem Biophys Res Commun*, 443: 556-61.
- Aruoma, O. I., and B. Halliwell. 1989. 'Inactivation of alpha 1-antiproteinase by hydroxyl radicals. The effect of uric acid', *FEBS Lett*, 244: 76-80.
- Battelli, M. G., L. Polito, and A. Bolognesi. 2014. 'Xanthine oxidoreductase in atherosclerosis pathogenesis: not only oxidative stress', *Atherosclerosis*, 237: 562-7.
- Becker, B. F. 1993. 'Towards the physiological function of uric acid', *Free Radic Biol Med*, 14: 615-31.
- Bos, M. J., P. J. Koudstaal, A. Hofman, J. C. Witteman, and M. M. Breteler. 2006. 'Uric acid is a risk factor for myocardial infarction and stroke: the Rotterdam study', *Stroke*, 37: 1503-7.
- Braga, T. T., M. F. Forni, M. Correa-Costa, R. N. Ramos, J. A. Barbuto, P. Branco, A. Castoldi, M. I. Hiyane, M. R. Davanzo, E. Latz, B. S. Franklin, A. J. Kowaltowski, and N. O. Camara. 2017. 'Soluble Uric Acid Activates the NLRP3 Inflammasome', *Sci Rep*, 7: 39884.
- Burner, U., P. G. Furtmuller, A. J. Kettle, W. H. Koppenol, and C. Obinger. 2000. 'Mechanism of reaction of myeloperoxidase with nitrite', *J Biol Chem*, 275: 20597-601.
- Bylund, J., K. L. Brown, C. Movitz, C. Dahlgren, and A. Karlsson. 2010. 'Intracellular generation of superoxide by the phagocyte NADPH oxidase: how, where, and what for?', *Free Radic Biol Med*, 49: 1834-45.
- Cameron, V. A., T. J. Mocatta, A. P. Pilbrow, C. M. Frampton, R. W. Troughton, A. M. Richards, and C. C. Winterbourn. 2006. 'Angiotensin type-1 receptor A1166C gene polymorphism correlates with oxidative stress levels in human heart failure', *Hypertension*, 47: 1155-61.
- Cantu-Medellin, N., and E. E. Kelley. 2013. 'Xanthine oxidoreductase-catalyzed reactive species generation: A process in critical need of reevaluation', *Redox Biol*, 1: 353-8.
- Carvalho, L. A. C., Jppb Lopes, G. H. Kaihami, R. P. Silva, A. Bruni-Cardoso, R. L. Baldini, and F. C. Meotti. 2018. 'Uric acid disrupts hypochlorous acid production and the bactericidal activity of HL-60 cells', *Redox Biol*, 16: 179-88.

- Carvalho, L. A., D. R. Truzzi, T. S. Fallani, S. V. Alves, J. C. Toledo Junior, O. Augusto, L. E. Netto, and F. C. Meotti. 2017. 'Urate hydroperoxide oxidizes human peroxiredoxin 1 and peroxiredoxin 2', *J Biol Chem*.
- Chen, C., J. M. Lü, and Q. Yao. 2016. 'Hyperuricemia-Related Diseases and Xanthine Oxidoreductase (XOR) Inhibitors: An Overview', *Med Sci Monit*, 22: 2501-12.
- Cho, Jaehyung, Daniel R. Kennedy, Lin Lin, Mingdong Huang, Glenn Merrill-Skoloff, Barbara C. Furie, and Bruce Furie. 2012. 'Protein disulfide isomerase capture during thrombus formation in vivo depends on the presence of $\beta 3$ integrins', *Blood*, 120: 647-55.
- Chuang, C. C., S. C. Shiesh, C. H. Chi, Y. F. Tu, L. I. Hor, C. C. Shieh, and M. F. Chen. 2006. 'Serum total antioxidant capacity reflects severity of illness in patients with severe sepsis', *Crit Care*, 10.
- Cicoira, M., L. Zanolla, A. Rossi, G. Golia, L. Franceschini, G. Brighetti, P. Zeni, and P. Zardini. 2002. 'Elevated serum uric acid levels are associated with diastolic dysfunction in patients with dilated cardiomyopathy', *Am Heart J*, 143: 1107-11.
- Corry, D. B., P. Eslami, K. Yamamoto, M. D. Nyby, H. Makino, and M. L. Tuck. 2008. 'Uric acid stimulates vascular smooth muscle cell proliferation and oxidative stress via the vascular renin-angiotensin system', *J Hypertens*, 26: 269-75.
- Cox, A. G., A. V. Peskin, L. N. Paton, C. C. Winterbourn, and M. B. Hampton. 2009. 'Redox potential and peroxide reactivity of human peroxiredoxin 3', *Biochemistry*, 48: 6495-501.
- Crisan, T. O., M. C. Cleophas, M. Oosting, H. Lemmers, H. Toenhake-Dijkstra, M. G. Netea, T. L. Jansen, and L. A. Joosten. 2015. 'Soluble uric acid primes TLR-induced proinflammatory cytokine production by human primary cells via inhibition of IL-1Ra', *Ann Rheum Dis*.
- Crışan, T. O., M. C. Cleophas, M. Oosting, H. Lemmers, H. Toenhake-Dijkstra, M. G. Netea, T. L. Jansen, and L. A. Joosten. 2016. 'Soluble uric acid primes TLR-induced proinflammatory cytokine production by human primary cells via inhibition of IL-1Ra', *Ann Rheum Dis*, 75: 755-62.
- Crışan, T. O., M. C. P. Cleophas, B. Novakovic, K. Erler, F. L. van de Veerdonk, H. G. Stunnenberg, M. G. Netea, C. A. Dinarello, and L. A. B. Joosten. 2017. 'Uric acid priming in human monocytes is driven by the AKT-PRAS40 autophagy pathway', *Proc Natl Acad Sci U S A*, 114: 5485-90.
- Cross, C. E., P. A. Motchnik, B. A. Bruener, D. A. Jones, H. Kaur, B. N. Ames, and B. Halliwell. 1992. 'Oxidative damage to plasma constituents by ozone', *FEBS Lett*, 298: 269-72.
- Culleton, B. F., M. G. Larson, W. B. Kannel, and D. Levy. 1999. 'Serum uric acid and risk for cardiovascular disease and death: the Framingham Heart Study', *Ann Intern Med*, 131: 7-13.
- Davies, K. J., A. Sevanian, S. F. Muakkassah-Kelly, and P. Hochstein. 1986. 'Uric acid-iron ion complexes. A new aspect of the antioxidant functions of uric acid', *Biochem J*, 235: 747-54.
- Davies, M. J. 2011. 'Myeloperoxidase-derived oxidation: mechanisms of biological damage and its prevention', *J Clin Biochem Nutr*, 48: 8-19.
- Davis, B. K., H. Wen, and J. P. Ting. 2011. 'The inflammasome NLRs in immunity, inflammation, and associated diseases', *Annu Rev Immunol*, 29: 707-35.
- Desideri, G., G. Castaldo, A. Lombardi, M. Mussap, A. Testa, R. Pontremoli, L. Punzi, and C. Borghi. 2014. 'Is it time to revise the normal range of serum uric acid levels?', *Eur Rev Med Pharmacol Sci*, 18: 1295-306.
- Doehner, W., and U. Landmesser. 2011. 'Xanthine oxidase and uric acid in cardiovascular disease: clinical impact and therapeutic options', *Semin Nephrol*, 31: 433-40.
- Domazou, A. S., H. Zhu, and W. H. Koppenol. 2012. 'Fast repair of protein radicals by urate', *Free Radic Biol Med*, 52: 1929-36.
- Drulović, J., I. Dujmović, N. Stojsavljević, S. Mesaros, S. Andjelković, D. Miljković, V. Perić, G. Dragutinović, J. Marinković, Z. Lević, and M. Mostarica Stojković. 2001. 'Uric acid levels in sera from patients with multiple sclerosis', *J Neurol*, 248: 121-6.
- Essex, David W. 2004. 'The role of thiols and disulfides in platelet function', *Antioxid Redox Signal*, 6: 736-46.
- Feig, D. I., D. H. Kang, and R. J. Johnson. 2008. 'Uric acid and cardiovascular risk', *N Engl J Med*, 359: 1811-21.

- Ford, E., M. N. Hughes, and P. Wardman. 2002. 'Kinetics of the reactions of nitrogen dioxide with glutathione, cysteine, and uric acid at physiological pH', *Free Radic Biol Med*, 32: 1314-23.
- Frei, B., R. Stocker, and B. N. Ames. 1988. 'Antioxidant defenses and lipid peroxidation in human blood plasma', *Proc Natl Acad Sci U S A*, 85: 9748-52.
- Gersch, C., S. P. Pali, W. Imaram, K. M. Kim, S. A. Karumanchi, A. Angerhofer, R. J. Johnson, and G. N. Henderson. 2009. 'Reactions of peroxynitrite with uric acid: formation of reactive intermediates, alkylated products and triuret, and in vivo production of triuret under conditions of oxidative stress', *Nucleosides Nucleotides Nucleic Acids*, 28: 118-49.
- Grainger, R., R. J. McLaughlin, A. A. Harrison, and J. L. Harper. 2013. 'Hyperuricaemia elevates circulating CCL2 levels and primes monocyte trafficking in subjects with inter-critical gout', *Rheumatology (Oxford)*, 52: 1018-21.
- Gur, M., D. Y. Sahin, Z. Elbasan, G. Y. Kalkan, A. Yildiz, Z. Kaya, B. Ozaltun, and M. Cayli. 2013. 'Uric acid and high sensitive C-reactive protein are associated with subclinical thoracic aortic atherosclerosis', *J Cardiol*, 61: 144-8.
- Gur, M., R. Yilmaz, R. Demirbag, and N. Aksoy. 2008. 'Relation of serum uric acid levels with the presence and severity of angiographic coronary artery disease', *Angiology*, 59: 166-71.
- Halliwell, Barry, and John M. C. Gutteridge. 2015. *Free Radicals in Biology and Medicine* (Oxford University Press: Oxford).
- Harris, C. M., and V. Massey. 1997. 'The reaction of reduced xanthine dehydrogenase with molecular oxygen. Reaction kinetics and measurement of superoxide radical', *J Biol Chem*, 272: 8370-9.
- Hediger, M. A., R. J. Johnson, H. Miyazaki, and H. Endou. 2005. 'Molecular physiology of urate transport', *Physiology (Bethesda)*, 20: 125-33.
- Ichida, K., H. Matsuo, T. Takada, A. Nakayama, K. Murakami, T. Shimizu, Y. Yamanashi, H. Kasuga, H. Nakashima, T. Nakamura, Y. Takada, Y. Kawamura, H. Inoue, C. Okada, Y. Utsumi, Y. Ikebuchi, K. Ito, M. Nakamura, Y. Shinohara, M. Hosoyamada, Y. Sakurai, N. Shinomiya, T. Hosoya, and H. Suzuki. 2012. 'Decreased extra-renal urate excretion is a common cause of hyperuricemia', *Nat Commun*, 3: 764.
- Iida, S., Y. Ohkubo, Y. Yamamoto, and A. Fujisawa. 2017. 'Parabanic acid is the singlet oxygen specific oxidation product of uric acid', *J Clin Biochem Nutr*, 61: 169-75.
- Johnson, R. J., G. L. Bakris, C. Borghi, M. B. Chonchol, D. Feldman, M. A. Lanasa, T. R. Merriman, O. W. Moe, D. B. Mount, L. G. Sanchez Lozada, E. Stahl, D. E. Weiner, and G. M. Chertow. 2018. 'Hyperuricemia, Acute and Chronic Kidney Disease, Hypertension, and Cardiovascular Disease: Report of a Scientific Workshop Organized by the National Kidney Foundation', *Am J Kidney Dis*, 71: 851-65.
- Johnson, R. J., E. A. Gaucher, Y. Y. Sautin, G. N. Henderson, A. J. Angerhofer, and S. A. Benner. 2008. 'The planetary biology of ascorbate and uric acid and their relationship with the epidemic of obesity and cardiovascular disease', *Med Hypotheses*, 71: 22-31.
- Johnson, R. J., and B. A. Rideout. 2004. 'Uric acid and diet--insights into the epidemic of cardiovascular disease', *N Engl J Med*, 350: 1071-3.
- Johnson, R. J., Y. Y. Sautin, W. J. Oliver, C. Roncal, W. Mu, L. Gabriela Sanchez-Lozada, B. Rodriguez-Iturbe, T. Nakagawa, and S. A. Benner. 2009. 'Lessons from comparative physiology: could uric acid represent a physiologic alarm signal gone awry in western society?', *J Comp Physiol B*, 179: 67-76.
- Kanellis, J., S. Watanabe, J. H. Li, D. H. Kang, P. Li, T. Nakagawa, A. Wamsley, D. Sheikh-Hamad, H. Y. Lan, L. Feng, and R. J. Johnson. 2003. 'Uric acid stimulates monocyte chemoattractant protein-1 production in vascular smooth muscle cells via mitogen-activated protein kinase and cyclooxygenase-2', *Hypertension*, 41: 1287-93.
- Kang, D. H., L. Han, X. Ouyang, A. M. Kahn, J. Kanellis, P. Li, L. Feng, T. Nakagawa, S. Watanabe, M. Hosoyamada, H. Endou, M. Lipkowitz, R. Abramson, W. Mu, and R. J. Johnson. 2005. 'Uric acid causes vascular smooth muscle cell proliferation by entering cells via a functional urate transporter', *Am J Nephrol*, 25: 425-33.

- Kaur, H., and B. Halliwell. 1990. 'Action of biologically-relevant oxidizing species upon uric acid. Identification of uric acid oxidation products', *Chem Biol Interact*, 73: 235-47.
- Kettle, A. J., R. F. Anderson, M. B. Hampton, and C. C. Winterbourn. 2007. 'Reactions of superoxide with myeloperoxidase', *Biochemistry*, 46: 4888-97.
- Kettle, A. J., and C. C. Winterbourn. 1997. 'Myeloperoxidase: a key regulator of neutrophil oxidant production', *Redox Rep*, 3: 3-15.
- Khosla, U. M., S. Zharikov, J. L. Finch, T. Nakagawa, C. Roncal, W. Mu, K. Krotova, E. R. Block, S. Prabhakar, and R. J. Johnson. 2005. 'Hyperuricemia induces endothelial dysfunction', *Kidney Int*, 67: 1739-42.
- Kittridge, K. J., and R. L. Willson. 1984. 'Uric acid substantially enhances the free radical-induced inactivation of alcohol dehydrogenase', *FEBS Lett*, 170: 162-4.
- Kono, H., C. J. Chen, F. Ontiveros, and K. L. Rock. 2010. 'Uric acid promotes an acute inflammatory response to sterile cell death in mice', *J Clin Invest*, 120: 1939-49.
- Krishnan, E., A. Hariri, O. Dabbous, and B. J. Pandya. 2012. 'Hyperuricemia and the echocardiographic measures of myocardial dysfunction', *Congest Heart Fail*, 18: 138-43.
- Kutzing, M. K., and B. L. Firestein. 2008. 'Altered uric acid levels and disease states', *J Pharmacol Exp Ther*, 324: 1-7.
- Kuwabara, Yoshimitsu, Tomoko Nishino, Ken Okamoto, Tomohiro Matsumura, Bryan T. Eger, Emil F. Pai, and Takeshi Nishino. 2003. 'Unique amino acids cluster for switching from the dehydrogenase to oxidase form of xanthine oxidoreductase', *Proceedings of the National Academy of Sciences*, 100: 8170-75.
- Leyva, F., S. Anker, J. W. Swan, I. F. Godsland, C. S. Wingrove, T. P. Chua, J. C. Stevenson, and A. J. Coats. 1997. 'Serum uric acid as an index of impaired oxidative metabolism in chronic heart failure', *Eur Heart J*, 18: 858-65.
- Li, M., X. Hu, Y. Fan, K. Li, X. Zhang, W. Hou, and Z. Tang. 2016. 'Hyperuricemia and the risk for coronary heart disease morbidity and mortality a systematic review and dose-response meta-analysis', *Sci Rep*, 6: 19520.
- Lotufo, P. A., C. P. Baena, I. S. Santos, and I. M. Bensenor. 2015. 'Serum Uric Acid and Prehypertension Among Adults Free of Cardiovascular Diseases and Diabetes: Baseline of the Brazilian Longitudinal Study of Adult Health (ELSA-Brasil)', *Angiology*, 67: 180-6.
- Lundqvist, H., P. Follin, L. Khalfan, and C. Dahlgren. 1996. 'Phorbol myristate acetate-induced NADPH oxidase activity in human neutrophils: only half the story has been told', *J Leukoc Biol*, 59: 270-9.
- Mandal, A. K., and D. B. Mount. 2015. 'The molecular physiology of uric acid homeostasis', *Annu Rev Physiol*, 77: 323-45.
- Manta, B., M. Hugo, C. Ortiz, G. Ferrer-Sueta, M. Trujillo, and A. Denicola. 2009. 'The peroxidase and peroxynitrite reductase activity of human erythrocyte peroxiredoxin 2', *Arch Biochem Biophys*, 484: 146-54.
- Maples, K. R., and R. P. Mason. 1988. 'Free radical metabolite of uric acid', *J Biol Chem*, 263: 1709-12.
- Marquez, L. A., and H. B. Dunford. 1995. 'Kinetics of oxidation of tyrosine and dityrosine by myeloperoxidase compounds I and II. Implications for lipoprotein peroxidation studies', *J Biol Chem*, 270: 30434-40.
- Marquez, L. A., H. B. Dunford, and H. Van Wart. 1990. 'Kinetic studies on the reaction of compound II of myeloperoxidase with ascorbic acid. Role of ascorbic acid in myeloperoxidase function', *J Biol Chem*, 265: 5666-70.
- Matsukawa, A., S. Miyazaki, T. Maeda, S. Tanase, L. Feng, S. Ohkawara, M. Yoshinaga, and T. Yoshimura. 1998. 'Production and regulation of monocyte chemoattractant protein-1 in lipopolysaccharide- or monosodium urate crystal-induced arthritis in rabbits: roles of tumor necrosis factor alpha, interleukin-1, and interleukin-8', *Laboratory investigation; a journal of technical methods and pathology*, 78: 973-85.

- Medzhitov, R., and C. Janeway, Jr. 2000. 'Innate immune recognition: mechanisms and pathways', *Immunol Rev*, 173: 89-97.
- Meisinger, C., W. Koenig, J. Baumert, and A. Döring. 2008. 'Uric acid levels are associated with all-cause and cardiovascular disease mortality independent of systemic inflammation in men from the general population: the MONICA/KORA cohort study', *Arterioscler Thromb Vasc Biol*, 28: 1186-92.
- Meotti, F. C., G. N. Jameson, R. Turner, D. T. Harwood, S. Stockwell, M. D. Rees, S. R. Thomas, and A. J. Kettle. 2011. 'Urate as a physiological substrate for myeloperoxidase: implications for hyperuricemia and inflammation', *J Biol Chem*, 286: 12901-11.
- Mineiro, M. F., E. D. Patricio, A. S. Peixoto, T. L. S. Araujo, R. P. da Silva, A. I. S. Moretti, F. S. Lima, F. R. M. Laurindo, and F. C. Meotti. 2020. 'Urate hydroperoxide oxidizes endothelial cell surface protein disulfide isomerase-A1 and impairs adherence', *Biochimica Et Biophysica Acta-General Subjects*, 1864.
- Mustard, J. F., E. A. Murphy, M. A. Ogryzlo, and H. A. Smythe. 1963. 'BLOOD COAGULATION AND PLATELET ECONOMY IN SUBJECTS WITH PRIMARY GOUT', *Can Med Assoc J*, 89: 1207-11.
- Nathan, C. 2006. 'Neutrophils and immunity: challenges and opportunities', *Nat Rev Immunol*, 6: 173-82.
- Ndrepepa, G. 2019. 'Myeloperoxidase - A bridge linking inflammation and oxidative stress with cardiovascular disease', *Clin Chim Acta*, 493: 36-51.
- Niskanen, L. K., D. E. Laaksonen, K. Nyssönen, G. Alfthan, H. M. Lakka, T. A. Lakka, and J. T. Salonen. 2004. 'Uric acid level as a risk factor for cardiovascular and all-cause mortality in middle-aged men: a prospective cohort study', *Arch Intern Med*, 164: 1546-51.
- Oda, M., Y. Satta, O. Takenaka, and N. Takahata. 2002. 'Loss of urate oxidase activity in hominoids and its evolutionary implications', *Mol Biol Evol*, 19: 640-53.
- Orowan, E. 1955. 'The origin of man', *Nature*, 175: 683-4.
- Paganoni, S., and M. A. Schwarzschild. 2017. 'Urate as a Marker of Risk and Progression of Neurodegenerative Disease', *Neurotherapeutics*, 14: 148-53.
- Patel, S. 2018. 'Danger-Associated Molecular Patterns (DAMPs): the Derivatives and Triggers of Inflammation', *Curr Allergy Asthma Rep*, 18: 63.
- Patricio, E. S., F. M. Prado, R. P. da Silva, L. A. Carvalho, M. V. Prates, T. Dadamos, M. Bertotti, P. Di Mascio, A. J. Kettle, and F. C. Meotti. 2015. 'Chemical Characterization of Urate Hydroperoxide, A Pro-oxidant Intermediate Generated by Urate Oxidation in Inflammatory and Photoinduced Processes', *Chem Res Toxicol*, 28: 1556-66.
- Peixoto Á, S., R. R. Geyer, A. Iqbal, D. R. Truzzi, A. I. Soares Moretti, F. R. M. Laurindo, and O. Augusto. 2018. 'Peroxynitrite preferentially oxidizes the dithiol redox motifs of protein-disulfide isomerase', *J Biol Chem*, 293: 1450-65.
- Proctor, P. 1970. 'Similar functions of uric acid and ascorbate in man?', *Nature*, 228: 868.
- Richette, Pascal, and Thomas Bardin. 2010. 'Gout', *The Lancet*, 375: 318-28.
- Rigby, K. M., and F. R. DeLeo. 2012. 'Neutrophils in innate host defense against *Staphylococcus aureus* infections', *Semin Immunopathol*, 34: 237-59.
- Rollins, B. J. 1996. 'Monocyte chemoattractant protein 1: a potential regulator of monocyte recruitment in inflammatory disease', *Mol Med Today*, 2: 198-204.
- Saksela, M., R. Lapatto, and K. O. Raivio. 1999. 'Irreversible conversion of xanthine dehydrogenase into xanthine oxidase by a mitochondrial protease', *FEBS Lett*, 443: 117-20.
- Santos, C. X., E. I. Anjos, and O. Augusto. 1999. 'Uric acid oxidation by peroxynitrite: multiple reactions, free radical formation, and amplification of lipid oxidation', *Arch Biochem Biophys*, 372: 285-94.
- Santus, R., L. K. Patterson, P. Filipe, P. Morliere, G. L. Hug, A. Fernandes, and J. C. Maziere. 2001. 'Redox reactions of the urate radical/urate couple with the superoxide radical anion, the tryptophan neutral radical and selected flavonoids in neutral aqueous solutions', *Free Radic Res*, 35: 129-36.

- Sautin, Y. Y., T. Nakagawa, S. Zharikov, and R. J. Johnson. 2007. 'Adverse effects of the classic antioxidant uric acid in adipocytes: NADPH oxidase-mediated oxidative/nitrosative stress', *Am J Physiol Cell Physiol*, 293: C584-96.
- Schwarzschild, M. A., S. R. Schwid, K. Marek, A. Watts, A. E. Lang, D. Oakes, I. Shoulson, A. Ascherio, C. Hyson, E. Gorbald, A. Rudolph, K. Kiebertz, S. Fahn, L. Gauger, C. Goetz, J. Seibyl, M. Forrest, and J. Ondrasik. 2008. 'Serum urate as a predictor of clinical and radiographic progression in Parkinson disease', *Arch Neurol*, 65: 716-23.
- Serbina, N. V., and E. G. Pamer. 2006. 'Monocyte emigration from bone marrow during bacterial infection requires signals mediated by chemokine receptor CCR2', *Nat Immunol*, 7: 311-7.
- Shi, Y. 2010. 'Caught red-handed: uric acid is an agent of inflammation', *J Clin Invest*, 120: 1809-11.
- Shi, Y., J. E. Evans, and K. L. Rock. 2003. 'Molecular identification of a danger signal that alerts the immune system to dying cells', *Nature*, 425: 516-21.
- Silva, R. P., L. A. C. Carvalho, E. S. Patricio, J. P. P. Bonifacio, A. B. Chaves-Filho, S. Miyamoto, and F. C. Meotti. 2018. 'Identification of urate hydroperoxide in neutrophils: A novel pro-oxidant generated in inflammatory conditions', *Free Radic Biol Med*, 126: 177-86.
- Simic, Michael G., and Slobodan V. Jovanovic. 1989. 'Antioxidation mechanisms of uric acid', *Journal of the American Chemical Society*, 111: 5778-82.
- So, A., and B. Thorens. 2010. 'Uric acid transport and disease', *J Clin Invest*, 120: 1791-9.
- Sofaer, J. A., and A. E. Emery. 1981. 'Genes for super-intelligence?', *J Med Genet*, 18: 410-3.
- Squadrito, G. L., R. Cueto, A. E. Splenser, A. Valavanidis, H. Zhang, R. M. Uppu, and W. A. Pryor. 2000. 'Reaction of uric acid with peroxynitrite and implications for the mechanism of neuroprotection by uric acid', *Arch Biochem Biophys*, 376: 333-7.
- Suzuki, T. 2007. 'Nitrosation of uric acid induced by nitric oxide under aerobic conditions', *Nitric Oxide*, 16: 266-73.
- Tanaka, Leonardo Y., Haniel A. Araújo, Gustavo K. Hironaka, Thaís L. S. Araujo, Celso K. Takimura, Andres I. Rodriguez, Annelise S. Casagrande, Paulo S. Gutierrez, Pedro Alves Lemos-Neto, and Francisco R. M. Laurindo. 2016. 'Peri/Epicellular Protein Disulfide Isomerase Sustains Vascular Lumen Caliber Through an Anticonstrictive Remodeling Effect', *Hypertension*, 67: 613-22.
- Terkeltaub, R. A. 2003. 'Clinical practice. Gout', *N Engl J Med*, 349: 1647-55.
- Terkeltaub, R., D. A. Bushinsky, and M. A. Becker. 2006. 'Recent developments in our understanding of the renal basis of hyperuricemia and the development of novel antihyperuricemic therapeutics', *Arthritis Res Ther*, 8 Suppl 1: S4.
- Thomas, M. J. 1992. 'Urate causes the human polymorphonuclear leukocyte to secrete superoxide', *Free Radic Biol Med*, 12: 89-91.
- Turner, R., S. O. Brennan, L. V. Ashby, N. Dickerhof, M. R. Hamzah, J. F. Pearson, L. K. Stamp, and A. J. Kettle. 2018. 'Conjugation of urate-derived electrophiles to proteins during normal metabolism and inflammation', *J Biol Chem*, 293: 19886-98.
- van Dalen, C. J., M. W. Whitehouse, C. C. Winterbourn, and A. J. Kettle. 1997. 'Thiocyanate and chloride as competing substrates for myeloperoxidase', *Biochem J*, 327 (Pt 2): 487-92.
- van der Vliet, A., J. P. Eiserich, B. Halliwell, and C. E. Cross. 1997. 'Formation of reactive nitrogen species during peroxidase-catalyzed oxidation of nitrite. A potential additional mechanism of nitric oxide-dependent toxicity', *J Biol Chem*, 272: 7617-25.
- Vásquez-Vivar, J., A. M. Santos, V. B. Junqueira, and O. Augusto. 1996. 'Peroxynitrite-mediated formation of free radicals in human plasma: EPR detection of ascorbyl, albumin-thiyl and uric acid-derived free radicals', *Biochem J*, 314 (Pt 3): 869-76.
- Volk, K. J., R. A. Yost, and A. Brajter-Toth. 1989. 'On-line electrochemistry/thermospray/tandem mass spectrometry as a new approach to the study of redox reactions: the oxidation of uric acid', *Anal Chem*, 61: 1709-17.
- Watanabe, S., D. H. Kang, L. Feng, T. Nakagawa, J. Kanellis, H. Lan, M. Mazzali, and R. J. Johnson. 2002. 'Uric acid, hominoid evolution, and the pathogenesis of salt-sensitivity', *Hypertension*, 40: 355-60.

- Wheeler, J. G., K. D. Juzwishin, G. Eiriksdottir, V. Gudnason, and J. Danesh. 2005. 'Serum uric acid and coronary heart disease in 9,458 incident cases and 155,084 controls: prospective study and meta-analysis', *PLoS Med*, 2: e76.
- Winterbourn, C. C., and A. J. Kettle. 2013. 'Redox reactions and microbial killing in the neutrophil phagosome', *Antioxid Redox Signal*, 18: 642-60.
- Winterbourn, C. C., A. J. Kettle, and M. B. Hampton. 2016. 'Reactive Oxygen Species and Neutrophil Function', *Annu Rev Biochem*, 85: 765-92.
- Winterbourn, Christine C. 2016. 'Reactive Oxygen Species and Neutrophil Function', *Annu. Rev. Biochem.*: 85:15.1–15.28.
- Wu, X. W., C. C. Lee, D. M. Muzny, and C. T. Caskey. 1989. 'Urate oxidase: primary structure and evolutionary implications', *Proc Natl Acad Sci U S A*, 86: 9412-6.
- Ximenes, Valdecir F., Ghassan J. Maghzal, Rufus Turner, Yoji Kato, Christine C. Winterbourn, and Anthony J. Kettle. 2010. "Serotonin as a physiological substrate for myeloperoxidase and its superoxide-dependent oxidation to cytotoxic tryptamine-4,5-dione." In *The Biochemical journal*, 285-93.
- Zarjou, Abolfazl, and Anupam Agarwal. 2011. 'Sepsis and Acute Kidney Injury', *Journal of the American Society of Nephrology*, 22: 999-1006.

Curriculum Vitae

Railmara Pereira da Silva

PhD in Biochemistry

Tel: (+55)-11-959347050

University of São Paulo

E-mail: railmara@iq.usp.br

748 Prof. Lineu Prestes Avenue São Paulo, Brazil

Education/Professional Experience

- 2015 - 2020 **PhD in Biochemistry**, Institute of Chemistry, Department of Biochemistry, University of São Paulo, Brazil (*Advisor: Dr Flavia Carla Meotti*)
- 2010 - 2015 **B.Sc. in Pharmacy**, Federal University of Sergipe, Brazil

Fellowships and Awards


- Society for Free Radical Research Australasia - Reactive Oxidants in Health and Disease - **YOUNG INVESTIGATOR AWARD** - Identification of Urate Hydroperoxide in Neutrophils: a Novel Pro-oxidant Generated in Inflammatory Conditions (2018). Auckland, New Zealand.
- Brazilian Society of Biochemistry and Molecular Biology - **AWARD FOR BEST POSTER** in the area of redox processes - Identification of Urate Hydroperoxide: A Pro-oxidant Intermediate Generated by Uric Acid Oxidation in Inflammation (2018). Joinville-SC (Brazil).
- Universidade Federal de Sergipe, UFS (Brazil) - **AWARD FOR BEST SCIENTIFIC WORK** in the area of biological sciences.
- FAPESP PhD (2015-2020) Scholarship.

Complementary Education

- 2019 - 2019- School of Advanced Science on Molecular Basis of Inflammatory Diseases. Center for Research in Inflammatory Diseases, USP, Brasil. 2019 – 2019. (Credit Hours: 100h).
- 2019-2019- Collaborator of MENINA CIÊNCIA - CIÊNCIA MENINA Project at Universidade Federal do ABC, Santo André-SP, Brazil (Credit Hours 30h)
- 2019 - 2019- Internship abroad. Center Free Radical Research at University of Otago, OTAGO, New Zealand.

- 2017 - 2017- Omic Sciences. 3^a School of Mass Spectrometry, BRMASS - Natal-RN, Brasil. (Credit Hours: 38h).
- 2015 - 2015 Scientific Initiation. Laboratory of Process Redox in Inflammation. Universidade de São Paulo, USP, Brasil. (Credit hours: (Credit Hours: 480h).
- 2014 - 2014 Internship abroad, Free Radicals Laboratory, Universidade de São Paulo, USP, Brazil. (Credit hours: 196h).
- 2014 - 2014 Course of Redox Processes in Biomedicine. Sociedade Brasileira de Bioquímica e Biologia Molecular, SBBQ, Brazil. (Credit Hours: 6h).
- 2013 - 2014 Internship: education in Pharmaceutical Care Services. Universidade Federal de Sergipe, UFS, Brazil. Credit hours: (480h).
- 2010 - 2014 Scientific Initiation: Redox process in pathologies related. Universidade Federal de Sergipe, UFS, Brazil.
- 2011 - 2011 Internship: Mitochondrial Genetics Research Laboratory. Universidade de São Paulo, USP, Brasil.

Publications

1. MINEIRO, MARCELA FRANCO; PATRICIO, ELIZIANE DE SOUZA; PEIXOTO, ÁLBERT SOUZA; ARAUJO, THAÍS LARISSA SILVA; **DA SILVA, RAILMARA PEREIRA**; MORETTI, ANA IOCHABEL SOARES ; LIMA, FILIPE SILVA; LAURINDO, FRANCISCO RAFAEL MARTINS; MEOTTI, FLAVIA CARLA . **Urate hydroperoxide oxidizes endothelial cell surface protein disulfide isomerase-A1 and impairs adherence.** BIOCHIMICA ET BIOPHYSICA ACTA-GENERAL SUBJECTS, v. 1864, p. 129481, 2020.
2. PINATTO-BOTELHO, MARCOS; **DA SILVA, RAILMARA PEREIRA**; ARCHILHA, MARCOS; GIROLDO, LILIAN; KUZNETSOV, ALEKSEY; MEOTTI, FLÁVIA; DOS SANTOS, ALCINDO. **Diethyl Selenodiglycolate: An Eco-Friendly Synthetic Antioxidant with Potential Application to Inflammatory Disorders.** JOURNAL OF THE BRAZILIAN CHEMICAL SOCIETY, v. 00, p. 1-10, 2020.
3. LETÍCIA F TERRA, ROSANGELA A M WAILEMANN, ANCÉLY F DOS SANTOS, VINICIUS M GOMES, **RAILMARA P SILVA**, ANNA LAPORTE, FLÁVIA C MEOTTI, WALTER R TERRA, GIUSEPPE PALMISANO, STEPHAN LORTZ, LETICIA LABRIOLA; **Heat Shock Protein B1 is a key mediator of prolactin-induced beta-cell cytoprotection against oxidative stress.** Free Radical Biology and Medicine, 2019.
4. BRUNO CHAUSSE, PAMELA A. KAKIMOTO, CAMILLE C. CALDEIRA DA SILVA, ADRIANO B. CHAVES-FILHO, MARCOS Y. YOSHINAGA, **RAILMARA PEREIRA DA SILVA**, SAYURI MIYAMOTO, ALICIA J. KOWALTOWSKI. **Distinct Metabolic Patterns During Microglial Remodeling by Oleate and Palmitate.** Biochemical Journal to Bioscience Reports, 2019.
5.  **RAILMARA P SILVA**, LARISSA A C CARVALHO, ELIZIANE S PATRICIO, JOÃO P P BONIFACIO, ADRIANO B CHAVES-FILHO, SAYURI MIYAMOTO, FLAVIA C MEOTTI . **Identification of urate hydroperoxide in neutrophils: A novel pro-oxidant generated in inflammatory conditions.** FREE RADICAL BIOLOGY AND MEDICINE., v.126, p.177 -

186, 2018.

6. RODRIGO BRITO SANTOS, **RAILMARA PEREIRA DA SILVA**, FELIPE AKIHIRO MELO OTSUKA, DANIELLE DE JESUS TRINDADE, ALINE COSTA SANTOS, HUMBERTO REIS MATOS. **An HPLC method for the determination of adenosine diphosphate: an important marker of hexokinase activity in metabolic diseases.** BIOMEDICAL CHROMATOGRAPHY, v. 19, p. e4473, 2018.
7. LARISSA A C CARVALHO, JOÃO P P B LOPES, GILBERTO H KAIHAMI, **RAILMARA P SILVA**, ALEXANDRE BRUNI-CARDOSO, REGINA L BALDINI, FLAVIA C MEOTTI. **Uric acid disrupts hypochlorous acid production and the bactericidal activity of HL-60 cells.** REDOX BIOLOGY., v.16, p.179 - 188, 2018.
8. VANDERSON S. BISPO, LUCAS S. DANTAS, ADRIANO B. CHAVES FILHO, ISABELLA F.D. PINTO, **RAILMARA P. DA SILVA**, FELIPE A.M. OTSUKA, RODRIGO B. SANTOS, ALINE C. SANTOS, DANIELLE J. TRINDADE, HUMBERTO R. MATOS **Reduction of the DNA damages, Hepatoprotective Effect and Antioxidant Potential of the Coconut Water, ascorbic and Caffeic Acids in Oxidative Stress Mediated by Ethanol.** ANAIS DA ACADEMIA BRASILEIRA DE CIENCIAS., v.89, p.1095 - 1109, 2017.
9. PATRÍCIO, ELIZIANE S.; PRADO, FERNANDA M.; **DA SILVA, RAILMARA P.**; CARVALHO, LARISSA A. C.; PRATES, MARCUS V. C.; DADAMOS, TONY; BERTOTTI, MAURO; DI MASCIO, PAOLO; KETTLE, ANTHONY J.; MEOTTI, FLAVIA C. **Chemical Characterization of Urate Hydroperoxide, A Pro-oxidant Intermediate Generated by Urate Oxidation in Inflammatory and Photoinduced Processes.** CHEMICAL RESEARCH IN TOXICOLOGY., v.39, p.150805160151008 - 2015.
10. ISABELLA F D PINTO, **RAILMARA P SILVA**, ADRIANO DE B CHAVES FILHO, LUCAS S DANTAS, VANDERSON S BISPO, ISAAC A MATOS, FELIPE A M OTSUKA, ALINE C SANTOS, HUMBERTO REIS MATOS. **Study of Antiglycation, Hypoglycemic, and Nephroprotective Activities of the Green Dwarf Variety Coconut Water (Cocos nucifera L.) in Alloxan-Induced Diabetic Rats.** JOURNAL OF MEDICINAL FOOD., v.18, p.150204114946002 - 2015.

Presentations in Events

1. **RAILMARA P. DA SILVA**, NICHOLAS J. MAGON, ANNA P. PILBROW, A. MARK RICHARDS³, FLAVIA C. MEOTTI AND ANTHONY J. KETTLE, **Oxidation of Uric Acid in Inflammation is Associated with Heart Failure in Patients** of the 3rd RIDC Redoxoma Meeting with the Advisory Committee, São Paulo, SP, Brazil, 2020.
2. **RAILMARA P. DA SILVA**, NICHOLAS J. MAGON, ANNA P. PILBROW, A. MARK RICHARDS³, FLAVIA C. MEOTTI AND ANTHONY J. KETTLE. **Generation of urate-derived electrophiles in patients with heart failure and diabetes**. 9th Meeting of SFRR (A+J). The Society for Free Radical Research Australasia. Sydney, Australia, 2019.
3. **RAILMARA P. DA SILVA**, NICHOLAS J. MAGON, ANNA P. PILBROW, LOUISA ASHBY, MARK RICHARDS, FLAVIA C. MEOTTI AND ANTHONY J. KETTLE. **Oxidation of Uric Acid in Inflammation is Associated with Heart Failure in Patients**. São Paulo School of Advanced Sciences on Molecular Basis of Inflammatory Diseases. Ribeirão Preto, SP; 2019.
4. **SILVA, R. P.**; CARVALHO, LARISSA A. C.; BONIFACIO, J. P. P.; PATRICIO, E. S.; FILHO, ADRIANO DE B. CHAVES; MYAMOTO, S.; MEOTTI, F. C. **Identification of Urate Hydroperoxide in Neutrophils: a Novel Pro-oxidant Generated in Inflammatory Conditions**, 2018. The 26th Meeting of the Society for Free Radical Research Australasia, Auckland, New Zealand (Congress, Oral Presentations).
5. **SILVA, R. P.**; **Identification of Urate Hydroperoxide: A Pro-oxidant Intermediate Generated by Uric Acid Oxidation in Inflammation**, 2018. Institute of Chemistry. São Paulo, SP-Brazil (Seminar, Presentations in Events).
6. **SILVA, R. P.**; CARVALHO, LARISSA A. C.; BONIFACIO, J. P. P.; PATRICIO, E. S.; FILHO, ADRIANO DE B. CHAVES; MYAMOTO, S.; MEOTTI, F. C. **Identification of urate hydroperoxide in neutrophils: A pro-oxidant generated by uric acid oxidation in inflammation**, 2018. 47th Annual Meeting of The Brazilian of Biochemistry and Molecular Society, Joinville, SC-Brazil. (Congress, Presentations in Events).
7. **RAILMARA P. DA SILVA**, ELIZIANE S. PATRÍCIO, JOÃO P.P. BONIFACIO, LARISSA A.C. CARVALHO, ADRIANO C.B. FILHO, LUIZ F. SOUZA, SAYURI MIYAMOTO, FLAVIA C MEOTTI. **Urate hydroperoxide: a new reported oxidant generated in inflammatory conditions**, 2018. "19th biennial meeting for the Society for Free Radical Research International, Lisboa, Portugal. (SFRR)"
8. **SILVA, R. P.**; PATRÍCIO, ELIZIANE S.; BONIFACIO, J. P. P.; CHAVES FILHO, A. B.; MYAMOTO, S.; MEOTTI, FLAVIA C. **Oxidative Metabolism of Uric Acid and Its Pro-oxidant Effect in Inflammatory Cells.**, 2017. 46th Annual Meeting of The Brazilian of Biochemistry and Molecular Society, Águas de Lindóia, SP-Brazil. (Congress, Presentations in Events).
9. MINEIRO, M.F., PATRICIO, E.S., LIMA, F.S., ARAUJO, T.L.S., MORETTI, A.I.S., **SILVA, R.P.**, LAURINDO, F.R.M, MEOTTI, F.C. **Urate Hydroperoxide Causes Endothelial Cell Disturbances And Oxidizes Cell Surface Protein Disulfide Isomerase**,

2017. 46th Annual Meeting of The Brazilian of Biochemistry and Molecular Society, Águas de Lindóia, SP-Brazil.

10. **SILVA, R. P.**; PATRICIO, E. S.; BONIFACIO, J. P. P.; MEOTTI, F. C. Pro-oxidant effect of uric acid metabolites in inflammatory cells, 2016. SFRBM/SFRRI 2016 (SFRBM 23rd Annual Meeting), San Francisco, CA-USA.2016 (Congress,Presentations in Events).
11. LARISSA A. C. CARVALHO, ELIZIANE DE SOUZA PATRÍCIO, JOÃO PEDRO PEREIRA BONIFACIO, **RAILMARA PEREIRA SILVA**, FLAVIA CARLA MEOTTI, Uric Acid Effects. 44th Annual Meeting of The Brazilian of Biochemistry and Molecular Society, Foz de Iguaçu, PR-Brazil. (Congress,Presentations in Events).